

Electromagnetic leptogenesis — an EFT-consistent analysis via Wilson coefficients. Part III. Probing light-neutrino masses and low-energy observables

Rin Takada^a

^a*Research Center for the Early Universe (RESCEU), Graduate School of Science, The University of Tokyo, 7-3-1 Hongo, Bunkyo, Tokyo 113-0033, Japan*

E-mail: takada-rin@resceu.s.u-tokyo.ac.jp

ABSTRACT: In this third part of our EFT-consistent analysis of electromagnetic leptogenesis, we confront the dipole operator that sources the baryon asymmetry with constraints from light-neutrino masses and low-energy observables. Starting from the UV completion and one-loop-matched Wilson coefficient C_{NB} of the gauge-invariant operator $\mathcal{O}_{NB} = (\bar{L}\sigma^{\mu\nu}P_R N)\tilde{H}B_{\mu\nu}$, we compute the radiatively induced Weinberg operator \mathcal{O}_5 and derive the light Majorana mass matrix generated by a double insertion of \mathcal{O}_{NB} . For the benchmarks that realise successful resonant electromagnetic leptogenesis at the electroweak scale, these contributions yield neutrino masses far below the scale implied by neutrino oscillation data, so that the observed neutrino masses must originate from additional interactions such as one of the seesaw mechanisms, and only in extreme corners of parameter space do they saturate the cosmological bound on $\sum m_\nu$. We also show that no additional Dirac neutrino mass is generated at one loop by the dipole operator alone. Furthermore, we derive the charged-lepton dipole operator $\mathcal{O}_{e\gamma}$ in LEFT, accounting for one-loop operator mixing in the symmetric phase and two-loop Barr–Zee–type graphs in the broken phase, and evolve its Wilson coefficient $C_{e\gamma}$ down to the muon and electron mass scales using QED renormalisation-group equations. The resulting analytic upper bounds on $\text{BR}(\mu \rightarrow e\gamma)$, the electron EDM, and $(g-2)_\mu$ lie many orders of magnitude below current experimental sensitivities throughout the BAU-compatible region. Electromagnetic leptogenesis in this EFT framework is therefore robust against present constraints from light-neutrino masses and low-energy dipole probes.

KEYWORDS: Leptogenesis, Electromagnetic leptogenesis, Baryon asymmetry of the Universe, Effective field theory, Wilson coefficients, Renormalization group, Right-handed neutrinos, Resonant leptogenesis, Weinberg operator, Light neutrino masses, Charged lepton flavor violation, Electron electric dipole moment, Muon anomalous magnetic moment

Contents

1	Introduction	1
2	Prerequisites	3
2.1	UV Lagrangian	3
2.2	Gauge-invariant operator \mathcal{O}_{NB} and Wilson coefficient C_{NB}	3
2.3	$\Delta L = 0$ four-point effective operators	4
2.4	Off-diagonal gauge mixing	4
2.5	RGE for C_{NB} and coupled running of SM couplings	4
2.6	Broken-phase dipole couplings	4
2.7	Broken-phase rate parameters	5
2.8	Electroweak window	6
3	Results I: Light-neutrino mass generation	6
3.1	Weinberg operator \mathcal{O}_5	6
3.2	Generation of the light Majorana neutrino mass	7
3.2.1	1PI self-energy of a light Majorana neutrino	7
3.2.2	Ultraviolet divergence and generation of the Majorana mass	8
3.3	Generation of the Dirac mass	9
3.4	Comparison with the observations	10
3.4.1	Comparison for standard parameter choice	11
3.4.2	Comparison for parameter values near theoretical limits	12
3.5	Summary of Results I	12
4	Generation of the electromagnetic dipole operator $\mathcal{O}_{e\gamma}$	13
4.1	Definitions and context	13
4.2	One-loop mixing and two-loop pure dipole	15
4.2.1	One-loop mixing in the symmetric phase	15
4.2.2	Two-loop pure dipole in the broken phase	15
4.3	Matrix representation of operator mixing	15
4.4	One-loop contribution to $C_{e\gamma}$ in the symmetric phase	16
4.5	Two-loop contribution to $C_{e\gamma}$ in the broken phase	18
4.5.1	Inner one-loop	18
4.5.2	Outer one-loop	20
5	Renormalisation-group running of $C_{e\gamma}$ in LEFT	21
5.1	One-loop RGE and solution for α	21
5.2	One-loop RGE and solution for $C_{e\gamma}$	23

6 Results II: Consistency with low-energy observables	24
6.1 Overview	25
6.2 Theory of low-energy observables	26
6.2.1 Branching ratio of $\mu \rightarrow e\gamma$	26
6.2.2 Electron EDM	27
6.2.3 Anomalous magnetic moments	28
6.3 Comparison with the observations	28
6.3.1 Comparison for standard parameter choice	30
6.3.2 Comparison for parameter values near theoretical limits	31
6.4 Quantitative explanation of the robustness of EMLG	32
6.4.1 Analytical upper bound for $\text{BR}(\mu \rightarrow e\gamma)$	32
6.4.2 Analytical upper bound for $ d_e , \Delta a_\mu $	33
6.5 Summary of Results II	34
7 Discussion and outlook	35
7.1 Lessons from Parts I–III and the EFT pipeline	35
7.2 Interplay of baryogenesis, light-neutrino masses, and low-energy observables	35
7.3 Outlook	36
8 Conclusions	37
A Calculation of the light Majorana neutrino masses m_ν	38
B Derivation of the Wilson coefficients $C_{e\gamma}$	41
B.1 One-loop operator mixing	41
B.2 Two-loop pure dipole	42
B.2.1 Inner one-loop	42
B.2.2 Outer one-loop	44
C One-loop β-function of QED	50
C.1 Renormalisation of QED	50
C.2 Fermion self-energy	51
C.3 Vacuum polarisation	52
C.4 Vertex correction	53
C.5 One-loop β -function	54

1 Introduction

The observed baryon asymmetry of the Universe (BAU) calls for dynamics that satisfy Sakharov’s three conditions [1]: baryon-number violation, C and CP violation, and a departure from thermal equilibrium. In the Standard Model (SM), anomalous electroweak transitions—sphalerons [2, 3]—violate $B + L$ while conserving $B - L$, thereby enabling

a lepton asymmetry to be partially converted into a baryon asymmetry. Fukugita and Yanagida showed that such a lepton asymmetry can be generated by out-of-equilibrium, CP-violating decays of heavy right-handed neutrinos, thereby providing the framework of leptogenesis [4]. This framework also aligns naturally with mechanisms for generating light-neutrino masses, such as the type-I seesaw [5–8]. See also standard reviews [9–11].

In this series of papers we investigate electromagnetic leptogenesis (EMLG), a variant of leptogenesis, in which the CP-violating source arises from a dimension-six electromagnetic dipole operator coupling right-handed neutrinos to lepton doublets and the hypercharge gauge field. The original proposal of Bell–Kayser–Law [12] treated the dipole couplings as free parameters at the decay scale. In contrast, our aim is to formulate EMLG within an effective field theory (EFT) framework, starting from the concrete UV completion and tracking the Wilson coefficient of the dipole operator from the high scale down to the electroweak scale, so that both baryogenesis and low-energy observables can be treated consistently.

Part I [13] embedded the Bell–Kayser–Law setup into the gauge-invariant operator $\mathcal{O}_{NB} = (\bar{L}\sigma^{\mu\nu}P_R N)\tilde{H}B_{\mu\nu}$ and matched its Wilson coefficient C_{NB} at one loop. This construction established an EFT “pipeline” from the UV Lagrangian to the freeze-out baryon asymmetry Y_B^{FO} . Gauge invariance requires a Higgs insertion, implying that the broken-phase dipole couplings scale as $\mu_{\alpha i} \propto v/(16\pi^2 M_\Psi^2)$, and that both the CP asymmetries and the washout rates scale as $\mu_{\alpha i}^2 \propto v^2/(16\pi^2 M_\Psi^2)^2$. This structural suppression drives low-scale, hierarchical EMLG far below the observed BAU. Part II [14] showed that this suppression can be overcome once the right-handed neutrinos become quasi-degenerate and the CP asymmetries are computed with the Pilaftsis–Underwood resummation [15]. In this resonant regime the self-energy contributions acquire Breit–Wigner enhancements while the washout saturates, allowing Y_B^{FO} to reach the observed BAU within a neutrino-oscillation-motivated window of the effective electromagnetic masses \tilde{m}_1^{EM} .

The present work, Part III, closes the EFT pipeline by confronting this dipole texture with light-neutrino masses and low-energy observables. Working with the UV benchmark of Part II that realises successful resonant EMLG, we compute the radiative Majorana masses generated via the Weinberg operator [16, 17] and derive the charged-lepton dipole operator $\mathcal{O}_{e\gamma}$ in LEFT, incorporating both one-loop operator mixing and two-loop Barr–Zee–type contributions [18, 19]. We then compare the resulting predictions for m_ν , $\mu \rightarrow e\gamma$, the electron EDM, and $(g-2)_\mu$ with current observations. For the experimental status of these observables we refer to MEG II Collaboration [20] for $\mu \rightarrow e\gamma$, JILA Collaboration [21] for the electron EDM, and Muon $g-2$ Collaboration [22] for $a_\mu = (g-2)_\mu/2$. Our main conclusion is that, although EMLG can account for the BAU, the associated radiative contributions to m_ν and to low-energy dipole observables remain safely below existing bounds throughout the BAU-compatible region. Only in extreme corners of parameter space are the cosmological limits on $\sum m_\nu < 0.12$ eV [23] exceeded.

This paper is organised as follows: in sec. 2 we briefly review the EFT pipeline developed in Part I and summarise the ingredients needed in the present analysis. Sec. 3 derives the light-neutrino masses induced by the electromagnetic dipole operator and compares them with oscillation, cosmological, and direct kinematic constraints. Sec. 4 computes

the one- and two-loop contributions to the charged-lepton dipole operator $\mathcal{O}_{e\gamma}$, and sec. 5 discusses the renormalisation-group evolution of its Wilson coefficient in LEFT. In sec. 6 we confront the resulting predictions with low-energy observables, and in sec. 7 we discuss the implications of our results and possible extensions. Sec. 8 contains our conclusions.

2 Prerequisites

2.1 UV Lagrangian

We consider a renormalisable UV completion with heavy fields whose decoupling generates gauge-invariant dimension-six operators with associated Wilson coefficients. Throughout, we work in the mass eigenbasis of the right-handed neutrinos. The Majorana mass matrix M_N is diagonalised via an Autonne–Takagi decomposition with a unitary matrix, and we denote the mass eigenstates by N_i ($i = 1, \dots, n_N$). Unless stated otherwise, Yukawa matrices and Wilson coefficients are expressed in this basis.

The field content extends the SM by right-handed neutrinos N_i , a vector-like fermion Ψ , and a charged scalar S . Here and in what follows, D_μ denotes the covariant derivative. The couplings λ_i and λ'_i mediate the N_i - Ψ - S interactions, while $y_{\alpha j}$ is the SM Dirac Yukawa coupling for L_α - \tilde{H} - N_j . We focus on the following UV Lagrangian [24]

$$\begin{aligned} \mathcal{L}_{\text{UV}} = & \mathcal{L}_{\text{SM}} + \bar{N}_i i\cancel{D} N_i + \bar{\Psi} (i\cancel{D} - M_\Psi) \Psi + |D_\mu S|^2 - V(H, S) \\ & - \left(\lambda'_i \bar{N}_i \Psi_R S + \lambda_i \bar{\Psi}_L N_i S^\dagger + \frac{1}{2} \bar{N} M_N N \right) \\ & - \left(y_{\alpha j} \bar{L}_\alpha \tilde{H} N_j + y_{j\alpha}^* \bar{N}_j \tilde{H}^\dagger L_\alpha \right), \end{aligned} \quad (2.1)$$

with the scalar potential

$$V(H, S) = M_S^2 |S|^2 + \lambda_S |S|^4 + \lambda_{HS} |H|^2 |S|^2, \quad (2.2)$$

where the three added species, N_i , Ψ , and S , are singlets under both $\text{SU}(3)_c$ and $\text{SU}(2)_L$, while their $\text{U}(1)_Y$ hypercharges are 0, +1, and –1, respectively. Integrating out Ψ and S at one loop generates the gauge-invariant dipole operator $\mathcal{O}_{NB,\alpha i} = (\bar{L}_\alpha \sigma^{\mu\nu} P_R N_i) \tilde{H} B_{\mu\nu}$ with Wilson coefficients $C_{NB,\alpha i}(\mu = M_\Psi)$, as derived in Part I, where μ denotes the renormalisation scale. In the present work, the Wilson coefficients $C_{NB,\alpha i}(\mu = \mu_{\text{ref}})$ obtained from this matching and subsequent running and evaluated at the electroweak reference scale $\mu_{\text{ref}} := 150$ GeV serve as the basic input for radiative neutrino masses and low-energy observables.

2.2 Gauge-invariant operator \mathcal{O}_{NB} and Wilson coefficient C_{NB}

One-loop matching at the scale $\mu = M_\Psi$ yields the gauge-invariant dipole operators [24–26]

$$\mathcal{O}_{NB,\alpha i} = (\bar{L}_\alpha \sigma^{\mu\nu} P_R N_i) \tilde{H} B_{\mu\nu}, \quad \sigma^{\mu\nu} := \frac{i}{2} [\gamma^\mu, \gamma^\nu], \quad \tilde{H} := i\sigma_2 H^*, \quad (2.3)$$

with $B_{\mu\nu} = \partial_\mu B_\nu - \partial_\nu B_\mu$, and the Wilson coefficients

$$C_{NB,\alpha i}(M_\Psi) = \sum_j \frac{g_1 Y_\Psi (\lambda_i \lambda'_j - \lambda_j \lambda'_i) y_{\alpha j} M_\Psi}{16\pi^2 M_j} \frac{1 - r + r \ln r}{(1 - r)^2}, \quad r := \frac{M_S^2}{M_\Psi^2}. \quad (2.4)$$

The flavour structure of C_{NB} is antisymmetric in the right-handed-neutrino indices, $C_{NB,\alpha i} \propto (\lambda_i \lambda'_j - \lambda_j \lambda'_i) y_{\alpha j}$, so only off-diagonal pairs with $i \neq j$ contribute. In particular, for a single right-handed neutrino generation, the coefficient vanishes identically; hence, at least two generations of right-handed neutrinos are required for this mechanism to operate.

2.3 $\Delta L = 0$ four-point effective operators

As in Parts I and II, the one-loop matching of the UV Lagrangian in eq. (2.1) onto operators with mass dimension $d \leq 6$ generates no additional independent $\Delta L = 0$ operators involving N_i . Lepton-number-conserving effects at this order can be absorbed into wave-function renormalisation and shifts of renormalisable parameters, so no local four-fermion N_i contact interaction appears in the low-energy EFT.

2.4 Off-diagonal gauge mixing

One-loop mixing into \mathcal{O}_{NW} does not arise in the symmetric phase. The off-diagonal two-point function $\langle B_\mu W_\nu^3 \rangle$ vanishes because the hypercharge-isospin sum over light fields satisfies $\sum_{\text{light}} YT^3 = 0$, so the UV matching yields \mathcal{O}_{NB} only. After electroweak symmetry breaking (EWSB), \mathcal{O}_{NB} is simply expressed in the physical basis using $B_{\mu\nu} = F_{\mu\nu} \cos \theta_W - Z_{\mu\nu} \sin \theta_W$; this is merely a change of basis, not an extra mixing.

2.5 RGE for C_{NB} and coupled running of SM couplings

We adopt the 't Hooft–Feynman gauge and the $\overline{\text{MS}}$ scheme. The Wilson coefficient obeys

$$\mu \frac{d}{d\mu} C_{NB} = -2\gamma_{NB} C_{NB}, \quad \gamma_{NB} = \frac{1}{2}(\gamma_L + \gamma_N + \gamma_H + \gamma_B), \quad (2.5)$$

where γ_i are the field anomalous dimensions. From the one-loop two-point functions the Wilson coefficient satisfies the RGE

$$\mu \frac{d}{d\mu} C_{NB,\alpha i}(\mu) = -\frac{1}{16\pi^2} \left(\frac{91}{12} g_1^2 + \frac{9}{4} g_2^2 - 3y_t^2 \right) C_{NB,\alpha i}(\mu). \quad (2.6)$$

In all our numerical results we evolve $\{g_1, g_2, g_3, y_t\}$ and C_{NB} simultaneously between $\mu = M_\Psi$ and the electroweak reference scale $\mu_{\text{ref}} = 150$ GeV [27, 28].

2.6 Broken-phase dipole couplings

After EWSB, the gauge-invariant operator \mathcal{O}_{NB} is expressed in the physical basis $B_{\mu\nu} = F_{\mu\nu} \cos \theta_W - Z_{\mu\nu} \sin \theta_W$, with $\tilde{H} \rightarrow (v/\sqrt{2} \ 0)^\top$. We therefore work with a single broken-phase dipole operator, which we still denote by \mathcal{O}_{NB} , simultaneously induces $N_i \rightarrow \nu_\alpha \gamma$ and $N_i \rightarrow \nu_\alpha Z$.

The effective interaction then reads [29, 30]

$$-\mathcal{L}_{\text{EFT}} \supset \frac{v}{\sqrt{2} M_\Psi^2} C_{NB,\alpha i}(\mu_{\text{ref}}) (\bar{\nu}_\alpha \sigma^{\mu\nu} P_R N_i) (F_{\mu\nu} \cos \theta_W - Z_{\mu\nu} \sin \theta_W) + \text{h.c.}, \quad (2.7)$$

from which it is convenient to define the dipole coupling $\mu_{\alpha i}$ by factoring out the electroweak angles:

$$-\mathcal{L}_{\text{EFT}} \supset \mu_{\alpha i} (\bar{\nu}_\alpha \sigma^{\mu\nu} P_R N_i) (F_{\mu\nu} - Z_{\mu\nu} \tan \theta_W) + \text{h.c.}, \quad (2.8)$$

with

$$\mu_{\alpha i} := \frac{v \cos \theta_W}{\sqrt{2} M_\Psi^2} C_{NB,\alpha i}(\mu_{\text{ref}}). \quad (2.9)$$

In the numerical calculation the Wilson coefficient is evolved down to the electroweak reference scale $\mu_{\text{ref}} = 150$ GeV. Choosing μ_{ref} is convenient, since the gauge couplings at this scale differ from their values at $\mu = m_Z \simeq 91.2$ GeV by less than 1%, well within one-loop accuracy. This choice fixes the scale at which C_{NB} is evaluated but does not change the definition of $\mu_{\alpha i}$.

2.7 Broken-phase rate parameters

Since the Z mode is suppressed only by phase-space factor and the weak mixing angle, we include both modes consistently in all rates and CP asymmetries.

The partial decay width into the photon mode for a given flavour reads [12, 31, 32]

$$\Gamma_{\gamma,\alpha i}^{\text{tree}} = \frac{|\mu_{\alpha i}|^2 M_i^3}{2\pi}, \quad (2.10)$$

and summing over α gives the total photon-mode width $\Gamma_{\gamma,i}^{\text{tree}}$. The partial width into the Z mode per flavour is

$$\Gamma_{Z,\alpha i}^{\text{tree}} = \frac{|\mu_{\alpha i}|^2 M_i^3}{2\pi} (1 - r_Z)^2 (1 + r_Z) \tan^2 \theta_W, \quad r_Z := \frac{m_Z^2}{M_i^2}, \quad (2.11)$$

and $\Gamma_{Z,i}^{\text{tree}} = \sum_\alpha \Gamma_{Z,\alpha i}^{\text{tree}}$. The total two-body decay widths are given by

$$\Gamma_i := \Gamma_{\gamma,i}^{\text{tree}} + \Gamma_{Z,i}^{\text{tree}}. \quad (2.12)$$

The decay parameters are defined as

$$K_i := \left. \frac{\Gamma_i}{H} \right|_{T=M_i}, \quad H(T) = 1.66 \sqrt{g_*} \frac{T^2}{M_{\text{Pl}}}, \quad (2.13)$$

where $H(T)$ is the Hubble parameter. Correspondingly, the effective electromagnetic neutrino masses \tilde{m}_i^{EM} and the reference values $m_*^{\text{EM}}(M_i)$ are defined such that $K_i = \tilde{m}_i^{\text{EM}} / m_*^{\text{EM}}(M_i)$ holds, namely [33]

$$\tilde{m}_i^{\text{EM}} := v^2 M_i \sum_\alpha |\mu_{\alpha i}|^2, \quad m_*^{\text{EM}}(M_i) := \frac{2\pi \cdot 1.66 \sqrt{g_*} v^2}{R_Z(M_i) M_{\text{Pl}}}, \quad (2.14)$$

with

$$R_Z(M_i) := 1 + (1 - r_Z)^2 (1 + r_Z) \tan^2 \theta_W, \quad r_Z := \frac{m_Z^2}{M_i^2}. \quad (2.15)$$

In our benchmark, $K_i = 1$ is realised for $\tilde{m}_i^{\text{EM}} = m_*^{\text{EM}}(M_i) \simeq 4.15 \times 10^{-4}$ eV.

The parameter \tilde{m}_i^{EM} provides a convenient measure of the overall size of the dipole couplings $\mu_{\alpha i}$. For fixed M_i , it determines both the total decay width Γ_i and the strength of the washout in the resonant electromagnetic leptogenesis dynamics studied in Part II.

2.8 Electroweak window

We model the electroweak window by the temperatures [34, 35]

$$\begin{aligned} T_{\text{EW}} &\simeq 160 \text{ GeV} & (\text{onset of the EWSB}), \\ T_{\text{sph}} &\simeq 130 \text{ GeV} & (\text{sphaleron freeze-out}), \end{aligned} \quad (2.16)$$

and choose $\mu_{\text{ref}} = 150$ GeV as our electroweak reference scale.

3 Results I: Light-neutrino mass generation

In this section we investigate, within the EFT framework, whether the electromagnetic dipole operator \mathcal{O}_{NB} can generate the observed light-neutrino masses m_ν . We introduce the Weinberg operator \mathcal{O}_5 together with its associated Wilson coefficient C_5 , and derive an analytic expression for m_ν based on dimensional regularisation and the additive renormalisation of C_5 . We then probe electromagnetic leptogenesis through m_ν by comparing the theoretical predictions with observational constraints, both for representative benchmark and for parameter choices pushed to the edge of theoretical validity.

3.1 Weinberg operator \mathcal{O}_5

In the electroweak-symmetric phase we define the Weinberg operator \mathcal{O}_5 by [16, 17]

$$\mathcal{O}_{5,\alpha\beta} := (\overline{L}_\alpha^c i\sigma_2 H)(H^\dagger i\sigma_2 L_\beta) = (L_\alpha^\dagger C i\sigma_2 H)(H^\dagger i\sigma_2 L_\beta), \quad (3.1)$$

where C is the charge-conjugation matrix and $i\sigma_2 := \epsilon_{ab}$ is used to raise and lower the $SU(2)_L$ indices. The hypercharges are $Y(L) = -\frac{1}{2}$ and $Y(H) = +\frac{1}{2}$, so the total hypercharge vanishes. The operator is a Lorentz scalar, and since two lepton doublets L with lepton number $L = +1$ appear, lepton number is violated by $\Delta L = 2$. Within the framework of our EFT, this operator has mass dimension $d = 5$ and is the unique dimension-five operator consistent with the Standard Model gauge symmetries.

The EFT Lagrangian that contains this Weinberg operator is

$$\mathcal{L}_5 = \frac{1}{2} C_{5,\alpha\beta} \mathcal{O}_{5,\alpha\beta} + \text{h.c.}, \quad (3.2)$$

and the Wilson coefficient is symmetric in flavour space, $C_{5,\alpha\beta} = C_{5,\beta\alpha}$.

After EWSB, substituting $H \rightarrow (0 \ v/\sqrt{2})^\dagger$ yields a mass term for the left-handed neutrinos ν_L :

$$\mathcal{L}_5 \rightarrow \frac{1}{2} C_{5,\alpha\beta} \frac{v^2}{2} \nu_{L_\alpha}^\dagger C \nu_{L_\beta} + \text{h.c.}, \quad (3.3)$$

so that

$$(m_\nu)_{\alpha\beta} = \frac{v^2}{2} C_{5,\alpha\beta}. \quad (3.4)$$

In other words, the light-neutrino mass matrix is determined by the Wilson coefficient C_5 of the Weinberg operator [36].

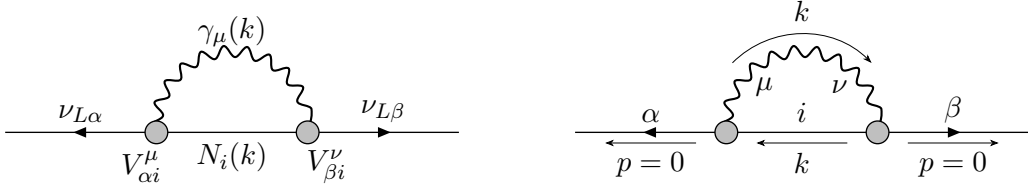


Figure 1. Contribution of the electromagnetic dipole operator to the Majorana mass of light-neutrinos.

3.2 Generation of the light Majorana neutrino mass

In what follows we work in the electroweak-broken phase with $H \rightarrow (0 \ v/\sqrt{2})^\top$. To extract the neutrino mass as the coefficient of $B(0)$ in the two-point function $\Sigma^{(LL)}(p) = A(p^2)\not{p}P_L + B(p^2)P_L$, we take the zero-external-momentum limit $p \rightarrow 0$ and compute the 1PI self-energy $\Sigma_{\alpha\beta}^{(LL)}(p \rightarrow 0)$ for the transition $\nu_{L\alpha} \rightarrow \nu_{L\beta}$ in the 't Hooft–Feynman gauge $\xi = 1$ and in the $\overline{\text{MS}}$ scheme (see also app. A).

3.2.1 1PI self-energy of a light Majorana neutrino

The effective Lagrangian in the broken phase reads

$$-\mathcal{L}_{\text{EFT}} \supset \mu_{\alpha i}(\bar{\nu}_\alpha \sigma^{\mu\nu} P_R N_i)(F_{\mu\nu} - Z_{\mu\nu} \tan \theta_W) + \text{h.c.}, \quad (3.5)$$

with dipole couplings

$$\mu_{\alpha i} = \frac{v \cos \theta_W}{\sqrt{2} M_\Psi^2} C_{NB,\alpha i}(\mu_{\text{ref}}). \quad (3.6)$$

From these, the corresponding broken-phase effective vertices, for $B = \gamma, Z$, are

$$V_{\alpha i}^\mu(k) = 2\mu_{\alpha i}^{(B)} \sigma^{\mu\rho} k_\rho P_R, \quad V_{\beta i}^\nu(k) = 2\mu_{\beta i}^{(B)} \sigma^{\nu\sigma} k_\sigma P_R, \quad (3.7)$$

where

$$\mu_{\alpha i}^{(\gamma)} = \mu_{\alpha i}, \quad \mu_{\alpha i}^{(Z)} = -\mu_{\alpha i} \tan \theta_W. \quad (3.8)$$

From the Feynman graph with one N_i and one gauge boson $B = \gamma, Z$ running in the loop (fig. 1), the 1PI self-energy

$$i\Sigma_{\alpha\beta}^{(LL)} = \sum_{i,B} \int \frac{d^n k}{(2\pi)^n} (2\mu_{\alpha i}^{(B)} \sigma^{\mu\rho} k_\rho P_R) \frac{i(k + M_i)}{k^2 - M_i^2} (2\mu_{\beta i}^{(B)} \sigma^{\nu\sigma} k_\sigma P_R) \frac{(-ig_{\mu\nu})}{k^2 - m_B^2}, \quad (3.9)$$

is obtained by

$$\Sigma_{\alpha\beta}^{(LL)} = \frac{3}{2\pi^2} \sum_{i,B} \mu_{\alpha i}^{(B)} \mu_{\beta i}^{(B)} M_i P_R \int_0^1 dx \Delta_B(x) \left[\frac{1}{\bar{\epsilon}} - \ln \frac{\Delta_B(x)}{\mu^2} + 1 \right], \quad (3.10)$$

where $\bar{\epsilon}^{-1} := \epsilon^{-1} - \gamma + \ln 4\pi$ and the function $\Delta_B(x)$ is defined as

$$\Delta_B(x) := m_B^2 x + M_i^2 (1 - x). \quad (3.11)$$

The parameter μ^2 carries the same mass dimension as $\Delta_B(x)$, namely dimension two. Eq. (3.10) exhibits an ultraviolet divergence proportional to ϵ^{-1} , and, in the language of EFT, it represents the operator mixing $\mathcal{O}_{NB} \times \mathcal{O}_{NB} \rightarrow \mathcal{O}_5$ [37]. Accordingly, the pole of eq. (3.10) is absorbed into the counterterm of \mathcal{O}_5 , while the finite part depends on the matching prescription.

Upon performing the integration over $\Delta_B(x)$, 1PI self-energy becomes

$$\Sigma_{\alpha\beta}^{(LL)} = \frac{3}{2\pi^2} \sum_{i,B} \mu_{\alpha i}^{(B)} \mu_{\beta i}^{(B)} M_i P_R \left[\frac{M_i^2 + m_B^2}{2} \left(\frac{1}{\bar{\epsilon}} + \frac{3}{2} \right) - \frac{M_i^4 \ln \frac{M_i^2}{\mu^2} - m_B^4 \ln \frac{m_B^2}{\mu^2}}{2(M_i^2 - m_B^2)} \right]. \quad (3.12)$$

3.2.2 Ultraviolet divergence and generation of the Majorana mass

Since $\Sigma_{\alpha\beta}^{(LL)}$ denotes the self-energy of left-handed neutrinos ν_L , the divergent part of eq. (3.12) is absorbed into the Weinberg operator \mathcal{O}_5 through renormalisation, as indicated by eqs. (3.3) and (3.4). In the $\overline{\text{MS}}$ scheme, one obtains

$$C_5^{(0)}(\mu) = \mu^{2\epsilon} [C_5(\mu) + \delta C_5(\mu)], \quad (3.13)$$

$$\delta C_{5,\alpha\beta}(\mu) = \frac{2}{v^2} \Sigma_{\text{div},\alpha\beta}^{(LL)} = \frac{3}{2\pi^2 v^2} \bar{\epsilon}^{-1} \sum_{i,B} \mu_{\alpha i}^{(B)} \mu_{\beta i}^{(B)} M_i (M_i^2 + m_B^2) P_R. \quad (3.14)$$

The counterterm δC_5 provides an explicit account of the operator mixing $\mathcal{O}_{NB} \times \mathcal{O}_{NB} \rightarrow \mathcal{O}_5$. Performing the sum over $B = \gamma, Z$ yields

$$\delta C_{5,\alpha\beta}(\mu) = \frac{3}{2\pi^2 v^2} \bar{\epsilon}^{-1} \sum_i \mu_{\alpha i} \mu_{\beta i} M_i P_R [M_i^2 (1 + \tan^2 \theta_W) + m_Z^2 \tan^2 \theta_W]. \quad (3.15)$$

Accordingly, the divergent term $-\frac{v^2}{2} \delta C_5$ cancels the UV divergence of $\Sigma_{\text{div}}^{(LL)}(p \rightarrow 0)$. In what follows, we drop the projection operator P_R associated with the neutrino mass term [31]:

$$\begin{aligned} (m_\nu)_{\alpha\beta}(\mu) &= \frac{v^2}{2} C_{5,\alpha\beta}(\mu) + \Sigma_{\text{finite},\alpha\beta}^{(LL)}(\mu) \\ &= \frac{v^2}{2} C_{5,\alpha\beta}(\mu) + \frac{3}{2\pi^2} \sum_i \mu_{\alpha i} \mu_{\beta i} M_i \left\{ \frac{3}{4} [M_i^2 (1 + \tan^2 \theta_W) + m_Z^2 \tan^2 \theta_W] \right. \\ &\quad \left. - \frac{M_i^2}{2} \ln \frac{M_i^2}{\mu^2} - \frac{M_i^4 \ln \frac{M_i^2}{\mu^2} - m_Z^4 \ln \frac{m_Z^2}{\mu^2}}{2(M_i^2 - m_Z^2)} \tan^2 \theta_W \right\}. \end{aligned} \quad (3.16)$$

Comparing the above with (3.4), one sees that m_ν receives an additional radiative contribution from the two-point function of the mass term. This correction is nothing but the finite part of the self-energy; it contains both $\ln(M_i^2/\mu^2)$ and $\ln(m_Z^2/\mu^2)$, reflecting the presence of two energy scales in the loop. In EFT language, renormalisation of a composite operator may require a lower-dimensional counterterm. Here, the one-loop graph with two insertions of the electromagnetic dipole operator \mathcal{O}_{NB} generates, in the ultraviolet, a divergence with the same structure as the dimension-five Weinberg operator \mathcal{O}_5 , which is absorbed by the counterterm of \mathcal{O}_5 . In the symmetric phase, this may be viewed as

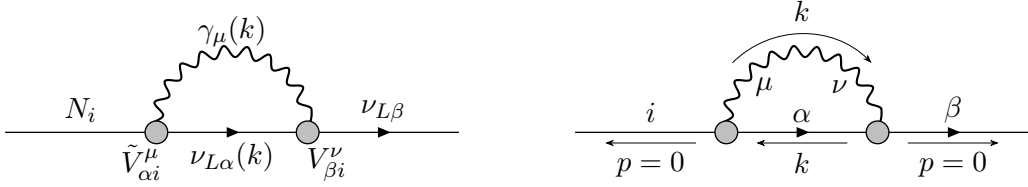


Figure 2. Contribution of the electromagnetic dipole operator to the Dirac mass m_D .

$\mathcal{O}_{NB} = (\bar{L}\sigma^{\mu\nu}P_R N)\tilde{H}B_{\mu\nu}$ ($d = 6$), whose double insertion combined with a gauge loop induces a Weinberg operator.

We match the UV-complete theory to the EFT at $\mu = M_\Psi$. In the UV we assume that the $\Delta L = 2$ Weinberg operator (3.1), (3.2) is not generated at tree level (forbidden by the UV symmetries and field content). Hence, we impose the boundary condition

$$C_5(M_\Psi) = 0. \quad (3.17)$$

It then follows that any $C_5(\mu)$ obtained at low energies arises entirely from operator mixing $\mathcal{O}_{NB} \times \mathcal{O}_{NB} \rightarrow \mathcal{O}_5$ within the EFT. On the other hand, the zero-momentum self-energy $\Sigma_{\alpha\beta}^{(LL)}(p \rightarrow 0)$ is UV-divergent and is absorbed by the $\overline{\text{MS}}$ counterterm δC_5 . With this subtraction, the physical mass in (3.16) becomes independent of the renormalisation scale μ . With the boundary condition (3.17), the first term in (3.16) vanishes at $\mu = M_\Psi$, so that the light-neutrino mass is given solely by the one-loop finite part,

$$(m_\nu)_{\alpha\beta}(M_\Psi) = \frac{3}{2\pi^2} \sum_i \mu_{\alpha i} \mu_{\beta i} M_i \left\{ \frac{3}{4} \left[M_i^2 (1 + \tan^2 \theta_W) + m_Z^2 \tan^2 \theta_W \right] - \frac{M_i^2}{2} \ln \frac{M_i^2}{M_\Psi^2} - \frac{M_i^4 \ln \frac{M_i^2}{M_\Psi^2} - m_Z^4 \ln \frac{m_Z^2}{M_\Psi^2}}{2(M_i^2 - m_Z^2)} \tan^2 \theta_W \right\}. \quad (3.18)$$

The expression (3.18) provides the light-neutrino mass entirely through the finite part. Consequently, if one evaluates at $\mu = M_\Psi$, the theoretical formula to be compared with observations is precisely (3.18). When evaluated at a different μ , the running $C_5(\mu)$ cancels the (counterterm-induced) logarithms and reproduces the same physical quantity.

The resulting 3×3 complex symmetric matrix m_ν is diagonalised by the Autonne–Takagi decomposition,

$$U_\nu^\dagger m_\nu U_\nu = \text{diag}(m_1, m_2, m_3), \quad m_i \geq 0, \quad (3.19)$$

where $\{m_i\}$ are the physical masses and U_ν denotes the neutrino part of the Pontecorvo–Maki–Nakagawa–Sakata (PMNS) matrix [38–42]. Since the experimental inputs Δm_{21}^2 and Δm_{31}^2 (NuFIT 6.0) [43] are fixed, we vary the theoretical inputs $\mu_{\alpha i}$ and compare the resulting m_i with the observations.

3.3 Generation of the Dirac mass

In this subsection we examine whether the electromagnetic dipole operator \mathcal{O}_{NB} can induce a Dirac mass. Throughout, the Dirac mass m_D denotes the coefficient of the mass term that

links the left-handed neutrino ν_L to the right-handed neutrino N , namely $-m_D \bar{\nu}_L N + \text{h.c.}$. In the broken phase, the dipole interaction reads

$$-\mathcal{L}_{\text{EFT}} \supset \mu_{\alpha i} (\bar{\nu}_{L\alpha} \sigma^{\mu\rho} k_\rho P_R N_i) (F_{\mu\nu} - Z_{\mu\nu} \tan \theta_W) + \text{h.c.}, \quad (3.20)$$

which couples ν_L , N , and a gauge field (photon or Z boson) at a single vertex. Hence, as depicted in fig. 2, one might attempt to construct a one-loop self-energy that connects the external legs N_i and $\nu_{L\beta}$. Using the broken-phase effective vertex

$$V_{\alpha i}^\mu(-k) = 2\mu_{\alpha i} \sigma^{\mu\rho}(-k_\rho) P_R, \quad (3.21)$$

the corresponding self-energy amplitude becomes

$$\begin{aligned} i\Sigma_{D,\alpha\beta} &= \sum_{i,B} \int \frac{d^n k}{(2\pi)^n} (-2\mu_{\alpha i}^{(B)*} \sigma^{\mu\rho} k_\rho P_L) \frac{ik}{k^2} (-2\mu_{\beta i}^{(B)} \sigma^{\nu\sigma} k_\sigma P_R) \frac{-ig_{\mu\nu}}{k^2} \\ &= 4 \sum_{i,B} \mu_{\alpha i}^{(B)*} \mu_{\beta i}^{(B)} \int \frac{d^n k}{(2\pi)^n} \frac{\sigma^{\mu\rho} k_\rho ik \sigma_\mu^\sigma k_\sigma}{k^4} P_R \\ &= 4(-1)^3 \sum_{i,B} \mu_{\alpha i}^{(B)*} \mu_{\beta i}^{(B)} \int \frac{d^n k}{(2\pi)^n} \frac{\sigma^{\mu\rho} k_\rho ik \sigma_\mu^\sigma k_\sigma}{k^4} P_R \\ &= -i\Sigma_{D,\alpha\beta}, \end{aligned} \quad (3.22)$$

where in the penultimate equality we have performed the change of variables $k \rightarrow -k$. The integration measure $d^n k$ and the denominator k^4 are invariant, while the numerator $\propto k_\rho ik k_\sigma$ picks up a factor $(-1)^3$ because it contains three powers of k . Hence, eq. (3.22) implies $i\Sigma_{D,\alpha\beta} = -i\Sigma_{D,\alpha\beta}$, and we conclude that

$$\Sigma_{D,\alpha\beta} = 0. \quad (3.23)$$

Therefore, a pure insertion of the electromagnetic dipole operator \mathcal{O}_{NB} does not generate a new Dirac mass at one loop. Within the EFT as a whole, a Dirac mass is already present through the Yukawa interaction inherited from the UV theory,

$$-\mathcal{L}_{\text{EFT}} \supset y_{\alpha j} \bar{L}_\alpha \tilde{H} N_j + \text{h.c.} \quad (3.24)$$

On the other hand, ref. [12] has shown that, rather than from a pure dipole contribution, a non-vanishing Dirac mass $m_D \neq 0$ can arise once the interference between the SM gauge interaction and the electromagnetic dipole operator is taken into account.

3.4 Comparison with the observations

In this subsection we evaluate eq. (3.18) at the UV scale $\mu = M_\Psi$ and compare the resulting prediction for the light-neutrino mass matrix m_ν , obtained within the EFT pipeline of Parts I and II, with three types of observational constraints: the cosmological bound on $\sum m_\nu$ from Planck 2018 + BAO [23], the global fit of the mass-squared differences from NuFIT 6.0 [44], and the direct upper limit on the effective electron-neutrino mass from KATRIN [45].

Expanding the light-neutrino mass generated by the electromagnetic dipole operator, eq. (3.18), in the regime $m_Z^2/M_i^2 \ll 1$, one finds the approximation

$$(m_\nu)_{\alpha\beta} \simeq \frac{3}{2\pi^2} \sum_i \mu_{\alpha i} \mu_{\beta i} M_i^3 (1 + \tan^2 \theta_W) \left(\frac{3}{4} - \frac{1}{2} \ln \frac{M_i^2}{M_\Psi^2} \right). \quad (3.25)$$

This expression makes manifest the suppression from the high scale M_Ψ to m_ν through the dipole couplings μ and the logarithm $\ln(M_i^2/M_\Psi^2)$. In other words, the prediction following from eq. (3.18) is expected to be far below the observational upper limits. In the numerical analysis below we shall therefore use the exact expression (3.18), rather than the approximation (3.25), when comparing with the observations.

3.4.1 Comparison for standard parameter choice

In Parts I and II our aim was to realise baryogenesis under realistic conditions, and we therefore worked with a single standard benchmark without attempting to weaken the suppression aggressively. In Part III our goal is instead to validate electromagnetic leptogenesis; accordingly we shall also consider alternative calculations at more extreme benchmarks that would not normally be adopted, in order to quantify the robustness of the mechanism. As a starting point, for the Part II values¹

$$(M_1, M_2, M_S, M_\Psi) \simeq (0.5, 0.5, 8, 10) \text{ TeV}, \quad |\lambda| \sim \mathcal{O}(10^{-2}), \quad |y_{\alpha j}| \sim \mathcal{O}(10^{-3}), \quad (3.26)$$

we obtain

$$m_1 \simeq 0 \text{ eV}, \quad m_2 \simeq 1.42 \times 10^{-15} \text{ eV}, \quad m_3 \simeq 2.63 \times 10^{-13} \text{ eV}, \quad (3.27)$$

and

$$\Delta m_{21}^2 \simeq 2.00 \times 10^{-30} \text{ eV}^2, \quad \Delta m_{31}^2 \simeq 6.93 \times 10^{-26} \text{ eV}^2. \quad (3.28)$$

In this case, $\sum m_\nu \simeq 2.65 \times 10^{-13} \text{ eV}$ is well below the cosmological bound $\sum m_\nu < 0.12 \text{ eV}$ from Planck + BAO [23], and Δm^2 are well below the NuFIT 6.0 determination of $\Delta m_{21}^2 = 7.49 \times 10^{-5} \text{ eV}^2$ and $\Delta m_{31}^2 = 2.513 \times 10^{-3} \text{ eV}^2$ [44]. Thus, the contribution to m_ν induced within EMLG is far below all current bounds. The observed light-neutrino masses must therefore be dominated by additional contributions to the Weinberg operator that are unrelated to the double insertion of \mathcal{O}_{NB} . In our EFT language this simply means that the Wilson coefficient C_5 receives, at the matching scale, a ‘‘hard’’ piece C_5^{UV} from some $\Delta L = 2$ dynamics in the UV, on top of the radiative piece C_5^{dipole} computed here. This UV contribution may be generated by a type-I seesaw involving the right-handed neutrinos $N_{1,2}$ that participate in electromagnetic leptogenesis, or by additional heavy states realising type-II [46–50] or type-III [51–53] seesaw mechanisms, even if their masses lie well above the electroweak scale. From the low-energy point of view all such possibilities are equivalent: they provide a boundary condition for C_5 , while the electromagnetic dipole operator supplies only a tiny radiative correction on top of it.

¹Throughout we assume quasi-degeneracy, $\Delta M/M \ll 1$. Wherever the dependence is analytic in ΔM (e.g. the one-loop expression for m_ν in eq. (3.18)), we set $M_1 \simeq M_2$ for simplicity. This approximation is not used in the CP-asymmetry calculation, where the resonant structure ($\Delta M \sim T$) must be retained.

3.4.2 Comparison for parameter values near theoretical limits

By contrast, for an extreme benchmark pushed to the edge of theoretical plausibility,

$$(M_1, M_2, M_S, M_\Psi) = (0.3, 0.3, 1, 3) \text{ TeV}, \quad |\lambda| \sim \mathcal{O}(1), \quad |y_{\alpha j}| \sim \mathcal{O}(10^{-2}), \quad (3.29)$$

we obtain

$$m_1 \simeq 1.29 \times 10^{-8} \text{ eV}, \quad m_2 \simeq 6.38 \times 10^{-3} \text{ eV}, \quad m_3 \simeq 1.19 \text{ eV}, \quad (3.30)$$

and

$$\Delta m_{21}^2 \simeq 4.07 \times 10^{-5} \text{ eV}^2, \quad \Delta m_{31}^2 \simeq 1.41 \text{ eV}^2. \quad (3.31)$$

The values in (3.30) satisfy the KATRIN upper limit $m_\beta < 0.45$ eV (90% C.L.) [45]. Recall that KATRIN constrains not an eigenvalue m_ν but the electron-type kinematic mass

$$m_\beta \coloneqq (|U_{e1}|^2 m_1^2 + |U_{e2}|^2 m_2^2 + |U_{e3}|^2 m_3^2)^{1/2}. \quad (3.32)$$

Using the standard mixing angles $\sin^2 \theta_{12} \simeq 0.30$, $\sin^2 \theta_{13} \simeq 0.022$ as given by NuFIT 6.0 [44], one finds from (3.30)

$$\begin{aligned} m_\beta &\simeq (|U_{e2}|^2 m_2^2 + |U_{e3}|^2 m_3^2)^{1/2} \\ &\simeq [0.30 \times (6.38 \times 10^{-3})^2 + 0.022 \times (1.19)^2]^{1/2} \text{ eV} \\ &\simeq 0.177 \text{ eV}. \end{aligned} \quad (3.33)$$

This satisfies the KATRIN 90% C.L. bound $m_\beta < 0.45$ eV [45]. On the other hand, $\sum m_\nu \simeq 1.20$ eV exceeds the Planck 2018 limit $\sum m_\nu < 0.12$ eV [23] by an order of magnitude, so that the dominant tension with observations originates from cosmology ($\sum m_\nu$), not from KATRIN. Thus, while EMLG can violate observational constraints for such extreme parameter choices, conversely one may say that within ranges where theoretical consistency is well preserved, EMLG is robust against constraints from light-neutrino masses.

3.5 Summary of Results I

The above analysis can be summarised as follows. Within the EFT framework defined in sec. 2, the light-neutrino mass matrix can be written schematically as

$$m_\nu = m_\nu^{\text{UV}} + m_\nu^{\text{dipole}}, \quad (3.34)$$

where m_ν^{dipole} is the finite contribution induced by the double insertion of \mathcal{O}_{NB} , and m_ν^{UV} collects all other contributions incorporated in the boundary value of C_5 at the matching scale. For the resonant EMLG benchmarks of Part II we find m_ν^{dipole} to be both parametrically and numerically negligible compared to the oscillation scale, so that the observed spectrum must be accounted for by m_ν^{UV} . In practice this term can originate from a minimal type-I seesaw using the same N_i that appear in electromagnetic leptogenesis, or from additional heavy fields realising type-II, or type-III seesaw dynamics; the details are immaterial for our purposes, since they enter the low-energy theory only through C_5 . Consequently, while baryogenesis and neutrino-mass generation may share degrees of freedom in the UV, their phenomenological effects in the EMLG setup studied here are effectively decoupled: the BAU depends only on the dipole couplings $\mu_{\alpha i}$, whereas the light-neutrino masses depend dominantly on C_5^{UV} .

4 Generation of the electromagnetic dipole operator $\mathcal{O}_{e\gamma}$

In this section we compute, for the electromagnetic dipole operator \mathcal{O}_{NB} introduced in Parts I and II, the one-loop and two-loop contributions to the Wilson coefficient $C_{e\gamma}$ of the charged-lepton dipole operator in LEFT [54]². After evolving $C_{e\gamma}$ to the LEFT scale with the RGE derived in the next section, we use it as a probe of low-energy observables (see also app. B).

4.1 Definitions and context

As dimension-six gauge-invariant operators in the electroweak-symmetric phase, we consider the “neutrino electromagnetic dipoles” that involve a right-handed neutrino, namely the operator \mathcal{O}_{NB} used in Parts I and II and the operator \mathcal{O}_{NW} , which did not enter those analyses:

$$\begin{aligned}\mathcal{O}_{NB,\alpha i} &:= (\bar{L}_\alpha \sigma^{\mu\nu} P_R N_i) \tilde{H} B_{\mu\nu}, \\ \mathcal{O}_{NW,\alpha i} &:= (\bar{L}_\alpha \sigma^{\mu\nu} \tau^I P_R N_i) \tilde{H} W_{\mu\nu}^I, \\ \sigma^{\mu\nu} &= \frac{i}{2} [\gamma^\mu, \gamma^\nu], \quad \tilde{H} = i\sigma_2 H^*,\end{aligned}\tag{4.1}$$

with $\alpha = e, \mu, \tau$ denoting lepton flavour and i the generation index of N . The Wilson coefficients $C_{NB,\alpha i}$ are obtained by one-loop matching onto our UV-complete model. In the symmetric phase there is no gauge-kinetic mixing between B_μ and W_ν^3 , so at the pre-EWSB matching only \mathcal{O}_{NB} is generated; the $SU(2)_L$ counterpart \mathcal{O}_{NW} is not induced at one loop.

In addition, SMEFT contains the dimension-six charged-lepton dipoles [29]

$$\mathcal{O}_{eB,\alpha\beta} = (\bar{L}_\alpha \sigma^{\mu\nu} P_R E_\beta) H B_{\mu\nu},\tag{4.2}$$

$$\mathcal{O}_{eW,\alpha\beta} = (\bar{L}_\alpha \sigma^{\mu\nu} \tau^I P_R E_\beta) H W_{\mu\nu}^I,\tag{4.3}$$

where $L_\alpha = (\nu_{L_\alpha} \ell_{L_\alpha})^\dagger$, the right-handed charged lepton is denoted E_β , and its mass by m_{ℓ_β} .

Working in the physical basis after electroweak symmetry breaking, one has

$$B_{\mu\nu} = F_{\mu\nu} \cos \theta_W - Z_{\mu\nu} \sin \theta_W, \quad W_{\mu\nu}^3 = F_{\mu\nu} \sin \theta_W + Z_{\mu\nu} \cos \theta_W.\tag{4.4}$$

Hence, in LEFT with $H \rightarrow (0 \ v/\sqrt{2})^\dagger$, the charged-lepton dipole

$$\mathcal{O}_{e\gamma,\alpha\beta} = (\bar{\ell}_\alpha \sigma^{\mu\nu} P_R E_\beta) F_{\mu\nu}\tag{4.5}$$

has the Wilson coefficient

$$C_{e\gamma,\alpha\beta} = \frac{v}{\sqrt{2}} (C_{eB,\alpha\beta} \cos \theta_W - C_{eW,\alpha\beta} \sin \theta_W).\tag{4.6}$$

Low-energy observables— $\mu \rightarrow e\gamma$, the electron EDM, and $(g-2)_\mu$ —can all be expressed solely in terms of this coefficient $C_{e\gamma}$.

²LEFT (Low-Energy Effective Field Theory) is the effective field theory below the electroweak-broken scale $\mu \lesssim \mu_{\text{ref}} = 150$ GeV. Since heavy SM degrees of freedom—Higgs, W , Z , top—are integrated out, the remaining light fields comprise a theory with gauge symmetry $SU(3)_c \times U(1)_{\text{em}}$.

Note that, upon inserting the Higgs VEV after EWSB, the operators \mathcal{O}_{eB} in (4.2) and \mathcal{O}_{eW} in (4.3) give

$$\mathcal{O}_{eB} \rightarrow \frac{v}{\sqrt{2}}(\bar{\ell}\sigma^{\mu\nu}P_R E)(F_{\mu\nu}\cos\theta_W - Z_{\mu\nu}\sin\theta_W) \quad (4.7)$$

$$\mathcal{O}_{eW} \rightarrow \frac{v}{\sqrt{2}}(\bar{\ell}\sigma^{\mu\nu}\tau^3 P_R E)(-F_{\mu\nu}\sin\theta_W - Z_{\mu\nu}\cos\theta_W) \quad (4.8)$$

where we used eq. (4.4) and $\tau^3 = -1$. Therefore, the coefficients of LEFT are

$$\begin{pmatrix} C_{e\gamma} \\ C_{eZ} \end{pmatrix} = \frac{v}{\sqrt{2}} \begin{pmatrix} \cos\theta_W & -\sin\theta_W \\ -\sin\theta_W & -\cos\theta_W \end{pmatrix} \begin{pmatrix} C_{eB} \\ C_{eW} \end{pmatrix}, \quad (4.9)$$

that is

$$C_{e\gamma} = \frac{v}{\sqrt{2}}(C_{eB}\cos\theta_W - C_{eW}\sin\theta_W), \quad (4.10)$$

$$C_{eZ} = -\frac{v}{\sqrt{2}}(C_{eB}\sin\theta_W + C_{eW}\cos\theta_W). \quad (4.11)$$

In our UV completion the one-loop matching in the electroweak-symmetric phase generates only the neutrino dipole \mathcal{O}_{NB} , while the $SU(2)_L$ counterpart \mathcal{O}_{NW} is absent; hence at one loop we impose

$$C_{NW}(\mu) = 0. \quad (4.12)$$

This follows from the fact that in the symmetric phase \mathcal{O}_{NB} arises at one loop whereas \mathcal{O}_{NW} does not. At the order we work, the one-loop operator mixing seeded by \mathcal{O}_{NB} preserves the gauge field entering the operator, so \mathcal{O}_{NB} mixes into \mathcal{O}_{eB} but not into \mathcal{O}_{eW} . Together with (4.12) this implies, for any renormalisation scale μ ,

$$C_{eW}(\mu) = 0. \quad (4.13)$$

After EWSB, and keeping μ generic, we have

$$C_{e\gamma}(\mu) = \frac{v}{\sqrt{2}}C_{eB}(\mu)\cos\theta_W, \quad (4.14)$$

$$C_{eZ}(\mu) = -\frac{v}{\sqrt{2}}C_{eB}(\mu)\sin\theta_W, \quad (4.15)$$

where $C_{eZ} = -C_{e\gamma}\tan\theta_W$. Below we shall set $\mu = \mu_{\text{ref}} = 150$ GeV when matching onto LEFT; all low-energy observables are then expressed in terms of $C_{e\gamma}(\mu_{\text{ref}})$. These coefficients follow from inserting the Higgs VEV and performing the neutral-gauge-basis rotation $(B_{\mu\nu}, W_{\mu\nu}^3) \rightarrow (F_{\mu\nu}, Z_{\mu\nu})$; the identification applies simultaneously to $C_{e\gamma}$ and C_{eZ} as in eq. (4.6). All low-energy observables depend only on $C_{e\gamma}$ in LEFT, not on C_{eZ} because the Z field is not dynamical below the electroweak scale and is integrated out long before the evolution to m_μ or m_e . Eliminating Z_ν through its equation of motion,

$$(\partial^2 + m_Z^2)Z_\nu = gJ_\nu^Z \quad \Rightarrow \quad Z_\nu \simeq \frac{g}{m_Z^2}J_\nu^Z + \dots, \quad (4.16)$$

shows that the operator proportional to C_{eZ} generates a derivative expansion,

$$Z_{\mu\nu} = \partial_{[\mu} Z_{\nu]} \Rightarrow Z_{\mu\nu} \simeq \frac{g}{m_Z^2} \partial_{[\mu} J_{\nu]}^Z + \dots, \quad (4.17)$$

so that each insertion carries two soft momenta—one from the dipole vertex $\sigma^{\mu\nu} q_\nu$ and another from $\partial_{[\mu} J_{\nu]}^Z$. The resulting amplitude therefore scales as $(q^2/m_Z^2)C_{eZ}$ relative to the photon dipole $C_{e\gamma}$. Taking $q^2 \simeq m_\ell^2$ for the external lepton mass gives

$$\left(\frac{m_\mu}{m_Z}\right)^2 \simeq 5 \times 10^{-7}, \quad \left(\frac{m_e}{m_Z}\right)^2 \simeq 1 \times 10^{-11}, \quad (4.18)$$

where the squared mass ratio arises because of the two derivatives in the gauge-invariant elimination of $Z_{\mu\nu}$. This suppression renders the C_{eZ} -induced local contribution negligible for all low-energy observables ($\mu \rightarrow e\gamma$, d_e , and $(g-2)_\mu$) compared with the photon dipole $C_{e\gamma}$. We thus describe the low-energy theory entirely in terms of $C_{e\gamma}$ at the reference scale $\mu_{\text{ref}} = 150$ GeV, which serves as the relevant LEFT coefficient for all subsequent phenomenological analyses.

4.2 One-loop mixing and two-loop pure dipole

4.2.1 One-loop mixing in the symmetric phase

In the symmetric phase, using one neutrino dipole operator \mathcal{O}_{NB} together with one charged-lepton Yukawa $y_e \bar{L}HE$ and one SM Dirac Yukawa $y_\nu \bar{L}\tilde{H}N$, a 1PI vertex function $\mathcal{V}_{\alpha\beta}^\rho$ is generated with external legs $(L_\alpha, E_\beta, H, B^\rho)$. This induces the operator mixing

$$\mathcal{O}_{NB} \xrightarrow[1\text{-loop}]{y_e, y_\nu} \mathcal{O}_{eB}. \quad (4.19)$$

The UV divergence ϵ^{-1} is absorbed by the additive renormalisation counterterm attached to the Wilson coefficient C_{eB} , and the coefficient of this counterterm gives the anomalous dimension γ_{eN} . After EWSB, this contribution is immediately mapped to $C_{e\gamma}$ via eq. (4.14); this is nothing more than a change of gauge basis.

4.2.2 Two-loop pure dipole in the broken phase

In the electroweak-broken phase, \mathcal{O}_{NB} itself provides the dipole couplings $\mu_{\alpha i}$ that connect $\nu_L N$ to γ or Z . Inserting \mathcal{O}_{NB} twice produces a double loop (“pure dipole”) from which $\mathcal{O}_{e\gamma}$ is generated. The graphs are of Barr–Zee type [18, 19]: the inner loop is the vacuum polarisation $\Pi_{\text{dipole}}^{\mu\nu}(p)$ built from $\nu_L N$ (with two dipole insertions on the gauge line), while the outer loop is a charged-lepton line that flips chirality through y_e and emits a photon. Because this two-loop contribution carries an extra loop factor $1/(16\pi^2)$, it is in general smaller than the one-loop contribution, but in this work we treat the two as coexisting.

4.3 Matrix representation of operator mixing

If we arrange the dipole-type operators as $(\mathcal{O}_{e\gamma} \ \mathcal{O}_{NB})^\dagger$, the operator mixing is expressed as

$$\mu \frac{d}{d\mu} \begin{pmatrix} \mathcal{O}_{e\gamma} \\ \mathcal{O}_{NB} \end{pmatrix} = \frac{1}{16\pi^2} \begin{pmatrix} \gamma_{ee} & \gamma_{eN} \\ \gamma_{Ne} & \gamma_{NN} \end{pmatrix} \begin{pmatrix} \mathcal{O}_{e\gamma} \\ \mathcal{O}_{NB} \end{pmatrix}, \quad (4.20)$$

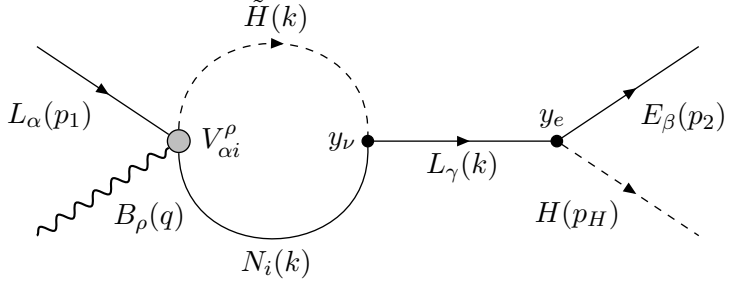


Figure 3. One-loop operator mixing in the electroweak-symmetric phase.

where γ_{ee} , γ_{eN} , γ_{Ne} , γ_{NN} are anomalous dimensions; $\gamma_{eN} \neq 0$ denotes the one-loop mixing, whereas γ_{Ne} would represent reverse mixing. However, in the symmetric phase $\mathcal{O}_{e\gamma}$ is a dimension-five operator containing (L, E, H) , whereas \mathcal{O}_{NB} is a dimension-six operator containing (L, N, \tilde{H}, B) . With SM fields alone there is no gauge-invariant structure that connects E and N at one loop, so $\mathcal{O}_{e\gamma} \rightarrow \mathcal{O}_{NB}$ cannot be generated at one loop and the reverse mixing does not exist: $\gamma_{Ne} = 0$. From the EFT power counting, a lower-dimensional operator cannot renormalise a higher-dimensional one in a mass-independent scheme, so reverse mixing from the downstream $\mathcal{O}_{e\gamma}$ back to the upstream \mathcal{O}_{NB} does not occur [55, 56]. The RGE for C_{NB} continues to be

$$\mu \frac{d}{d\mu} C_{NB,\alpha i} = -\frac{1}{16\pi^2} \left(\frac{91}{12} g_1^2 + \frac{9}{4} g_2^2 - 3y_t^2 \right) C_{NB,\alpha i}, \quad (4.21)$$

as in eq. (2.6).

4.4 One-loop contribution to $C_{e\gamma}$ in the symmetric phase

In matching Wilson coefficients of effective operators, it suffices (i) to keep only the lowest term in the momentum expansion appropriate to a local operator (for operators without derivatives, setting all external momenta to zero is adequate), and (ii) to note that the UV structure (the $\bar{\epsilon}^{-1}$ pole) together with the scheme-fixed finite part does not depend on how the external momenta are routed. Hence, as long as no infrared singularity is induced, one may set all external momenta to zero. For an electromagnetic dipole operator, however, the gauge leg must retain its momentum q , because $B_{\mu\nu} \propto q_\mu \varepsilon_\nu - q_\nu \varepsilon_\mu$ is linear in q . All other external legs can be set to zero (the heavy internal masses provide the scale). In dimensional regularisation the resulting scaleless integrals vanish, leaving only the required UV part.

We compute the 1PI vertex $\mathcal{V}_{\alpha\beta}^\rho$ shown in fig. 3, with external legs $L_\alpha(p_1)$, $E_\beta(p_2)$, $H(p_H)$, and $B^\rho(q)$. To extract the UV divergence it is sufficient to set external momenta to zero. We work in the 't Hooft–Feynman gauge and the $\overline{\text{MS}}$ scheme. From the graph in fig. 3, one obtains

$$\begin{aligned} i\mathcal{V}_{\alpha\beta}^\rho &= \sum_{\gamma,i} \int \frac{d^n k}{(2\pi)^n} \left[-2 \frac{C_{NB,\alpha i}(\mu)}{M_\Psi^2} \sigma^{\rho\lambda} q_\lambda P_R \right] \frac{i(k + M_i)}{k^2 - M_i^2} \frac{i}{k^2} (-iy_{\nu,\gamma i} P_L) \frac{i k}{k^2} (-iy_{e,\gamma\beta} P_R) \\ &= \frac{1}{16\pi^2} \sum_i \frac{C_{NB,\alpha i}(\mu)}{M_\Psi^2} (y_e^\gamma y_\nu)_{\beta i} \left(\frac{1}{\bar{\epsilon}} - \ln \frac{M_i^2}{\mu^2} + 1 \right) (2\sigma^{\rho\lambda} q_\lambda P_R), \end{aligned} \quad (4.22)$$

with $\bar{\epsilon}^{-1} := \epsilon^{-1} - \gamma + \ln 4\pi$. In an EFT, the Feynman rule for a local operator is that the corresponding vertex carries a factor iC . We therefore identify the amplitude $i\mathcal{V}$ computed in the full theory with the factor iC multiplying the corresponding local operator in the EFT. Since the effective operator \mathcal{O}_a contains all spinor/Lorentz structures, the Wilson coefficient C_a is a scalar factor. That is, the operator structure $2\sigma^{\rho\lambda}q_\lambda P_R$ of \mathcal{O}_{eB} is contained in not C_{eB} but \mathcal{O}_{eB} , so the unrenormalised Wilson coefficient $C_{eB}^{(0)}$ is

$$C_{eB,\alpha\beta}^{(0)}(\mu) = \frac{1}{16\pi^2} \sum_i \frac{C_{NB,\alpha i}(\mu)}{M_\Psi^2} (y_e^\intercal y_\nu)_{\beta i} \left(\frac{1}{\bar{\epsilon}} - \ln \frac{M_i^2}{\mu^2} + 1 \right). \quad (4.23)$$

Cancelling the divergence with $C_{eB}^{(0)} = \mu^{2\epsilon}(C_{eB} + \delta C_{eB})$ yields

$$\delta C_{eB,\alpha\beta}(\mu) = \frac{1}{16\pi^2} \sum_i \frac{C_{NB,\alpha i}(\mu)}{M_\Psi^2} (y_e^\intercal y_\nu)_{\beta i} \frac{1}{\bar{\epsilon}}, \quad (4.24)$$

and the renormalised coefficient

$$C_{eB,\alpha\beta}(\mu) = \frac{1}{16\pi^2} \sum_i \frac{C_{NB,\alpha i}(\mu)}{M_\Psi^2} (y_e^\intercal y_\nu)_{\beta i} \left(1 - \ln \frac{M_i^2}{\mu^2} \right). \quad (4.25)$$

At this one-loop order, only $\mathcal{O}_{NB} \rightarrow \mathcal{O}_{eB}$ is generated. Thus, using eq. (4.14),

$$\begin{aligned} (C_{e\gamma}^{(1)})_{\alpha\beta}(\mu) &= \frac{v}{\sqrt{2}} C_{eB,\alpha\beta}(\mu) \cos \theta_W \\ &= \frac{1}{16\pi^2} \sum_i \frac{v \cos \theta_W}{\sqrt{2} M_\Psi^2} C_{NB,\alpha i}(\mu) (y_e^\intercal y_\nu)_{\beta i} \left(1 - \ln \frac{M_i^2}{\mu^2} \right). \end{aligned} \quad (4.26)$$

Here and henceforth the renormalisation scale μ is taken to be the same on both sides: eq. (4.26) is a pure EWSB basis rotation and therefore holds for any μ , provided the Wilson coefficients are evaluated at that same scale. In practice, we set $\mu = \mu_{\text{ref}} = 150$ GeV onto LEFT matching and subsequently evolve $C_{e\gamma}$ in LEFT:

$$\begin{aligned} (C_{e\gamma}^{(1)})_{\alpha\beta}(\mu_{\text{ref}}) &= \frac{1}{16\pi^2} \sum_i \frac{v \cos \theta_W}{\sqrt{2} M_\Psi^2} C_{NB,\alpha i}(\mu_{\text{ref}}) (y_e^\intercal y_\nu)_{\beta i} \left(1 - \ln \frac{M_i^2}{\mu_{\text{ref}}^2} \right) \\ &= \frac{1}{16\pi^2} \sum_i \mu_{\alpha i} (y_e^\intercal y_\nu)_{\beta i} \left(1 - \ln \frac{M_i^2}{\mu_{\text{ref}}^2} \right), \end{aligned} \quad (4.27)$$

where, by definition,

$$\mu_{\alpha i} = \frac{v \cos \theta_W}{\sqrt{2} M_\Psi^2} C_{NB,\alpha i}(\mu_{\text{ref}}). \quad (4.28)$$

After performing the matching at $\mu_{\text{ref}} = 150$ GeV, the coefficient $C_{e\gamma}^{(1)}$ is evolved in the LEFT by means of the QED RGE down to the low-energy scales $\mu = m_\mu, m_e$, which correspond to the experimental observables.

In summary, the one-loop mixing piece generally carries off-diagonal flavour components ($\alpha \neq \beta$); the flavour structure in eq. (4.27) thus induces CLFV.

4.5 Two-loop contribution to $C_{e\gamma}$ in the broken phase

As a physical picture, in the electroweak-broken phase the operator \mathcal{O}_{NB} itself yields dipole couplings $\mu_{\alpha i}$ that connect ν_L - N to γ or Z . If one inserts \mathcal{O}_{NB} twice in the inner loop (the ν_L - N ‘‘bubble’’), an effective vertex $h\gamma B$ is generated with the gauge-invariant tensor

$$T_1^{\mu\rho}(p, q) = g^{\mu\rho}(q \cdot r) - q^\rho r^\mu, \quad (4.29)$$

namely

$$i\mathcal{V}_{h\gamma B}^{\mu\rho}(p, q) = \mathcal{C}_B T_1^{\mu\rho}(p, q), \quad \mathcal{C}_B = -\frac{5c_B}{2\pi^2 v} \sum_{\alpha', i} |\mu_{\alpha' i}|^2 \left(\frac{1}{\epsilon} - \ln \frac{M_i^2}{\mu^2} + 2 \right), \quad (4.30)$$

with $c_\gamma = 1$ and $c_Z = -\tan \theta_W$. This structure satisfies the Ward–Takahashi identity; once it is passed to the outer loop, only the dipole structure $\sigma^{\mu\nu} q_\nu$ survives.

In the outer loop, the chirality flip on the charged-lepton line is provided by the Yukawa coupling y_{ℓ_β} , yielding a three-point 1PI amplitude with external legs $(\ell_\alpha, E_\beta, A^\mu)$. The crucial point here is that the inner flavour sum closes as $\sum_{\alpha', i} |\mu_{\alpha' i}|^2$, so that the final result is flavour-diagonal:

$$(C_{e\gamma}^{(2)})_{\alpha\beta} \propto \delta_{\alpha\beta} y_{\ell_\beta} \sum_{\alpha', i} |\mu_{\alpha' i}|^2 \sum_{B=\gamma, Z} c_B g_{L_\beta}^{(B)} I_B(m_h^2, m_B^2), \quad (4.31)$$

where $g_{L_\beta}^\gamma = e Q_{\ell_\beta}$ and $g_{L_\beta}^Z = e(T_3 - Q_{\ell_\beta} \sin^2 \theta_W)/(\sin \theta_W \cos \theta_W)$. The function $I_B(m_h^2, m_B^2)$ is a finite (scheme-independent) outer-loop function; any μ -dependence is entirely contained in the prefactor \mathcal{C}_B . Consequently, CLFV is not generated by the two-loop pure-dipole alone; the CLFV effects are those of the one-loop mixing in sec. 4.4.

After EWSB, substituting $\tilde{H} \rightarrow (0 \ (v + h)/\sqrt{2})^\top$ into \mathcal{O}_{NB} yields

$$\begin{aligned} -\mathcal{L}_{\text{LEFT}} \supset & \mu_{\alpha i} \bar{\nu}_\alpha \sigma^{\mu\nu} P_R N_i (F_{\mu\nu} - Z_{\mu\nu} \tan \theta_W) \\ & + \frac{h}{v} \mu_{\alpha i} \bar{\nu}_\alpha \sigma^{\mu\nu} P_R N_i (F_{\mu\nu} - Z_{\mu\nu} \tan \theta_W), \end{aligned} \quad (4.32)$$

and, as in Parts I and II, the dipole couplings are given in (4.28). When the external gauge boson carries incoming momentum q , the effective vertices are defined—as functions of the particle flow $\nu \rightarrow N$ and of whether the dipole couples with or without h —as

$$V_{\alpha i}^\mu(q) = -2\mu_{\alpha i} \sigma^{\mu\lambda} q_\lambda P_R, \quad V_{\alpha i}^{(Z)\mu}(q) = 2 \tan \theta_W \mu_{\alpha i} \sigma^{\mu\lambda} q_\lambda P_R, \quad (4.33)$$

$$V_{\alpha i}^{(h)\mu}(q) = -\frac{2}{v} \mu_{\alpha i} \sigma^{\mu\lambda} q_\lambda P_R, \quad V_{\alpha i}^{(hZ)\mu}(q) = \frac{2 \tan \theta_W}{v} \mu_{\alpha i} \sigma^{\mu\lambda} q_\lambda P_R. \quad (4.34)$$

When the particle flow is reversed, $N \rightarrow \nu$, the corresponding effective vertex, denoted by \tilde{V} , is obtained from V by replacing $\mu \rightarrow \mu^*$ and $P_R \rightarrow P_L$.

4.5.1 Inner one-loop

The external legs of the inner loop are $h(p)$, $\gamma^\mu(q)$, and $B^\rho(-p - q)$. In fig. 4 there are two insertions of \mathcal{O}_{NB} ; according to (4.32), one of the effective vertices carries the factor h/v . Symmetrising the amplitude under the interchange of the two gauge fields,

$$i\mathcal{V}_{h\gamma B}^{\mu\rho}(p, q) = i \left[\mathcal{V}_{(h\gamma)B}^{\mu\rho}(p, q) + \mathcal{V}_{\gamma(hB)}^{\mu\rho}(p, q) \right], \quad (4.35)$$

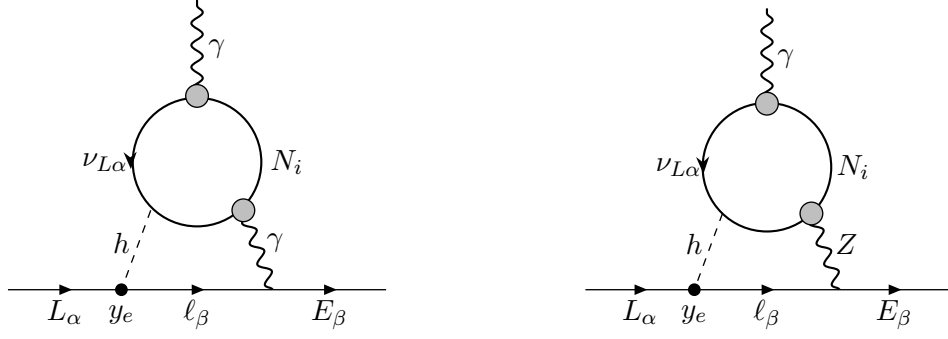


Figure 4. Two-loop Barr-Zee-type graphs in the broken phase.

with the two pieces defined as follows.

(i) When h attaches to the γ -vertex side, taking $r = -(p + q)$,

$$iV_{(h\gamma)B}^{\mu\rho} = \sum_{\alpha',i} \int \frac{d^n k}{(2\pi)^n} \left(-\frac{2}{v} \mu_{\alpha'i} \sigma^{\mu\nu} q_\nu P_R \right) \frac{i(\not{k} + M_i)}{k^2 - M_i^2} \left(-2c_B \mu_{\alpha'i}^* \sigma^{\rho\lambda} r_\lambda P_L \right) \frac{i(\not{k} + \not{p})}{(k + p)^2}. \quad (4.36)$$

(ii) When h attaches to the B -vertex side,

$$iV_{\gamma(hB)}^{\mu\rho} = \sum_{\alpha',i} \int \frac{d^n k}{(2\pi)^n} \left(-2\mu_{\alpha'i} \sigma^{\mu\nu} q_\nu P_R \right) \frac{i(\not{k} + M_i)}{k^2 - M_i^2} \left(-\frac{2c_B}{v} \mu_{\alpha'i}^* \sigma^{\rho\lambda} r_\lambda P_L \right) \frac{i(\not{k} + \not{p})}{(k + p)^2}, \quad (4.37)$$

with $B = \gamma, Z$, $c_\gamma = 1$, $c_Z = -\tan \theta_W$.

Adding (i) and (ii) gives

$$\begin{aligned} iV_{h\gamma B}^{\mu\rho}(p, q) &= -\frac{8c_B}{v} \sum_{\alpha',i} |\mu_{\alpha'i}|^2 \int \frac{d^n k}{(2\pi)^n} \frac{\text{tr}[(\sigma^{\mu\nu} q_\nu P_R)(\not{k} + M_i)(\sigma^{\rho\lambda} r_\lambda P_L)(\not{k} + \not{p})]}{(k^2 - M_i^2)(k + p)^2} \\ &= -\frac{5c_B}{2\pi^2 v} [g^{\mu\rho}(q \cdot r) - q^\rho r^\mu] \sum_{\alpha',i} |\mu_{\alpha'i}|^2 \left(\frac{1}{\bar{\epsilon}} - \ln \frac{M_i^2}{\mu^2} + 2 \right), \end{aligned} \quad (4.38)$$

with $\mu_{\alpha'i}$ as in (4.28). Here, truncating the local-operator expansion at the lowest order $\mathcal{O}(q)$,

$$T_1^{\mu\rho}(p, q) := g^{\mu\rho}(q \cdot r) - q^\rho r^\mu \simeq -g^{\mu\rho}(q \cdot p) + p^\mu q^\rho, \quad (4.39)$$

which is nothing but the gauge-invariant tensor of the electromagnetic dipole. Therefore, the effective vertex to be passed to the outer loop can be written as

$$iV_{h\gamma B}^{\mu\rho}(p, q) = \mathcal{C}_B T_1^{\mu\rho}(p, q), \quad (4.40)$$

where the coefficient \mathcal{C}_B is defined as

$$\mathcal{C}_B = -\frac{5c_B}{2\pi^2 v} \sum_{\alpha',i} |\mu_{\alpha'i}|^2 \left(\frac{1}{\bar{\epsilon}} - \ln \frac{M_i^2}{\mu^2} + 2 \right), \quad (4.41)$$

with $c_\gamma = 1$ and $c_Z = -\tan \theta_W$.

4.5.2 Outer one-loop

The external legs of the outer loop are a left-handed charged lepton, a right-handed charged lepton, and an external photon $(\ell_\alpha, E_\beta, A^\mu)$. The object produced at the end is $\mathcal{O}_{e\gamma}$, while in the inner loop run the Higgs h and a gauge boson $B = \gamma, Z$. The vertices are

$$h\bar{\ell}_\beta E_\beta : -iy_{e_\beta} P_R, \quad B\bar{\ell}\ell : -ig_{L_\beta}^{(B)} \gamma_\rho P_L, \quad h\gamma B : i\mathcal{V}_{h\gamma B}^{\mu\rho}. \quad (4.42)$$

Writing the outer 1PI amplitude for each $B = \gamma, Z$, we have

$$\begin{aligned} i\Gamma_{\alpha\beta}^{(B)\mu}(q) &= \delta_{\alpha\beta} \int \frac{d^n p}{(2\pi)^n} \frac{i\cancel{p}}{p^2} (-ig_{L_\beta}^{(B)} \delta_{\alpha\gamma} \gamma_\rho P_L) \frac{i}{p^2 - m_h^2} \\ &\quad \times \frac{i(\cancel{p} + \cancel{q})}{(p+q)^2} (-iy_{e_\beta} \delta_{\gamma\beta}) \frac{-ig^{\rho\sigma}}{(p+q)^2 - m_B^2} [i\mathcal{V}_\sigma^\mu(p, q)] \\ &= \delta_{\alpha\beta} g_{L_\beta}^{(B)} y_{e_\beta} \mathcal{C}_B \int \frac{d^n p}{(2\pi)^n} \frac{\cancel{p} \gamma_\rho (\cancel{p} + \cancel{q}) T_1^{\mu\rho}(p, q) P_R}{p^2(p^2 - m_h^2)(p+q)^2[(p+q)^2 - m_B^2]}, \end{aligned} \quad (4.43)$$

where $i\mathcal{V}_\sigma^\mu(p, q)$ is the inner one-loop effective vertex and we substituted $i\mathcal{V}_\sigma^\mu = i\mathcal{C}_B T_{1\sigma}^\mu$. After evaluating the loop integral and using the Gordon identity, we obtain

$$i\Gamma_{\alpha\beta}^{(B)\mu}(q) = \frac{i}{2\sqrt{2}v} \delta_{\alpha\beta} g_{L_\beta}^{(B)} \mathcal{C}_B (2\sigma^{\mu\nu} q_\nu P_R) I_B(m_h^2, m_B^2), \quad (4.44)$$

and

$$I_B(a, b) := \int \frac{d^n p}{(2\pi)^n} \frac{q \cdot p}{(p^2 - a)(p+q)^2[(p+q) - b]}. \quad (4.45)$$

It follows that $I_B(q^2 \rightarrow 0)$ reduces to a constant $i/(32\pi^2)$, independent of whether $a = m_h^2$ or $b = m_B^2$ [57, 58]. Substituting this into (4.44), we obtain

$$\Gamma_{\alpha\beta}^{(B)\mu}(q) = -\frac{1}{64\sqrt{2}\pi^2 v} \sum_{B=\gamma, Z} c_B g_{L_\beta}^{(B)} \mathcal{C}_B (2\sigma^{\mu\nu} q_\nu P_R), \quad (4.46)$$

and hence, taking (4.41) into account, the Wilson coefficient induced at two loops is

$$(C_{e\gamma}^{(2)})_{\alpha\beta}(\mu) = \frac{5\sqrt{2}e}{(16\pi^2)^2 v^2} \delta_{\alpha\beta} \sum_{\alpha', i} |\mu_{\alpha'i}|^2 \left(Q_{\ell_\beta} - \frac{T_3 - Q_{\ell_\beta} \sin^2 \theta_W}{\cos^2 \theta_W} \right) \left(\frac{1}{\bar{\epsilon}} - \ln \frac{M_i^2}{\mu^2} + 2 \right), \quad (4.47)$$

with $c_\gamma = 1$, $c_Z = -\tan \theta_W$. The combination $eg_{L_\beta}^{(B)}$ is the gauge coupling of B to the left-handed lepton after electroweak mixing, so that

$$g_{\ell_\beta} := Q_{\ell_\beta} - \frac{T_3 - Q_{\ell_\beta} \sin^2 \theta_W}{\cos^2 \theta_W} = Q_{\ell_\beta} (1 + \tan^2 \theta_W) - \frac{T_3}{\cos^2 \theta_W} = \frac{Q_{\ell_\beta} - T_3}{\cos^2 \theta_W}, \quad (4.48)$$

where Q_{ℓ_β} is the electric charge in units of e ; for a charged lepton $Q_\ell = -1$. T_3 is the third component of weak isospin; for a left-handed lepton doublet the charge component is $T_3 = -1/2$ whereas the right-handed charged-lepton has $T_3 = 0$. The Weinberg angle θ_W satisfies $\sin^2 \theta_W = 0.231$, $\cos^2 \theta_W = 0.769$. Under these benchmark values,

$$g_\ell := g_{\ell_\beta} \simeq -0.650, \quad \beta = e, \mu, \tau. \quad (4.49)$$

Finally, to cancel the divergence in (4.47), we renormalise the Wilson coefficient in the same way as in (4.23)–(4.25), using $C_{e\gamma}^{(0)} = \mu^{2\epsilon}(C_{e\gamma} + \delta C_{e\gamma})$:

$$\delta C_{e\gamma, \alpha\beta}(\mu) = \frac{5\sqrt{2}e}{(16\pi^2)^2 v^2} \delta_{\alpha\beta} \sum_{\alpha',i} |\mu_{\alpha'i}|^2 g_{\ell_\beta} \frac{1}{\epsilon} \quad (4.50)$$

and

$$C_{e\gamma, \alpha\beta}(\mu) = \frac{5\sqrt{2}e}{(16\pi^2)^2 v^2} \delta_{\alpha\beta} \sum_{\alpha',i} |\mu_{\alpha'i}|^2 g_{\ell_\beta} \left(2 - \ln \frac{M_i^2}{\mu^2} \right). \quad (4.51)$$

Therefore, the renormalised two-loop contribution to $C_{e\gamma}$ is given by

$$(C_{e\gamma}^{(2)})_{\alpha\beta}(\mu) = \frac{5\sqrt{2}e}{(16\pi^2)^2 v^2} \delta_{\alpha\beta} \sum_{\alpha',i} |\mu_{\alpha'i}|^2 g_{\ell_\beta} \left(2 - \ln \frac{M_i^2}{\mu^2} \right). \quad (4.52)$$

At the EWSB matching point we set $\mu = \mu_{\text{ref}} = 150$ GeV and evaluate both $C_{e\gamma}^{(1)}$ and $C_{e\gamma}^{(2)}$ at this common scale. In particular,

$$(C_{e\gamma}^{(2)})_{\alpha\beta}(\mu_{\text{ref}}) = \frac{5\sqrt{2}e}{(16\pi^2)^2 v^2} \delta_{\alpha\beta} \sum_{\alpha',i} |\mu_{\alpha'i}|^2 g_{\ell_\beta} \left(2 - \ln \frac{M_i^2}{\mu_{\text{ref}}^2} \right). \quad (4.53)$$

We then define the matched Wilson coefficient

$$(C_{e\gamma})_{\alpha\beta}(\mu_{\text{ref}}) = (C_{e\gamma}^{(1)})_{\alpha\beta}(\mu_{\text{ref}}) + (C_{e\gamma}^{(2)})_{\alpha\beta}(\mu_{\text{ref}}), \quad (4.54)$$

given by eqs. (4.27) and (4.53). This coefficient is subsequently evolved to $\mu = m_\mu, m_e$ by the QED RGE in LEFT.

5 Renormalisation-group running of $C_{e\gamma}$ in LEFT

5.1 One-loop RGE and solution for α

From app. C we obtain the one-loop QED β -function

$$\beta(e) = \frac{e^3}{12\pi^2}. \quad (5.1)$$

Rewriting (5.1) in terms of the fine-structure constant $\alpha := e^2/(4\pi)$,

$$\frac{d\alpha}{d \ln \mu} = \frac{e}{2\pi} \beta(e) = \frac{e^4}{24\pi^3} = \frac{2}{3\pi} \alpha^2. \quad (5.2)$$

Here, from (C.40) we see that at one loop the renormalisation of the electric charge $\delta Z_e^{(1)}$ is fixed solely by the photon wave-function renormalisation constant $\delta Z_3^{(1)}$, and $\delta Z_3^{(1)}$ itself is obtained by linearly summing the vacuum-polarisation contributions of all charged Dirac fields. Therefore, for a flavour f of electric charge Q_f and colour multiplicity N_c^f , the 1PI two-point function (C.20) receives a contribution proportional to $N_c^f Q_f^2$. From (C.21) its UV divergence is

$$e^2 \Pi_{2,f}^{\text{div}}(q^2) = \frac{e^2 N_c^f Q_f^2}{12\pi^2} \epsilon^{-1}. \quad (5.3)$$

Summing over all flavours then gives

$$e^2 \Pi_2^{\text{div}}(q^2) = \sum_f e^2 \Pi_{2,f}^{\text{div}}(q^2) = \frac{e^2}{12\pi^2} \epsilon^{-1} \left(\sum_f N_c^f Q_f^2 \right). \quad (5.4)$$

Extracting only the UV-divergent part of the 1PI two-point function, which leads to (C.23), so

$$\delta Z_3^{(1)} + e^2 \Pi_2^{\text{div}} = 0 \quad \Rightarrow \quad \delta Z_3^{(1)} = -\frac{e^2}{12\pi^2} \epsilon^{-1} \left(\sum_f N_c^f Q_f^2 \right) + \mathcal{O}(e^4). \quad (5.5)$$

As in app. C, because the bare electric charge $e_0 = \mu^\epsilon e Z_e$ is μ -independent, repeating the steps of (C.42)–(C.46) with the N_c^f and Q_f weights included yields the one-loop QED β -function

$$\beta(e) = \frac{e^3}{12\pi^2} \sum_f N_c^f Q_f^2. \quad (5.6)$$

Here the factor $\sum N_c^f Q_f^2$ arises because the coefficient of the divergent part of $\delta Z_3^{(1)}$ is the linear sum of vacuum-polarisation contributions from each charged Dirac flavour. N_c^f is the colour multiplicity, and Q_f^2 comes from the two photon couplings eQ_f in the loop. In the $\overline{\text{MS}}$ scheme, when $\mu < m_f$ the flavour f decouples and is removed from the sum by matching across the mass threshold. In this case, (5.2) can be rewritten as

$$\mu \frac{d\alpha}{d\mu} = \beta_1 \alpha^2, \quad \beta_1 := \frac{2}{3\pi} \sum_f N_c^f Q_f^2, \quad (5.7)$$

which is nothing but the RGE for $\alpha(\mu)$.

We now solve the RGE (5.7) for $\alpha(\mu)$. Separating variables gives

$$\frac{d\alpha}{d\ln\mu} = \beta_1 \alpha^2 \quad \Rightarrow \quad \frac{d\alpha}{\alpha^2} = \beta_1 d\ln\mu. \quad (5.8)$$

Choosing a reference scale μ_0 and the initial condition $\alpha(\mu_0) := \alpha_0$, we integrate to obtain

$$\int_{\alpha_0}^{\alpha(\mu)} \frac{d\alpha}{\alpha^2} = \beta_1 \int_{\mu_0}^{\mu} d\ln\mu, \quad (5.9)$$

namely

$$\frac{1}{\alpha(\mu)} = \frac{1}{\alpha_0} - \beta_1 \ln \frac{\mu}{\mu_0} \quad \Leftrightarrow \quad \alpha(\mu) = \frac{\alpha_0}{1 - \beta_1 \alpha_0 \ln \frac{\mu}{\mu_0}}. \quad (5.10)$$

When the denominator is close to unity, the solution may be expanded as

$$\alpha(\mu) \simeq \alpha_0 \left(1 + \beta_1 \alpha_0 \ln \frac{\mu}{\mu_0} + \dots \right). \quad (5.11)$$

As an example, when the Wilson coefficient $C_{e\gamma}$ is evaluated at the scale $\mu_{\text{ref}} = 150$ GeV, the active flavours are $f = \{e, \mu, \tau, u, c, d, s, b\}$ (the top quark is inactive since $m_t \simeq 172$ GeV). Consequently,

$$\sum_f N_c^f Q_f^2 = \underbrace{3 \times [1 \times (-1)^2]}_{e, \mu, \tau} + \underbrace{2 \times [3 \times (2/3)^2]}_{u, c} + \underbrace{3 \times [3 \times (-1/3)^2]}_{d, s, b} = \frac{20}{3}. \quad (5.12)$$

Hence, from the definition (5.7),

$$\beta_1 = \frac{2}{3\pi} \cdot \frac{20}{3} = \frac{40}{9\pi}. \quad (5.13)$$

Substituting this into the second form of (5.10) gives the one-loop QED running coupling,

$$\alpha(\mu) = \frac{\alpha(\mu_0)}{1 - \frac{40}{9\pi} \alpha(\mu_0) \ln \frac{\mu}{\mu_0}}. \quad (5.14)$$

5.2 One-loop RGE and solution for $C_{e\gamma}$

Finally, we determine the one-loop RGE for $C_{e\gamma}$ in the all-legs renormalisation scheme. Since $\mathcal{O}_{e\gamma} = (\bar{\ell} \sigma^{\mu\nu} P_R E) F_{\mu\nu}$, the external fields renormalise as

$$\ell_0 = \sqrt{Z_2} \ell, \quad E_0 = \sqrt{Z_2} E, \quad A_{0\mu} = \sqrt{Z_3} A_\mu. \quad (5.15)$$

It follows that, in the all-legs scheme,

$$\mathcal{O}_{0e\gamma} = (\bar{\ell}_0 \sigma^{\mu\nu} P_R E_0) F_{0\mu\nu} = (Z_2^2 Z_3)^{1/2} \mathcal{O}_{e\gamma}, \quad (5.16)$$

so the wave-function renormalisation factors of the external legs can be absorbed into the Wilson coefficient:

$$C_{0e\gamma} = Z_{e\gamma} C_{e\gamma}, \quad Z_{e\gamma} := (Z_2^2 Z_3)^{-1/2}, \quad (5.17)$$

where the operator insertion $C_{0e\gamma} \mathcal{O}_{0e\gamma} = C_{e\gamma} \mathcal{O}_{e\gamma}$ is finite. Taking the UV poles of $\delta Z_2^{(1)}$ and $\delta Z_3^{(1)}$ from (C.17) and (C.24), we obtain

$$\delta Z_2^{(1)}|_{\text{UV}} = -\frac{\alpha}{4\pi} \epsilon^{-1} Q_\ell^2, \quad \delta Z_3^{(1)}|_{\text{UV}} = -\frac{\alpha}{3\pi} \epsilon^{-1} \left(\sum_f N_c^f Q_f^2 \right) \quad (5.18)$$

Taking into account that the lepton self-energy counterterm $\delta Z_2^{(1)}$ carries the squared electric charge Q_ℓ^2 of the charged lepton, while the vacuum-polarisation counterterm $\delta Z_3^{(1)}$ contains the sum over all electrically charged species that can run in QED, eq. (5.17) implies

$$Z_{e\gamma}|_{\text{UV}} = 1 - \delta Z_2^{(1)}|_{\text{UV}} - \frac{1}{2} \delta Z_3^{(1)}|_{\text{UV}} = 1 + \frac{\alpha}{4\pi} \epsilon^{-1} Q_\ell^2 + \frac{\alpha}{6\pi} \epsilon^{-1} \left(\sum_f N_c^f Q_f^2 \right). \quad (5.19)$$

Hence, the anomalous dimension induced by $Z_{e\gamma}$ is [26, 59]

$$\gamma_{e\gamma} := \frac{1}{2} \left(\mu \frac{\partial}{\partial \mu} \ln Z_{e\gamma} \right)_{e_0, \epsilon} = \frac{1}{2} (-2) \left(\frac{\partial}{\partial \epsilon^{-1}} \right)_{e, \mu} \delta Z_{e\gamma}^{(1)} = -\frac{\alpha}{4\pi} \left(Q_\ell^2 + \frac{2}{3} \sum_f N_c^f Q_f^2 \right). \quad (5.20)$$

Acting with $\mu(d/d\mu)$ on both sides of the first relation in (5.17), at fixed e_0, ϵ , gives

$$0 = \mu \frac{d}{d\mu} (Z_{e\gamma} C_{e\gamma})_{e_0, \epsilon} = \left(\mu \frac{d}{d\mu} Z_{e\gamma} \right)_{e_0, \epsilon} C_{e\gamma} + Z_{e\gamma} \left(\mu \frac{d}{d\mu} C_{e\gamma} \right)_{e_0, \epsilon}. \quad (5.21)$$

Using the definition of $\gamma_{e\gamma}$,

$$\gamma_{e\gamma} := \frac{1}{2} \left(\mu \frac{\partial}{\partial \mu} \ln Z_{e\gamma} \right)_{e_0, \epsilon} \Rightarrow \mu \frac{d}{d\mu} Z_{e\gamma} = 2\gamma_{e\gamma} Z_{e\gamma}. \quad (5.22)$$

From (5.21) and (5.22), we obtain

$$\mu \frac{d}{d\mu} C_{e\gamma} = -2\gamma_{e\gamma} C_{e\gamma}. \quad (5.23)$$

Substituting eq. (5.20) into eq. (5.23) yields the QED one-loop RGE for the dipole coefficient $C_{e\gamma}$, consistent with the LEFT anomalous dimensions of ref. [56]:

$$\mu \frac{d}{d\mu} C_{e\gamma}(\mu) = \frac{\alpha}{2\pi} \left(Q_\ell^2 + \frac{2}{3} \sum_f N_c^f Q_f^2 \right) C_{e\gamma}(\mu). \quad (5.24)$$

As an illustration, at $\mu_{\text{ref}} = 150$ GeV one has $\sum_f N_c^f Q_f^2 = 20/3$, so the coefficient in parentheses becomes $1 + \frac{2}{3} \cdot \frac{20}{3} = \frac{49}{9}$:

$$\mu \frac{d}{d\mu} C_{e\gamma}(\mu) = \frac{49\alpha(\mu)}{18\pi} C_{e\gamma}(\mu). \quad (5.25)$$

We now express the solution of the RGE (5.24) in terms of the running coupling $\alpha(\mu)$. The one-loop RGE for α is (5.7), whose solution is given by the second relation in (5.10). Combining with (5.24) and working at one-loop accuracy,

$$\frac{d \ln C_{e\gamma}}{d \ln \mu} = \frac{\mathcal{Q}^2}{2\pi} \alpha(\mu), \quad \frac{d \ln \alpha}{d \ln \mu} = \beta_1 \alpha(\mu), \quad \mathcal{Q}^2 := Q_\ell^2 + \frac{2}{3} \sum_f N_c^f Q_f^2. \quad (5.26)$$

Therefore,

$$\frac{d \ln C_{e\gamma}}{d \ln \alpha} = \frac{\mathcal{Q}^2}{2\pi \beta_1}. \quad (5.27)$$

Since the r.h.s. is a constant, separating variables and integrating gives

$$\ln \frac{C_{e\gamma}(\mu)}{C_{e\gamma}(\mu_0)} = \frac{\mathcal{Q}^2}{2\pi \beta_1} \ln \frac{\alpha(\mu)}{\alpha(\mu_0)} \Rightarrow C_{e\gamma}(\mu) = C_{e\gamma}(\mu_0) \left[\frac{\alpha(\mu)}{\alpha(\mu_0)} \right]^{\mathcal{Q}^2/(2\pi \beta_1)}. \quad (5.28)$$

Using the one-loop running of $\alpha(\mu)$ from (5.10),

$$C_{e\gamma}(\mu) = C_{e\gamma}(\mu_0) \left[1 - \beta_1 \alpha(\mu_0) \ln \frac{\mu}{\mu_0} \right]^{-\mathcal{Q}^2/(2\pi \beta_1)}. \quad (5.29)$$

Thus the one-loop RGE admits a closed-form solution for $C_{e\gamma}(\mu)$.

6 Results II: Consistency with low-energy observables

In this section we start from the set of broken-phase neutrino dipole couplings $\{\mu_{\alpha i}\}$ that arise in electromagnetic leptogenesis and construct the Wilson coefficient $C_{e\gamma, \alpha\beta}$ of the charged-lepton dipole operator $\mathcal{O}_{e\gamma, \alpha\beta} = (\bar{\ell}_\alpha \sigma^{\mu\nu} P_R E_\beta) F_{\mu\nu}$ with right-handed charged lepton denoted by E_β . We then examine, in a quantitative and global manner, the consistency of this framework with three observables: (i) $\mu \rightarrow e\gamma$, (ii) the electron EDM d_e , and (iii) the muon anomalous magnetic moment $(g-2)_\mu$ (hereafter also denoted $\Delta a_\mu := (g-2)_\mu/2$). In this way we visualise how the baryon asymmetry generated by electromagnetic leptogenesis can coexist with bounds from low-energy experiments.

6.1 Overview

In this subsection, we restate the workflow used in this paper:

1. Upstream input (before EWSB): starting from the gauge-invariant dipole operator \mathcal{O}_{NB} obtained by UV matching, we evolve its Wilson coefficient $C_{NB}(M_\Psi)$ downwards using the one-loop RGE in the symmetric phase,

$$\mu \frac{d}{d\mu} C_{NB,\alpha i}(\mu) = -\frac{1}{16\pi^2} \left(\frac{91}{12} g_1^2 + \frac{9}{4} g_2^2 - 3y_t^2 \right) C_{NB,\alpha i}(\mu), \quad (6.1)$$

simultaneously with the SM couplings $\{g_1, g_2, g_3, y_t\}$, down to $\mu_{\text{ref}} = 150$ GeV.

2. Moving to the broken phase (near μ_{ref}): we define the broken-phase neutrino-photon dipole couplings

$$\mu_{\alpha i} = \frac{v \cos \theta_W}{\sqrt{2} M_\Psi^2} C_{NB,\alpha i}(\mu_{\text{ref}}), \quad (6.2)$$

which will later feed the generation of the charged-lepton dipoles $\mathcal{O}_{e\gamma}$.

3. One-loop operator mixing: a single insertion of \mathcal{O}_{NB} together with the SM Yukawas y_e , y_ν generates \mathcal{O}_{eB} at one loop, which is mapped to $\mathcal{O}_{e\gamma}$ after EWSB. The corresponding Wilson coefficient is

$$(C_{e\gamma}^{(1)})_{\alpha\beta}(\mu) = \frac{1}{16\pi^2} \sum_i \frac{v \cos \theta_W}{\sqrt{2} M_\Psi^2} C_{NB,\alpha i}(\mu) (y_e^\top y_\nu)_{\beta i} \left(1 - \ln \frac{M_i^2}{\mu^2} \right). \quad (6.3)$$

Furthermore, at the matching scale $\mu_{\text{ref}} = 150$ GeV we obtain

$$(C_{e\gamma}^{(1)})_{\alpha\beta}(\mu_{\text{ref}}) = \frac{1}{16\pi^2} \sum_i \mu_{\alpha i} (y_e^\top y_\nu)_{\beta i} \left(1 - \ln \frac{M_i^2}{\mu_{\text{ref}}^2} \right) \quad (6.4)$$

A single mixing generates charged-lepton-flavour-violating (CLFV) entries with $\alpha \neq \beta$.

4. Two-loop pure dipole (Barr-Zee type): in the broken phase two insertion of $\mu_{\alpha i}$ induce $\mathcal{O}_{e\gamma}$ at two loops. The result can be written as

$$(C_{e\gamma}^{(2)})_{\alpha\beta}(\mu) = \frac{5\sqrt{2} e}{(16\pi^2)^2 v^2} \delta_{\alpha\beta} \sum_{\alpha',i} |\mu_{\alpha' i}|^2 \left(Q_{\ell_\beta} - \frac{T_3 - Q_{\ell_\beta} \sin^2 \theta_W}{\cos^2 \theta_W} \right) \left(2 - \ln \frac{M_i^2}{\mu^2} \right). \quad (6.5)$$

This contribution is essentially flavour-diagonal; CLFV arises predominantly from the one-loop piece.

5. Matching of the Wilson coefficient $C_{e\gamma}$: after matching at $\mu_{\text{ref}} = 150$ GeV, we use $C_{e\gamma} = C_{e\gamma}^{(1)} + C_{e\gamma}^{(2)}$.
6. QED running in LEFT ($\mu_{\text{ref}} \sim m_Z \rightarrow m_\mu, m_e$): below the electroweak scale $\mu_{\text{ref}} = 150$ GeV or $m_Z \simeq 91.2$ GeV, the relevant RGE in LEFT reads

$$\mu \frac{d}{d\mu} C_{e\gamma}(\mu) = \frac{\alpha(\mu)}{2\pi} \left(Q_\ell^2 + \frac{2}{3} \sum_f N_c^f Q_f^2 \right) C_{e\gamma}(\mu). \quad (6.6)$$

At $\mu_{\text{ref}} = 150$ GeV, one has $\frac{2}{3} \sum_f N_c^f Q_f^2 = \frac{40}{9}$. In Part III, although a two-loop contribution to the Wilson coefficient $C_{e\gamma}^{(2)}$ as in eq. (6.5) is included, its running is taken to be governed by the one-loop RGE (6.6).

7. Comparison between theory and experiment: we take as a common horizontal axis the effective electromagnetic neutrino mass $\tilde{m}_1^{\text{EM}} \propto K_1$, and confront the allowed region from the low-energy observables

$$\begin{aligned} \text{BR}(\mu \rightarrow e\gamma) &\propto |(C_{e\gamma})_{e\mu}(m_\mu)|^2 + |(C_{e\gamma})_{\mu e}(m_\mu)|^2, \\ d_e &\propto \text{Im}(C_{e\gamma})_{ee}(m_e), \quad \Delta a_\mu \propto \text{Re}(C_{e\gamma})_{\mu\mu}(m_\mu), \end{aligned} \quad (6.7)$$

with the region preferred by the BAU. In our analysis we use the symmetric-phase one-loop EFT RGE (6.1) for $\mu \geq \mu_{\text{ref}} = 150$ GeV, and the broken-phase one-loop QED RGE (6.6) for $\mu \leq \mu_{\text{ref}}$.

6.2 Theory of low-energy observables

6.2.1 Branching ratio of $\mu \rightarrow e\gamma$

In LEFT the relevant effective interaction is

$$-\mathcal{L}_{\text{LEFT}} \supset (C_{e\gamma})_{e\mu}(\bar{e}\sigma^{\mu\nu}P_R\mu)F_{\mu\nu} + (C_{e\gamma})_{\mu e}(\bar{e}\sigma^{\mu\nu}P_L\mu)F_{\mu\nu}. \quad (6.8)$$

Inserting the on-shell photon field strength $F_{\mu\nu} \rightarrow i(q_\mu\varepsilon_\nu - q_\nu\varepsilon_\mu)$, with $\varepsilon \cdot q = 0$, the tree-level amplitude for $\mu \rightarrow e\gamma$ becomes

$$i\mathcal{M} = 2i\varepsilon_\mu^*(q)q_\nu\bar{u}_e(p)[(C_{e\gamma})_{e\mu}\sigma^{\mu\nu}P_R + (C_{e\gamma})_{\mu e}\sigma^{\mu\nu}P_L]u_\mu(k), \quad (6.9)$$

where k and p denote the incoming muon and outgoing electron four-momenta, respectively. After taking the absolute square, averaging over the initial spin and summing over the final polarisations, one finds

$$|\mathcal{M}|^2 = -2q_\nu q_\beta \text{tr}[\not{p}(A\sigma^{\mu\nu}P_R + B\sigma^{\mu\nu}P_L)(\not{k} + m_\mu)(A^*\sigma_\mu^\beta P_L + B^*\sigma_\mu^\beta P_R)], \quad (6.10)$$

with $A := (C_{e\gamma})_{e\mu}$ and $B := (C_{e\gamma})_{\mu e}$. Here, we have taken $m_e \rightarrow 0$. Using $[\sigma^{\mu\nu}, \gamma_5] = 0$, one has $\sigma^{\mu\nu}P_R = P_R\sigma^{\mu\nu}$ and $\sigma^{\mu\nu}P_L = P_L\sigma^{\mu\nu}$. Rearranging the trace in the second line of eq. (6.10), we obtain

$$\text{tr}[\dots] = \frac{|A|^2 + |B|^2}{2} \text{tr}(\not{p}\sigma^{\mu\nu}\not{k}\sigma_\mu^\beta). \quad (6.11)$$

Here $P_{R,L} = (1 \pm \gamma_5)/2$, and we used the vanishing of traces with an odd number of γ matrices (including one γ_5):

$$\text{tr}(\not{p}\sigma^{\mu\nu}\sigma_\mu^\beta) = 0, \quad \text{tr}(\not{p}\sigma^{\mu\nu}\sigma_\mu^\beta\gamma_5) = 0. \quad (6.12)$$

Employing the identities

$$[\gamma^\rho, \sigma^{\mu\nu}] = 2i(g^{\rho\mu}\gamma^\nu - g^{\rho\nu}\gamma^\mu), \quad (6.13)$$

$$\sigma^{\mu\nu}\sigma_\mu^\beta = 3g^{\nu\beta} - 2i\sigma^{\nu\beta}, \quad (6.14)$$

$$\text{tr}(\gamma^\rho\gamma^\sigma\sigma^{\alpha\beta}) = 4i(g^{\rho\beta}g^{\sigma\alpha} - g^{\rho\alpha}g^{\sigma\beta}), \quad (6.15)$$

we find

$$\text{tr}(\not{p}\sigma^{\mu\nu}\not{k}\sigma_\mu^\beta) = 4\left[g^{\nu\beta}(k\cdot p) - 2(k^\nu p^\beta + k^\beta p^\nu)\right]. \quad (6.16)$$

Substituting (6.16) into (6.11) gives

$$\text{tr}[\dots] = 2(|A|^2 + |B|^2)\left[g^{\nu\beta}(k\cdot p) - 2(k^\nu p^\beta + k^\beta p^\nu)\right]. \quad (6.17)$$

Inserting this back into (6.10), we obtain

$$\overline{|\mathcal{M}|^2} = 16(k\cdot q)^2(|A|^2 + |B|^2), \quad (6.18)$$

where we used momentum conservation $k = p + q$ as well as $(k - q)^2 = p^2 = m_e^2$, so that $k\cdot q = (m_\mu^2 - m_e^2)/2 \simeq m_\mu^2/2$ in the limit $m_e \rightarrow 0$. Hence,

$$\overline{|\mathcal{M}|^2} = 16\left(\frac{m_\mu^2}{2}\right)^2(|A|^2 + |B|^2) = 4m_\mu^4\left[|(C_{e\gamma})_{e\mu}(m_\mu)|^2 + |(C_{e\gamma})_{\mu e}(m_\mu)|^2\right]. \quad (6.19)$$

With $\|\mathbf{q}\| = m_\mu/2$ and the two-body phase-space factor $\Phi_2 = \|\mathbf{q}\|/(8\pi m_\mu^2)$, the partial width reads [60]

$$\Gamma(\mu \rightarrow e\gamma) = \frac{\overline{|\mathcal{M}|^2}}{16\pi m_\mu} = \frac{m_\mu^3}{4\pi}\left[|(C_{e\gamma})_{e\mu}(m_\mu)|^2 + |(C_{e\gamma})_{\mu e}(m_\mu)|^2\right]. \quad (6.20)$$

At low energies the dominant muon decay is $\mu^- \rightarrow e^-\bar{\nu}_e\nu_\mu$, described by the charged-current Lagrangian

$$-\mathcal{L}_{\text{CC}} = \frac{g_w}{\sqrt{2}}[\bar{e}\gamma^\alpha(1 - \gamma_5)\nu_e + \bar{\nu}_\mu\gamma^\alpha(1 - \gamma_5)\mu]W_\alpha^- + \text{h.c.} \quad (6.21)$$

Here, we define the Fermi coupling constant G_F by $\frac{G_F}{\sqrt{2}} := \frac{g_w^2}{8M_W^2}$ with the weak coupling constant g_w and the mass of the W boson M_W . Neglecting the electron mass gives the total width [61]

$$\Gamma_\mu^{\text{SM}}(\mu \rightarrow e\nu\bar{\nu}) = \frac{G_F^2 m_\mu^5}{192\pi^3}. \quad (6.22)$$

Combining eqs. (6.20) and (6.22), the branching ratio becomes

$$\text{BR}(\mu \rightarrow e\gamma) = \frac{\Gamma(\mu \rightarrow e\gamma)}{\Gamma_\mu^{\text{SM}}} = \frac{48\pi^2}{G_F^2 m_\mu^2}\left[|(C_{e\gamma})_{e\mu}(m_\mu)|^2 + |(C_{e\gamma})_{\mu e}(m_\mu)|^2\right]. \quad (6.23)$$

6.2.2 Electron EDM

The LEFT effective Lagrangian containing the EDM term can be written as

$$\begin{aligned} -\mathcal{L}_{\text{LEFT}} &\supset C_{ee}\bar{e}\sigma^{\mu\nu}P_R eF_{\mu\nu} + C_{ee}^*\bar{e}\sigma^{\mu\nu}P_L eF_{\mu\nu} \\ &= \frac{1}{2}(C_{ee} + C_{ee}^*)\bar{e}\sigma^{\mu\nu}eF_{\mu\nu} + \frac{1}{2}(C_{ee} - C_{ee}^*)\bar{e}\sigma^{\mu\nu}\gamma_5 eF_{\mu\nu} \\ &= \text{Re } C_{ee}\bar{e}\sigma^{\mu\nu}eF_{\mu\nu} + i\text{Im } C_{ee}\bar{e}\sigma^{\mu\nu}\gamma_5 eF_{\mu\nu}, \end{aligned} \quad (6.24)$$

where we have defined $C_{ee} := (C_{e\gamma})_{ee}$ and $P_{R,L} = (1 \pm \gamma_5)/2$. The standard definition of the EDM is [62]

$$\mathcal{L}_{\text{EDM}} = -\frac{i}{2}d_e\bar{e}\sigma^{\mu\nu}\gamma_5 eF_{\mu\nu}. \quad (6.25)$$

Matching the two expressions yields

$$d_e(\mu = m_e) = 2|\text{Im}(C_{e\gamma})_{ee}(m_e)|. \quad (6.26)$$

The overall sign is convention-dependent, so absolute values are compared in practice. When evaluating (6.26) numerically, convert the result from natural units [GeV^{-1}] to [cm] by multiplying with $\hbar c = 1.97327 \times 10^{-14} \text{ GeV cm}$.

6.2.3 Anomalous magnetic moments

With the effective interaction

$$\mathcal{L}_{\text{MDM}} = \frac{e}{4m_\ell} a_\ell \bar{\ell} \sigma^{\mu\nu} \ell F_{\mu\nu}, \quad a_\ell = a_\ell^{\text{SM}} + \Delta a_\ell, \quad (6.27)$$

and the LEFT Lagrangian

$$-\mathcal{L}_{\text{LEFT}} \supset \text{Re}(C_{e\gamma})_{\ell\ell} \bar{\ell} \sigma^{\mu\nu} \ell F_{\mu\nu}, \quad (6.28)$$

one finds [63]

$$\Delta a_\ell = \frac{4m_\ell}{e} \text{Re}(C_{e\gamma})_{\ell\ell}(m_\ell), \quad \ell = e, \mu. \quad (6.29)$$

In this work, we consider the muon anomalous magnetic moment ($\ell = \mu$).

6.3 Comparison with the observations

In this subsection, we study how the three low-energy observables

$$\text{BR}(\mu \rightarrow e\gamma), \quad |d_e|, \quad |\Delta a_\mu|, \quad (6.30)$$

depend on \tilde{m}_1^{EM} , and we analytically estimate the sizes of the theoretical curves relative to the corresponding experimental bounds for (i) standard parameter values and (ii) parameter values near theoretical limits. As derived in sec. 6.2, each observable scales with the components of the Wilson coefficient $C_{e\gamma}$ according to

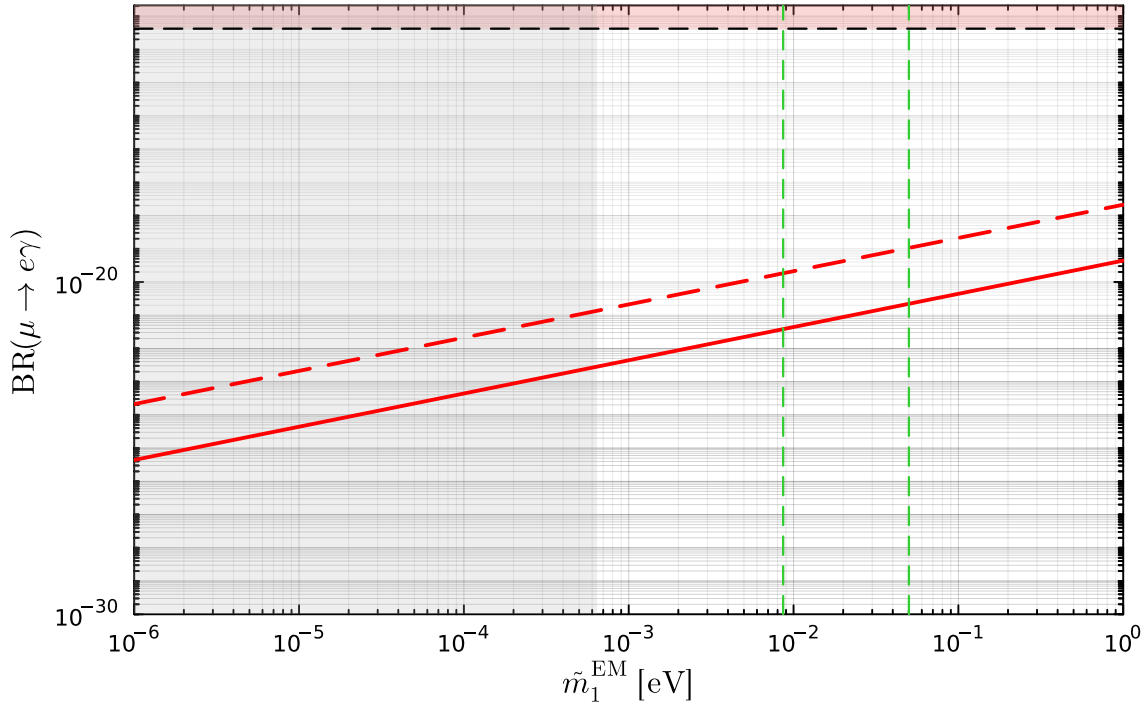
$$\begin{aligned} \text{BR}(\mu \rightarrow e\gamma) &\propto |(C_{e\gamma})_{e\mu}(m_\mu)|^2 + |(C_{e\gamma})_{\mu e}(m_\mu)|^2, \\ |d_e| &\propto |\text{Im}(C_{e\gamma})_{ee}(m_e)|, \\ |\Delta a_\mu| &\propto |\text{Re}(C_{e\gamma})_{\mu\mu}(m_\mu)|. \end{aligned} \quad (6.31)$$

On the other hand, by definition the effective electromagnetic neutrino mass on the horizontal axis is

$$\tilde{m}_1^{\text{EM}} = v^2 M_1 \sum_\alpha |\mu_{\alpha 1}|^2 \propto \frac{v^4 M_1}{M_\Psi^4} |C_{NB}(\mu_{\text{ref}})|^2, \quad (6.32)$$

so that, through the chain $C_{NB} \rightarrow C_{e\gamma}$, the relations in (6.31) inherit a dependence on \tilde{m}_1^{EM} .

CLFV : $\mu \rightarrow e\gamma$



eEDM

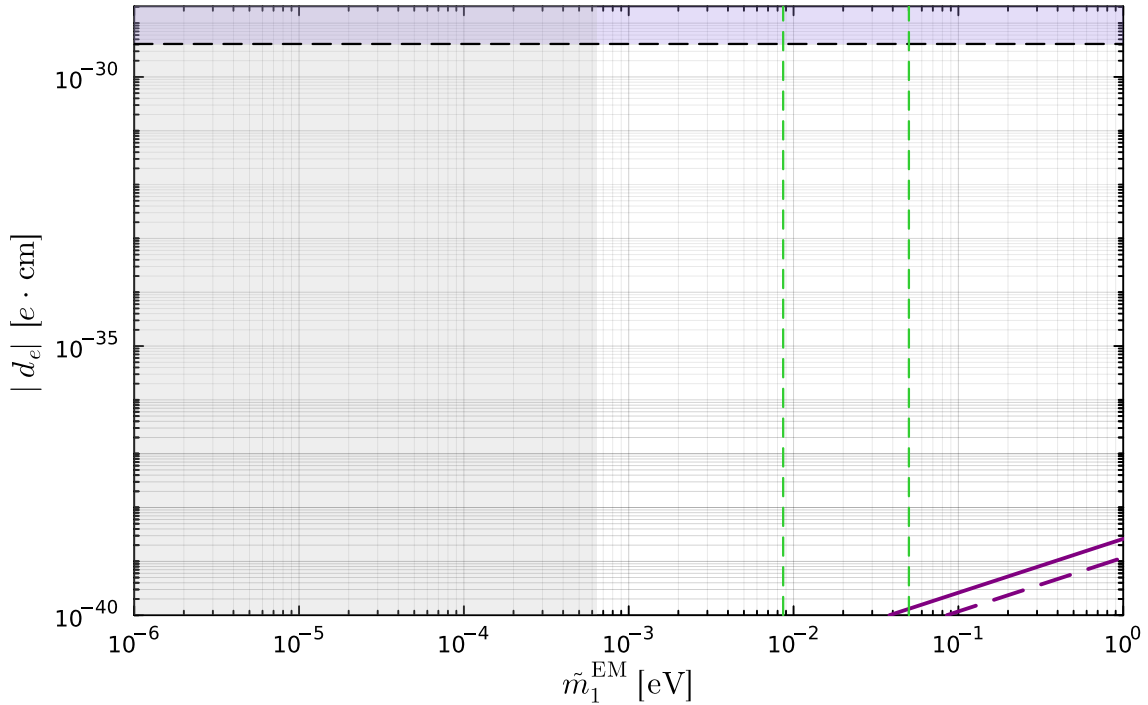


Figure 5. Comparison between the theoretical lines for the low-energy observables at the standard parameter choice (solid lines) and at the extreme benchmark (dashed lines), and the corresponding experimental bounds, where the region above each black dashed line is excluded. The theoretical lines are computed within the effective field theory derived from our UV model, and the experimental constraints are shown as rectangles with the same colour as their corresponding lines. (continued below)

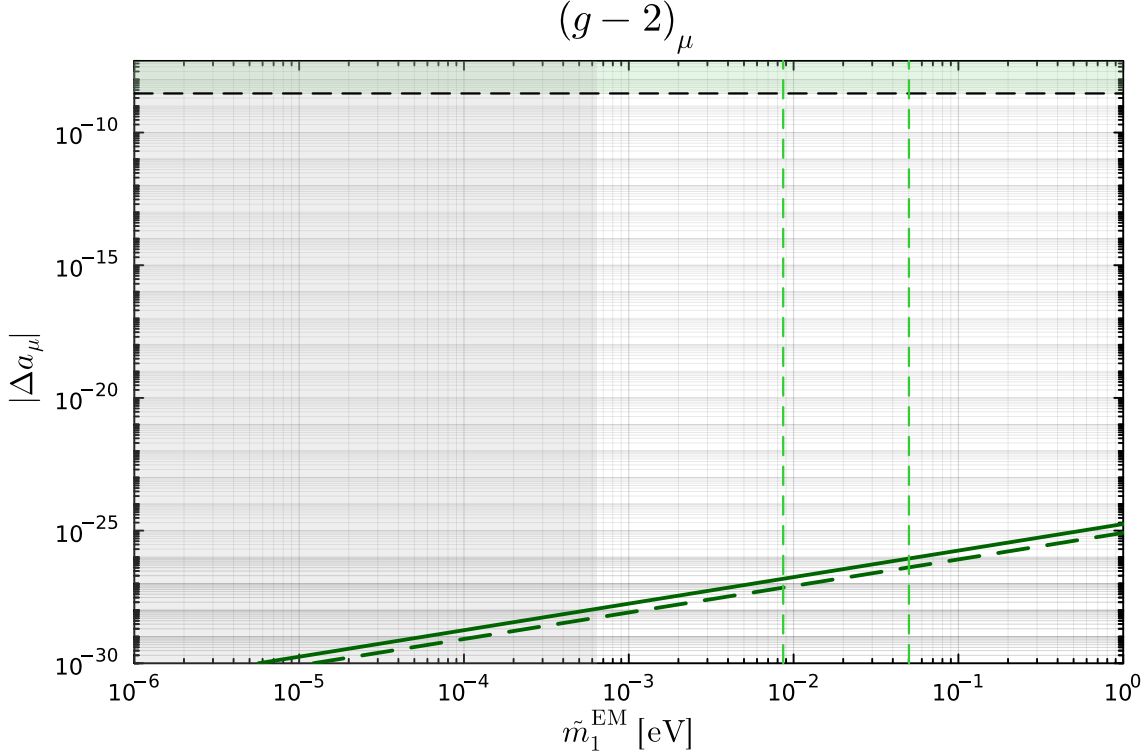


Figure 5. (continued) The gray rectangle denotes the parameter region $\tilde{m}_1^{\text{EM}} \lesssim 6.4 \times 10^{-4}$ eV in which resonant electromagnetic leptogenesis fails to reproduce the observed BAU, while the green dashed lines indicate, as in Parts I and II, the range of \tilde{m}_1^{EM} suggested by neutrino-oscillation observations. In the region where the observed BAU can be reproduced, the theoretical lines for $\text{BR}(\mu \rightarrow e\gamma)$, $|d_e|$, and $|\Delta a_\mu|$, given in eqs. (6.23), (6.26), and (6.29), lie well below the experimental upper limits in eq. (6.34) for both benchmarks and therefore satisfy all present observational bounds. Unlike the case of the light-neutrino Majorana mass discussed in sec. 3, none of the lines at the extreme benchmark crosses its experimental bound. For both $|d_e|$ and $|\Delta a_\mu|$, the enhancement at the extreme benchmark is even smaller than in the standard-parameter case.

6.3.1 Comparison for standard parameter choice

For the standard benchmark adopted in sec. 3.4.1,

$$(M_1, M_2, M_S, M_\Psi) \simeq (0.5, 0.5, 8, 10) \text{ TeV}, \quad |\lambda| \sim \mathcal{O}(10^{-2}), \quad |y_{\alpha j}| \sim \mathcal{O}(10^{-3}), \quad (6.33)$$

the low-energy observables are represented analytically by the straight lines shown in fig. 5. The experimental upper limits, plotted as the corresponding rectangular exclusion regions in those figures, are [20–22, 63]

$$\begin{aligned} \text{BR}(\mu \rightarrow e\gamma)_{\text{max}} &= 1.5 \times 10^{-13}, & \text{(MEG II Collaboration),} \\ |d_e|_{\text{max}} &= 4.1 \times 10^{-30} \text{ e cm}, & \text{(JILA Collaboration),} \\ |\Delta a_\mu|_{\text{max}} &= 3.0 \times 10^{-9}, & \text{(Muon } g-2 \text{ Collaboration).} \end{aligned} \quad (6.34)$$

Since, for all three observables, the theoretical lines lie below the excluded bands throughout the \tilde{m}_1^{EM} range, electromagnetic leptogenesis is consistent with current experimental

constraints—apart from the gray region corresponding to $\tilde{m}_1^{\text{EM}} \lesssim 6.4 \times 10^{-4}$ eV, where the produced BAU falls below the observed value. The vertical dashed green lines show the oscillation-motivated neutrino-mass window [44] as in Parts I and II.

As for the muon anomalous magnetic moment, the measurement by the Muon $g - 2$ Collaboration [22] reads

$$a_\mu^{\text{exp}} = 116\,592\,059(22) \times 10^{-11}, \quad (6.35)$$

while the Standard Model prediction currently available is [63]

$$a_\mu^{\text{SM}} = 116\,591\,810(43) \times 10^{-11}. \quad (6.36)$$

Taking the difference yields

$$\begin{aligned} |\Delta a_\mu|_{\text{obs}} &= a_\mu^{\text{exp}} - a_\mu^{\text{SM}} = [116\,592\,059(22) - 116\,591\,810(43)] \times 10^{-11} \\ &= 249 \times 10^{-11} \pm \sqrt{22^2 + 43^2} \times 10^{-11} \\ &\simeq (2.49 \pm 0.48) \times 10^{-9}, \end{aligned} \quad (6.37)$$

where the uncertainty at 1σ is obtained by adding the experimental and theoretical errors in quadrature. This band can be used as a target for potential UV completions. In particular, even if our prediction lies well below the observed discrepancy (fig. 5), the model is not excluded by the $(g - 2)_\mu$ data.

6.3.2 Comparison for parameter values near theoretical limits

We next consider the same extreme benchmark as in sec. 3.4.2,

$$(M_1, M_2, M_S, M_\Psi) = (0.3, 0.3, 1, 3) \text{ TeV}, \quad |\lambda| \sim \mathcal{O}(1), \quad |y_{\alpha j}| \sim \mathcal{O}(10^{-2}). \quad (6.38)$$

The theoretical lines and experimental bounds are displayed in fig. 5. None of the theoretical lines enters the excluded regions; in fact, for the eEDM and $|\Delta a_\mu|$ the theory lines lie well on the “safe side”, even farther from the experimental limits. Thus, unlike the situation in sec. 3.4 where observational constraints could be violated, no such tension appears here. Let us understand why.

Our low-energy observables are controlled by the charged-lepton dipole operator through $C_{e\gamma}$, which is the sum of the one-loop operator mixing and the two-loop pure-dipole (Barr–Zee type) contribution:

$$C_{e\gamma} = C_{e\gamma}^{(1)} + C_{e\gamma}^{(2)}. \quad (6.39)$$

Both pieces are loop-suppressed and involve small Yukawa couplings. In fact, from (6.4) and (6.5) one has, schematically,

$$\begin{aligned} (C_{e\gamma}^{(1)})_{\alpha\beta}(\mu_{\text{ref}}) &\propto \frac{1}{16\pi^2} \sum_i \mu_{\alpha i} (y_e^\top y_\nu)_{\beta i} \left(1 - \ln \frac{M_i^2}{\mu_{\text{ref}}^2} \right), \\ (C_{e\gamma}^{(2)})_{\alpha\beta}(\mu_{\text{ref}}) &\propto \frac{e}{(16\pi^2)^2 v^2} \delta_{\alpha\beta} \sum_{\alpha',i} |\mu_{\alpha' i}|^2 \left(2 - \ln \frac{M_i^2}{\mu_{\text{ref}}^2} \right), \end{aligned} \quad (6.40)$$

so that the one-loop term carries a factor $1/(16\pi^2)$ and is further suppressed by $\mu_{\alpha i}$ and Yukawa couplings, while the two-loop term scales as $1/[(16\pi^2)^2 v^2]$ and with $\sum_{\alpha',i} |\mu_{\alpha'i}|^2$. Since the horizontal axis behaves as $\tilde{m}_1^{\text{EM}} \propto \sum |\mu_{\alpha 1}|^2$, and for our benchmarks one flavour combination dominates the sum, the overall growth of $C_{e\gamma}$ with \tilde{m}_1^{EM} is at most

$$C_{e\gamma}^{(1)} \propto \sqrt{\tilde{m}_1^{\text{EM}}}, \quad C_{e\gamma}^{(2)} \propto \tilde{m}_1^{\text{EM}}. \quad (6.41)$$

Consequently, even at the extreme benchmark, the induced effects remain modest and the theoretical lines fail to reach the experimentally excluded regions in fig. 5.

A crucial point is that the coefficient $C_{e\gamma}(q^2 = 0)$, which controls the low-energy dipole observables, does not experience the resonant enhancement. The width-regularised pole in the right-handed neutrino self-energy amplifies the CP-violating decay rate and hence the baryon asymmetry, but the on-shell photon vertex is analytic at the resonance and therefore does not inherit this pole. As a result, the baryon asymmetry can be resonantly enhanced without driving the low-energy observables to unacceptably large values.

6.4 Quantitative explanation of the robustness of EMLG

The effective electromagnetic neutrino mass \tilde{m}_1^{EM} that appears in electromagnetic leptogenesis controls the size of the low-energy dipole interactions. With only mild QED running, the low-energy effects arise either from one-loop operator mixing, which scales as $\sqrt{\tilde{m}_1^{\text{EM}}}$, or from two-loop Barr-Zee-type graphs, which scale linearly with \tilde{m}_1^{EM} . We derive analytic upper bounds for $\text{BR}(\mu \rightarrow e\gamma)$, $|d_e|$ and $|\Delta a_\mu|$, and show that they lie well below current sensitivities in the parameter regions compatible with the BAU.

In the EFT description of EMLG, the Wilson coefficient of the dipole operator in LEFT is the sum of the one-loop mixing before EWSB and the two-loop pure-dipole term after EWSB,

$$C_{e\gamma} = C_{e\gamma}^{(1)} + C_{e\gamma}^{(2)}. \quad (6.42)$$

Both pieces admit analytic upper bounds. Writing them in terms of the quantity $\tilde{m}_1^{\text{EM}} := v^2 M_i \sum |\mu_{\alpha i}|^2$ defined in eq. (6.32), focusing for definiteness on the first heavy neutrino N_1 , one obtains theory estimates well separated from the present sensitivities (LFV/EDM/ $g - 2$).

6.4.1 Analytical upper bound for $\text{BR}(\mu \rightarrow e\gamma)$

From eq. (6.3), the one-loop mixing contribution at a generic scale μ reads

$$C_{e\gamma}^{(1)}(\mu) = \frac{1}{16\pi^2} \frac{v \cos \theta_W}{\sqrt{2} M_\Psi^2} C_{NB,\alpha 1}(\mu) (y_e^\intercal y_\nu)_{\beta 1} \left(1 - \ln \frac{M_1^2}{\mu^2} \right). \quad (6.43)$$

Taking the absolute value and using the spectral norm, we obtain

$$|C_{e\gamma}^{(1)}(\mu)| \leq \frac{c_1(\mu)}{16\pi^2} \frac{v \cos \theta_W}{\sqrt{2} M_\Psi^2} C_{NB,\alpha 1}(\mu) \|y_e y_\nu\|_2 \left(\sum_\alpha |y_{\alpha 1}|^2 \right)^{1/2}, \quad c_1(\mu) := \left| 1 - \ln \frac{M_1^2}{\mu^2} \right|. \quad (6.44)$$

Using the sub-multiplicativity $\|y_e y_\nu\|_2 \leq \|y_e\|_2 \|y_\nu\|_2$ and $\|y_e\|_2 = \max\{|y_e|, |y_\mu|, |y_\tau|\} = |y_\tau| \simeq \sqrt{2} m_\tau / v$, and evaluating the bound at $\mu = \mu_{\text{ref}}$, we obtain

$$|C_{e\gamma}^{(1)}(\mu_{\text{ref}})| \leq \frac{c_1(\mu_{\text{ref}})}{16\pi^2} \mu_{\alpha 1} \frac{\sqrt{2} m_\tau}{v} \|y_\nu\|_2 \left(\frac{\tilde{m}_1^{\text{EM}}}{v^2 M_1} \right)^{1/2}, \quad (6.45)$$

where we have used the definition (6.2) and $\sum |\mu_{\alpha 1}|^2 = \tilde{m}_1^{\text{EM}} / (v^2 M_1)$.

In order to compare with the $\mu \rightarrow e\gamma$ observations, we need the coefficient evaluated at the muon scale $\mu = m_\mu$. The QED RGE in LEFT, eq. (6.6), implies a simple multiplicative running

$$C_{e\gamma}(m) = \mathcal{R}(m, \mu_{\text{ref}}) C_{e\gamma}(\mu_{\text{ref}}), \quad (6.46)$$

with

$$\mathcal{R}(m, \mu_{\text{ref}}) := \exp \left[\int_{\mu_{\text{ref}}}^m \frac{d\mu'}{\mu'} \frac{\alpha(\mu')}{2\pi} \left(Q_\ell^2 + \frac{2}{3} \sum_f N_c^f Q_f^2 \right) \right]. \quad (6.47)$$

Approximating α and the flavour-universal charge factor in the exponent as constants over the relatively short running interval between μ_{ref} and m_ℓ ($\ell = e, \mu$) gives

$$\mathcal{R}(m, \mu_{\text{ref}}) \simeq \left(\frac{m}{\mu_{\text{ref}}} \right)^\kappa, \quad \kappa := \frac{\alpha}{2\pi} \left(Q_\ell^2 + \frac{2}{3} \sum_f N_c^f Q_f^2 \right) \simeq 6 \times 10^{-3}. \quad (6.48)$$

Hence, $|\mathcal{R}(m_e, \mu_{\text{ref}})| \simeq 0.92$ and $|\mathcal{R}(m_\mu, \mu_{\text{ref}})| \simeq 0.95$; the running induces only a few-to-ten-per-cent rescaling. In what follows we therefore evaluate $C_{e\gamma}^{(1)}(m_\mu)$ and $C_{e\gamma}^{(2)}(m_e)$ at μ_{ref} and, for analytic bounds, set $|\mathcal{R}| \simeq 1$; keeping \mathcal{R} would simply multiply the bounds below by an $\mathcal{O}(1)$ factor. Inserting the bound (6.45) into (6.23) yields

$$\text{BR}(\mu \rightarrow e\gamma) \lesssim \frac{48\pi^2}{G_F^2 m_\mu^2} \left[\frac{c_1(\mu_{\text{ref}})}{16\pi^2} \frac{\sqrt{2} m_\tau}{v} \|y_\nu\|_2 \right]^2 \left(\frac{\tilde{m}_1^{\text{EM}}}{v^2 M_1} \right). \quad (6.49)$$

Substituting the typical numerical values $G_F = 1.1664 \times 10^{-5}$ GeV $^{-2}$, $m_\mu = 0.10566$ GeV, $m_\tau = 1.77682$ GeV, $c_1(\mu_{\text{ref}}) = |1 - \ln(500^2/150^2)| \simeq 1.41$, and $v = 246$ GeV, the CLFV upper bound becomes

$$\text{BR}(\mu \rightarrow e\gamma) \lesssim 8.6 \times 10^{-17} \left(\frac{c_1}{1.41} \right)^2 \left(\frac{\|y_\nu\|_2}{10^{-2}} \right)^2 \left(\frac{500 \text{ GeV}}{M_1} \right) \left(\frac{\tilde{m}_1^{\text{EM}}}{0.01 \text{ eV}} \right). \quad (6.50)$$

This is more than three orders of magnitude below the current upper limit 1.5×10^{-13} [20] (MEG II Collaboration).

6.4.2 Analytical upper bound for $|d_e|$, $|\Delta a_\mu|$

From the broken-phase result (6.5), we have

$$(C_{e\gamma}^{(2)})_{\beta\beta}(\mu) = \frac{5\sqrt{2} e}{(16\pi^2)^2 v^2} \left[\sum_\alpha \mu_{\alpha 1}^2 g_{\ell_\beta} \left(2 - \ln \frac{M_1^2}{\mu^2} \right) \right]. \quad (6.51)$$

Using (6.32), $\sum |\mu_{\alpha 1}|^2 = \tilde{m}_1/(v^2 M_1)$, and taking absolute values we obtain

$$|(C_{e\gamma}^{(2)})_{\beta\beta}(\mu)| \leq \frac{5\sqrt{2}e}{(16\pi^2)^2} |g_{\ell_\beta}| c_2(\mu) \left(\frac{\tilde{m}_1^{\text{EM}}}{v^4 M_1} \right), \quad c_2(\mu) := \left| 2 - \ln \frac{M_1^2}{\mu^2} \right|, \quad (6.52)$$

which shows that the two-loop contribution grows only linearly with \tilde{m}_1^{EM} .

The eEDM bound follows from (6.26):

$$|d_e| = 2|C_{ee}(m_e)|(\hbar c) \leq \frac{10\sqrt{2}e}{(16\pi^2)^2} |\mathcal{R}(m_e, \mu_{\text{ref}})| |g_{\ell_\beta}| c_2(\mu_{\text{ref}}) \left(\frac{\tilde{m}_1^{\text{EM}}}{v^4 M_1} \right) (\hbar c). \quad (6.53)$$

Using $\hbar c = 1.97327 \times 10^{-14}$ GeV cm, $v = 246$ GeV, $e = \sqrt{4\pi\alpha} = 0.3028$ and $|g_{\ell_\beta}| \simeq 0.650$, and taking $c_2(\mu_{\text{ref}}) = |2 - \ln(500^2/150^2)| \simeq 0.408$, we obtain

$$|d_e| \lesssim 4.9 \times 10^{-42} e \text{ cm} \left(\frac{c_2}{0.408} \right) \left(\frac{|g_{\ell_\beta}|}{0.650} \right) \left(\frac{500 \text{ GeV}}{M_1} \right) \left(\frac{\tilde{m}_1^{\text{EM}}}{0.01 \text{ eV}} \right), \quad (6.54)$$

which is twelve orders of magnitude below the present bound $4.1 \times 10^{-30} e \text{ cm}$ [21] (JILA Collaboration).

Finally, inserting the same bound into (6.29) gives for the muon anomalous magnetic moment

$$|\Delta a_\mu| = \frac{4m_\mu}{e} |\text{Re } C_{\mu\mu}(m_\mu)| \leq \frac{20\sqrt{2}}{(16\pi^2)^2} m_\mu |g_{\ell_\mu}| c_2(\mu_{\text{ref}}) \left(\frac{\tilde{m}_1^{\text{EM}}}{v^4 M_1} \right), \quad (6.55)$$

and therefore

$$|\Delta a_\mu| \leq 1.7 \times 10^{-28} \left(\frac{c_2}{0.408} \right) \left(\frac{|g_{\ell_\beta}|}{0.650} \right) \left(\frac{500 \text{ GeV}}{M_1} \right) \left(\frac{\tilde{m}_1^{\text{EM}}}{0.01 \text{ eV}} \right), \quad (6.56)$$

more than nineteen orders of magnitude below the upper edge of the currently allowed band $|\Delta a_\mu|_{\text{max}} = 3.0 \times 10^{-9}$ [22, 63] (Muon $g-2$ Collaboration).

6.5 Summary of Results II

The low-energy implications of electromagnetic leptogenesis are governed by the same dipole texture that sources the baryon asymmetry. The relevant LEFT coefficient $C_{e\gamma}$ receives only a one-loop mixing contribution and a two-loop Barr–Zee–type term, both of which are suppressed by loop factors $(16\pi^2)^{-1}$, by powers of v^{-2} , and by M_1^{-1} , so that they remain small even at the resonant value of the parameters. Since the low-energy dipole observables scale at most as $\sqrt{\tilde{m}_1^{\text{EM}}}$ (from $C_{e\gamma}^{(1)}$) or linearly with \tilde{m}_1^{EM} (from $C_{e\gamma}^{(2)}$), even for the largest values of \tilde{m}_1^{EM} compatible with successful electromagnetic leptogenesis, the predicted CLFV, eEDM, and $(g-2)_\mu$ signals remain many orders of magnitude below current experimental sensitivities. The additional QED running between μ_{ref} and $m_{e,\mu}$ merely induces an $\mathcal{O}(1)$ rescaling and does not modify these conclusions.

7 Discussion and outlook

7.1 Lessons from Parts I–III and the EFT pipeline

In this work, we have completed a three-part, EFT-consistent analysis of electromagnetic leptogenesis (EMLG). In Part I, we embedded the Bell–Kayser–Law formalism [12] into the gauge-invariant operator

$$\mathcal{O}_{NB} = (\bar{L}\sigma^{\mu\nu}P_R N)\tilde{H}B_{\mu\nu}, \quad (7.1)$$

matched its Wilson coefficient at one loop and evolved it to the electroweak scale. Gauge invariance forces a Higgs insertion, so that the broken-phase dipole scales as

$$\mu_{\alpha i} \propto \frac{1}{16\pi^2} \frac{v}{M_\Psi^2}, \quad (7.2)$$

which in turn implies that both the CP-violating sources and the washout rates scale as μ^2 . In the non-resonant, hierarchical regime, this “production and washout in lockstep” drives the freeze-out baryon asymmetry down to $Y_B^{\text{FO}} \lesssim 10^{-17}$, far below the observed value $Y_B^{\text{obs}} \simeq 8.7 \times 10^{-11}$ [23].

Part II demonstrated that this structural suppression can be overcome once the right-handed neutrinos become quasi-degenerate and the CP asymmetries are computed with the Pilaftsis–Underwood resummation [15]. In the limit $|M_2 - M_1| \sim \Gamma_2/2$, the self-energy contribution develops a Breit–Wigner enhancement while the washout saturates, allowing us to reach $Y_B^{\text{FO}} \gtrsim 10^{-9}$ across the oscillation-motivated window for the effective mass \tilde{m}_1^{EM} . As shown in Part II, a Froggatt–Nielsen charge assignment [64] in the UV Yukawa sector naturally realises the dipole texture $\{\mu_{\alpha i}\}$ and the quasi-degenerate right-handed neutrino spectrum required for resonance, while keeping all couplings perturbative.

Part III closes the EFT pipeline by confronting the same dipole texture with light-neutrino masses and low-energy observables. The central message is that, in the region of parameter space where resonant EMLG accounts for the observed BAU, the induced contributions to m_ν , $\text{BR}(\mu \rightarrow e\gamma)$, $|d_e|$, and $|\Delta a_\mu|$ are either negligible or, in extreme corners of parameter space, only in mild tension with the cosmological bound on $\sum m_\nu$.

Throughout this work we use the BAU-compatible window in \tilde{m}_i^{EM} derived in Part II. That analysis was performed in a broken-phase, dipole-decay-dominated setup with Maxwell–Boltzmann statistics, a fully flavoured spectator treatment and an instantaneous electroweak crossover, while $2 \leftrightarrow 2$ scatterings mediated by \mathcal{O}_{NB} were neglected; these approximations are expected to induce only $\mathcal{O}(1)$ uncertainties in Y_B^{FO} .

7.2 Interplay of baryogenesis, light-neutrino masses, and low-energy observables

The results of secs. 3 and 6 highlight that the entire phenomenology of our EMLG setup is controlled by a single object—the dipole texture $\{\mu_{\alpha i}\}$. Two insertions of \mathcal{O}_{NB} generate a light Majorana mass at one loop and it scales as

$$(m_\nu)_{\alpha\beta} \sim \frac{1}{16\pi^2} \sum_i \mu_{\alpha i} \mu_{\beta i} M_i^3. \quad (7.3)$$

Using the explicit relation $\mu \rightarrow v C_{NB}/M_\Psi^2$ and our one-loop matching for C_{NB} , this contribution is strongly suppressed and remains well below the observed neutrino mass scale throughout the parameter space relevant for EMLG.

On the other hand, the low-energy observables probe the same texture through the LEFT dipole coefficient

$$C_{e\gamma} = C_{e\gamma}^{(1)} + C_{e\gamma}^{(2)}, \quad (7.4)$$

where the one-loop mixing contribution grows at most as $\sqrt{\tilde{m}_1^{\text{EM}}}$ and the two-loop Barr–Zee term scales linearly with \tilde{m}_1^{EM} . Both terms are loop-suppressed and involve small Yukawa couplings, leading to analytic upper bounds such as

$$\text{BR}(\mu \rightarrow e\gamma) \lesssim 10^{-16}, \quad |d_e| \lesssim 10^{-42} \text{ e cm}, \quad |\Delta a_\mu| \lesssim 10^{-28}, \quad (7.5)$$

within the BAU-compatible region—several (or many) orders of magnitude below current experimental limits. Since the resonant enhancement responsible for the baryon asymmetry does not feed into the low-energy dipole coefficients, resonant EMLG can efficiently generate the BAU while remaining essentially invisible to current CLFV, eEDM, and $(g-2)_\mu$ searches.

To stress-test these conclusions we have also examined an extreme benchmark at the edge of perturbative control, with $M_{1,2} \simeq 0.3$ TeV, $M_\Psi \simeq 3$ TeV and $|\lambda| \sim \mathcal{O}(1)$. In this corner of parameter space the dipole-induced Majorana masses actually overshoot the cosmological bound on Σm_ν by almost an order of magnitude ($\Sigma m_\nu \simeq 1.20$ eV for the benchmark in eq. (3.29)), and are therefore in strong tension with cosmology, while still remaining compatible with the present KATRIN limit [45]. By contrast, the predicted rates for $\mu \rightarrow e\gamma$, $|d_e|$, and $|\Delta a_\mu|$ remain far below their current experimental bounds, so this benchmark quantifies how close electromagnetic leptogenesis can come to existing data before one exceeds the theoretical limit.

7.3 Outlook

The present work completes our three-part EFT analysis of electromagnetic leptogenesis. Parts I and II established that, once the Bell–Kayser–Law framework [12] is embedded into a gauge-invariant EFT, the dipole operator inherits strong loop and heavy-mass-scale suppressions that drastically reduce the CP asymmetries at low scales. Resonant enhancement from quasi-degenerate right-handed neutrinos overcomes this structural suppression and restores successful baryogenesis. In Part III we have shown that, for the same Wilson coefficients, radiative neutrino masses and low-energy dipole observables remain safely below current bounds.

Several directions warrant further investigation. First, it would be interesting to revisit high-scale implementations of EMLG in which the dipole operators are already present in the symmetric phase and the relevant decays are three-body processes $N_k \rightarrow \ell_j \phi V$ with $V = B, W$. In such setups the leading CP asymmetries arise at two loops [12], in contrast to the one-loop source in our low-scale scenario. A dedicated study is required to determine whether the resonant self-energy enhancement can yield a viable BAU in this high-scale regime.

Second, our analysis focused on a minimal EFT in which all new effects are incorporated in the single operator \mathcal{O}_{NB} . A more general treatment within the full ν SMEFT [65, 66] or LEFT operator bases would allow electromagnetic leptogenesis to coexist with other dimension-six interactions that violate lepton flavour or CP. Such operators could modify both the washout pattern in the early Universe and the correlations among $\mu \rightarrow e\gamma$, EDMs, and $(g-2)_\ell$ at low energies. A global EFT fit in the full ν SMEFT or LEFT basis, in which the Wilson coefficients of \mathcal{O}_{NB} and all other relevant operators are constrained simultaneously by cosmological and laboratory data, would provide a more model-independent test of whether a dipole contribution to leptogenesis is required or still allowed.

Finally, our results strongly indicate that the electromagnetic dipole operator by itself can provide only a tiny radiative correction to the light-neutrino mass matrix. The dominant contribution must originate from additional $\Delta L = 2$ interactions, incorporated in the Weinberg operator at low scales. Within our EFT pipeline this is most conveniently parametrised by supplementing the renormalisable EMLG UV Lagrangian

$$\begin{aligned} \mathcal{L}_{\text{UV}} = & \mathcal{L}_{\text{SM}} + \bar{N}_i i\cancel{D} N_i + \bar{\Psi} (i\cancel{D} - M_\Psi) \Psi + |D_\mu S|^2 - V(H, S) \\ & - \left(\lambda'_i \bar{N}_i \Psi_R S + \lambda_i \bar{\Psi}_L N_i S^\dagger + \frac{1}{2} \bar{N} M_{NN} N \right) \\ & - \left(y_{\alpha j} \bar{L}_\alpha \tilde{H} N_j + y_{j\alpha}^* \bar{N}_j \tilde{H}^\dagger L_\alpha \right), \end{aligned} \quad (7.6)$$

with whatever heavy states are responsible for generating the leading piece of C_5 . A possible UV origin of C_5 is a minimal type-I seesaw realised by the same N_i that appear in electromagnetic leptogenesis (2.1). Alternatively, one may introduce scalar triplets, or fermion triplets that realise type-II, or type-III seesaw dynamics with masses at the electroweak scale or well above it. From the viewpoint of our analysis these possibilities differ only in the boundary condition for C_5 , while the dipole operator \mathcal{O}_{NB} controls the CP-violating source of the BAU. In the present work we have focussed exclusively on the dipole-driven source of the BAU, effectively switching off any contribution from Yukawa-induced vanilla leptogenesis.³ A natural extension would be to explore scenarios in which both dipole- and Yukawa-induced asymmetries are present and to quantify how the two mechanisms coexist or interfere within a unified UV completion.

8 Conclusions

In this work, we have completed the EFT-consistent programme of electromagnetic leptogenesis initiated in Parts I and II. Starting from the UV completion and electromagnetic dipole operator $\mathcal{O}_{NB} = (\bar{L} \sigma^{\mu\nu} P_R N) \tilde{H} B_{\mu\nu}$, we have derived the radiative contributions to light-neutrino masses and to the charged-lepton dipole operator $\mathcal{O}_{e\gamma}$ in LEFT, and confronted them with present observations on m_ν , $\mu \rightarrow e\gamma$, the electron EDM, and $(g-2)_\mu$. Throughout, we employ the benchmark dipole textures and the mass spectra that realise resonant EMLG at the electroweak scale and interpret our results in terms of the BAU-compatible window in \tilde{m}_1^{EM} identified in Part II.

³ “Vanilla leptogenesis” refers to the standard type-I seesaw scenario in which CP-violating Yukawa interactions of heavy Majorana neutrinos generate the BAU.

In summary, our analysis leads to the following main conclusions:

- Radiative Majorana masses induced by the electromagnetic dipole operator are generically tiny; only in extreme corners of parameter space can they exceed the cosmological bound on $\sum m_\nu$. Therefore, they cannot by themselves account for the observed neutrino spectrum and must be supplemented by additional contributions to the Weinberg operator, for example those arising from type-I, type-II, or type-III seesaw dynamics in the UV.
- The same dipole texture that yields successful resonant EMLG produces contributions to $\text{BR}(\mu \rightarrow e\gamma)$, $|d_e|$, and $|\Delta a_\mu|$ that lie many orders of magnitude below present limits throughout the BAU-compatible region.
- Analytic bounds derived from the EFT pipeline show that this suppression of low-energy dipole observables is structural: it follows from gauge invariance, loop factors, and heavy scales, and from the fact that the resonant enhancement responsible for the BAU does not propagate to the on-shell dipole coefficient $C_{e\gamma}(q^2 = 0)$.
- Taken together with Parts I and II, these results establish electromagnetic leptogenesis at the electroweak scale as a viable and internally consistent baryogenesis mechanism whose low-energy imprints are expected to remain elusive for the foreseeable future.

These conclusions close the three-part EFT analysis of electromagnetic leptogenesis and provide a coherent baseline against which more general EFT extensions and UV completions can be systematically explored.

Acknowledgments

The author is grateful to A. Ishige, K. Hotokezaka, R. Jinno, and R. Namba for helpful discussions and suggestions related to this work.

A Calculation of the light Majorana neutrino masses m_ν

In this appendix we derive eq. (3.18), namely the Majorana masses of the light-neutrinos induced by the electromagnetic dipole operator \mathcal{O}_{NB} , following the discussion in sec. 3.2.

To extract the Majorana mass matrix induced by \mathcal{O}_{NB} within the EFT, it is convenient to analyse the 1PI two-point function of the left-handed neutrinos in the broken phase. For external states $\nu_{L\alpha} \rightarrow \nu_{L\beta}$ with momentum p , Lorentz covariance and chirality imply the decomposition

$$\Sigma_{\alpha\beta}^{(LL)}(p) = A_{\alpha\beta}(p^2) \not{p} P_L + B_{\alpha\beta}(p^2) P_R, \quad (\text{A.1})$$

where $A_{\alpha\beta}(p^2)$ and $B_{\alpha\beta}(p^2)$ are scalar form factors. The term proportional to $\not{p} P_L$ renormalises the kinetic term, whereas the chirality-flipping form factor $B_{\alpha\beta}(p^2)$ has the same spinor structure as a Majorana mass insertion. In the absence of a tree-level Weinberg operator, the full inverse propagator reads

$$S_{\alpha\beta}^{-1}(p) = \not{p} P_L \delta_{\alpha\beta} - \Sigma_{\alpha\beta}^{(LL)}(p). \quad (\text{A.2})$$

The physical Majorana masses are defined by the pole of $S(p)$. For vanishing tree-level mass and to leading order in the loop expansion, the pole condition near $p^2 = 0$ yields

$$(m_\nu)_{\alpha\beta} \simeq B_{\alpha\beta}(0), \quad (\text{A.3})$$

where the effect of $A_{\alpha\beta}(0)$ contributes only at higher loop order through wave-function renormalisation. Since only heavy fields with masses $M_i, m_Z \gg p$ propagate in the loop, the form factors are analytic at $p^2 = 0$ and higher-derivative terms are suppressed by p^2/M^2 . Thus, for matching onto the Weinberg operator \mathcal{O}_5 , it is sufficient to evaluate $\Sigma_{\alpha\beta}^{(LL)}(p)$ at vanishing external momentum and identify $B_{\alpha\beta}(0)$ with the radiatively induced Majorana mass matrix.

We begin by computing the one-particle-irreducible (1PI) self-energy in the 't Hooft–Feynman gauge, using dimensional regularisation and the $\overline{\text{MS}}$ scheme. From the Feynman graph containing one right-handed neutrino N_i and one gauge boson $B = \gamma, Z$ running in the loop (fig. 1), the self-energy is

$$\begin{aligned} i\Sigma_{\alpha\beta}^{(LL)} &= \sum_{i,B} \int \frac{d^n k}{(2\pi)^n} (2\mu_{\alpha i}^{(B)} \sigma^{\mu\rho} k_\rho P_R) \frac{i(\not{k} + M_i)}{k^2 - M_i^2} (2\mu_{\beta i}^{(B)} \sigma^{\nu\sigma} k_\sigma P_R) \frac{(-ig_{\mu\nu})}{k^2 - m_B^2} \\ &= 4 \sum_{i,B} \mu_{\alpha i}^{(B)} \mu_{\beta i}^{(B)} \int \frac{d^n k}{(2\pi)^n} \frac{\sigma^{\mu\rho} k_\rho P_R (\not{k} + M_i) P_R \sigma_\mu^\sigma k_\sigma}{(k^2 - M_i^2)(k^2 - m_B^2)} \\ &= 4 \sum_{i,B} \mu_{\alpha i}^{(B)} \mu_{\beta i}^{(B)} M_i \int \frac{d^n k}{(2\pi)^n} \frac{\sigma^{\mu\rho} k_\rho \sigma_\mu^\sigma k_\sigma P_R}{(k^2 - M_i^2)(k^2 - m_B^2)} \\ &= 4(n-1) \sum_{i,B} \mu_{\alpha i}^{(B)} \mu_{\beta i}^{(B)} M_i \int \frac{d^n k}{(2\pi)^n} \frac{k^2 P_R}{(k^2 - M_i^2)(k^2 - m_B^2)}. \end{aligned} \quad (\text{A.4})$$

Here we have made use of the identity

$$\sigma^{\mu\nu} \sigma^{\rho\sigma} = i(g^{\nu\rho} \sigma^{\mu\sigma} - g^{\mu\rho} \sigma^{\nu\sigma} - g^{\nu\sigma} \sigma^{\mu\rho} + g^{\mu\sigma} \sigma^{\nu\rho}) + (g^{\mu\rho} g^{\nu\sigma} - g^{\mu\sigma} g^{\nu\rho}), \quad (\text{A.5})$$

which yields

$$\begin{aligned} \sigma^{\mu\rho} \sigma_\mu^\sigma &= i(g_\mu^\rho \sigma^{\mu\sigma} - g_\mu^\mu \sigma^{\rho\sigma} - g^{\rho\sigma} \sigma_\mu^\mu + g^{\mu\sigma} \sigma_\mu^\rho) + (g_\mu^\mu g^{\rho\sigma} - g^{\mu\sigma} g_\mu^\rho) \\ &= i(\sigma^{\rho\sigma} - n\sigma^{\rho\sigma} + \sigma^{\rho\sigma}) + (ng^{\rho\sigma} - g^{\rho\sigma}) \\ &= i(2-n)\sigma^{\rho\sigma} + (n-1)g^{\rho\sigma}. \end{aligned} \quad (\text{A.6})$$

Using the antisymmetry of $\sigma^{\mu\nu}$, one obtains the contracted identity

$$\sigma^{\mu\rho} k_\rho \sigma_\mu^\sigma k_\sigma = (n-1)k^2. \quad (\text{A.7})$$

Applying the Feynman-parameter formula to the denominator of eq. (A.4),

$$\begin{aligned} \frac{1}{(k^2 - M_i^2)(k^2 - m_B^2)} &= \int_0^1 dx \frac{1}{[(k^2 - m_B^2)x + (k^2 - M_i^2)(1-x)]^2} \\ &= \int_0^1 dx \frac{1}{[m_B^2 x + M_i^2(1-x) - k^2]^2}, \end{aligned} \quad (\text{A.8})$$

and performing the loop integral in dimensional regularisation, one finds

$$\begin{aligned}
i\Sigma_{\alpha\beta}^{(LL)} &= 4(n-1) \sum_{i,B} \mu_{\alpha i}^{(B)} \mu_{\beta i}^{(B)} M_i \int_0^1 dx \int \frac{d^n k}{(2\pi)^n} \frac{k^2 P_R}{[m_B^2 x + M_i^2(1-x) - k^2]^2} \\
&= -4(n-1) \sum_{i,B} \mu_{\alpha i}^{(B)} \mu_{\beta i}^{(B)} M_i \int_0^1 dx \frac{i\Gamma(1-\frac{n}{2})}{(4\pi)^{\frac{n}{2}} \Gamma(2)} \frac{(n/2)P_R}{[m_B^2 x + M_i^2(1-x)]^{1-\frac{n}{2}}} \\
&= -2in(n-1) \sum_{i,B} \mu_{\alpha i}^{(B)} \mu_{\beta i}^{(B)} M_i P_R \\
&\quad \times \frac{1}{16\pi^2} \left[-\frac{2}{4-n} + (\gamma - 1) - \ln 4\pi \right] \int_0^1 dx \Delta_B(x) \left[1 - \frac{4-n}{2} \ln \frac{\Delta_B(x)}{\mu^2} \right] \\
&= \frac{3i}{2\pi^2} \sum_{i,B} \mu_{\alpha i}^{(B)} \mu_{\beta i}^{(B)} M_i P_R \int_0^1 dx \Delta_B(x) \left[\frac{1}{\epsilon} - (\gamma - 1) + \ln 4\pi - \ln \frac{\Delta_B(x)}{\mu^2} \right] \\
&= \frac{3i}{2\pi^2} \sum_{i,B} \mu_{\alpha i}^{(B)} \mu_{\beta i}^{(B)} M_i P_R \int_0^1 dx \Delta_B(x) \left[\frac{1}{\epsilon} - \ln \frac{\Delta_B(x)}{\mu^2} + 1 \right], \tag{A.9}
\end{aligned}$$

where we have introduced the usual ‘‘infinite part’’ $\bar{\epsilon}^{-1} := \epsilon^{-1} - \gamma + \ln 4\pi$ in the $\overline{\text{MS}}$ scheme, and defined

$$\Delta_B(x) := m_B^2 x + M_i^2(1-x). \tag{A.10}$$

Carrying out the integrals over $\Delta_B(x)$, we obtain from eq. (A.9)

$$\int_0^1 dx \Delta_B(x) = \int_0^1 dx [M_i^2 + (m_B^2 - M_i^2)x] = \frac{M_i^2 + m_B^2}{2}, \tag{A.11}$$

$$\begin{aligned}
\int_0^1 dx \Delta_B(x) \ln \frac{\Delta_B(x)}{\mu^2} &= \frac{1}{M_i^2 - m_B^2} \int_{u=m_B^2}^{M_i^2} du u \ln \frac{u}{\mu^2} \\
&= \frac{1}{2(M_i^2 - m_B^2)} \left(M_i^4 \ln \frac{M_i^2}{\mu^2} - m_B^4 \ln \frac{m_B^2}{\mu^2} \right) - \frac{M_i^2 + m_B^2}{4}, \tag{A.12}
\end{aligned}$$

so we obtain from eq. (A.9),

$$\Sigma_{\alpha\beta}^{(LL)} = \frac{3}{2\pi^2} \sum_{i,B} \mu_{\alpha i}^{(B)} \mu_{\beta i}^{(B)} M_i P_R \left[\frac{M_i^2 + m_B^2}{2} \left(\frac{1}{\epsilon} + \frac{3}{2} \right) - \frac{M_i^4 \ln \frac{M_i^2}{\mu^2} - m_B^4 \ln \frac{m_B^2}{\mu^2}}{2(M_i^2 - m_B^2)} \right]. \tag{A.13}$$

Since $\Sigma_{\alpha\beta}^{(LL)}$ is the self-energy of the left-handed neutrino $\nu_{L\alpha}$, its divergent part is absorbed into the renormalisation of the Weinberg operator \mathcal{O}_5 . In the $\overline{\text{MS}}$ scheme,

$$C_5^{(0)}(\mu) = \mu^{2\epsilon} [C_5(\mu) + \delta C_5(\mu)], \tag{A.14}$$

$$\begin{aligned}
\delta C_{5,\alpha\beta}(\mu) &= \frac{2}{v^2} \Sigma_{\text{div},\alpha\beta}^{(LL)} \\
&= \frac{3}{2\pi^2 v^2} \bar{\epsilon}^{-1} \sum_{i,B} \mu_{\alpha i}^{(B)} \mu_{\beta i}^{(B)} M_i (M_i^2 + m_B^2) P_R. \tag{A.15}
\end{aligned}$$

Performing the sum over $B = \gamma, Z$, we obtain

$$\delta C_{5,\alpha\beta}(\mu) = \frac{3}{2\pi^2 v^2} \bar{\epsilon}^{-1} \sum_i \mu_{\alpha i} \mu_{\beta i} M_i P_R [M_i^2(1 + \tan^2 \theta_W) + m_Z^2 \tan^2 \theta_W]. \tag{A.16}$$

Thus, the term $-v^2\delta C_5/2$ cancels the UV divergence of $\Sigma^{(LL)}(p \rightarrow 0)$. In what follows, we omit the chiral projector P_R that accompanies m_ν :

$$\begin{aligned}
(m_\nu)_{\alpha\beta}(\mu) &= \frac{v^2}{2} C_{5,\alpha\beta}(\mu) + \Sigma_{\text{finite},\alpha\beta}^{(LL)}(\mu) \\
&= \frac{v^2}{2} C_{5,\alpha\beta}(\mu) + \frac{3}{2\pi^2} \sum_i \mu_{\alpha i} \mu_{\beta i} M_i \\
&\quad \times \left\{ \frac{3}{4} [M_i^2 (1 + \tan^2 \theta_W) + m_Z^2 \tan^2 \theta_W] \right. \\
&\quad \left. - \frac{M_i^2}{2} \ln \frac{M_i^2}{\mu^2} - \frac{M_i^4 \ln \frac{M_i^2}{\mu^2} - m_Z^4 \ln \frac{m_Z^2}{\mu^2}}{2(M_i^2 - m_Z^2)} \tan^2 \theta_W \right\} \quad (\text{A.17})
\end{aligned}$$

At the matching scale $\mu = M_\Psi$ we impose the boundary condition $C_5(M_\Psi) = 0$, which reflects the absence of a tree-level Weinberg operator \mathcal{O}_5 in the UV completion and removes the first term in eq. (A.17). The light-neutrino mass at $\mu = M_\Psi$ is then given entirely by the finite one-loop contribution

$$\begin{aligned}
(m_\nu)_{\alpha\beta}(M_\Psi) &= \frac{3}{2\pi^2} \sum_i \mu_{\alpha i} \mu_{\beta i} M_i \left\{ \frac{3}{4} [M_i^2 (1 + \tan^2 \theta_W) + m_Z^2 \tan^2 \theta_W] \right. \\
&\quad \left. - \frac{M_i^2}{2} \ln \frac{M_i^2}{M_\Psi^2} - \frac{M_i^4 \ln \frac{M_i^2}{M_\Psi^2} - m_Z^4 \ln \frac{m_Z^2}{M_\Psi^2}}{2(M_i^2 - m_Z^2)} \tan^2 \theta_W \right\}. \quad (\text{A.18})
\end{aligned}$$

The explicit μ -dependence in eq. (A.17) thus simply reflects the usual reshuffling of logarithms between the running coefficient $C_5(\mu)$ and the finite loop part, leaving $(m_\nu)_{\alpha\beta}$ independent of the renormalisation scale.

B Derivation of the Wilson coefficients $C_{e\gamma}$

B.1 One-loop operator mixing

In this appendix we derive the one-loop contribution $C_{e\gamma}^{(1)}$, following the analysis of sec. 4.4.

We begin by computing the 1PI vertex function $\mathcal{V}_{\alpha\beta}^\rho$ associated with the operator \mathcal{O}_{eB} , with external legs $(L_\alpha(p_1), E_\beta(p_2), H(p_H), B^\rho(q))$. Since we are interested only in the UV divergence that renormalises the local dipole operator, it is sufficient to set all external momenta to zero except for the gauge leg, which must retain the momentum q appearing in the field strength. Working in the 't Hooft–Feynman gauge and in the $\overline{\text{MS}}$ scheme, the internal propagators are

$$S_L(k) = \frac{i\cancel{k}}{k^2}, \quad S_N(k) = \frac{i(\cancel{k} + M_i)}{k^2 - M_i^2}, \quad \Delta_{\tilde{H}}(k) = \frac{i}{k^2}. \quad (\text{B.1})$$

From the 1PI graph in fig. 3 the vertex function is

$$i\mathcal{V}_{\alpha\beta}^\rho = \sum_{\gamma,i} \int \frac{d^n k}{(2\pi)^n} \left(-2 \frac{C_{NB,\alpha i}}{M_\Psi^2} \sigma^{\rho\lambda} q_\lambda P_R \right) \frac{i(\cancel{k} + M_i)}{k^2 - M_i^2} \cdot \frac{i}{k^2} (-iy_{\nu,\gamma i} P_L) \frac{i\cancel{k}}{k^2} (-iy_{e,\gamma\beta} P_R)$$

$$\begin{aligned}
&= -2i \sum_i \frac{C_{NB,\alpha i}}{M_\Psi^2} (y_e^\top y_\nu)_{\beta i} \int \frac{d^n k}{(2\pi)^n} \frac{\sigma^{\rho\lambda} q_\lambda P_R(\not{k} + M_i) P_L \not{k} P_R}{k^4(k^2 - M_i^2)} \\
&= -2i \sum_i \frac{C_{NB,\alpha i}}{M_\Psi^2} (y_e^\top y_\nu)_{\beta i} \int \frac{d^n k}{(2\pi)^n} \frac{\sigma^{\rho\lambda} q_\lambda P_R \not{k}^2 P_R}{k^4(k^2 - M_i^2)} \\
&= -2i \sum_i \frac{C_{NB,\alpha i}}{M_\Psi^2} (y_e^\top y_\nu)_{\beta i} \int \frac{d^n k}{(2\pi)^n} \frac{\sigma^{\rho\lambda} q_\lambda P_R}{k^2(k^2 - M_i^2)}. \tag{B.2}
\end{aligned}$$

Thus, the numerator in eq. (B.2) has the same $\sigma^{\mu\nu} k_\nu P_R$ structure as the operator \mathcal{O}_{eB} . Applying the Feynman-parameter formula to the denominator of eq. (B.2), we obtain

$$\frac{1}{k^2(k^2 - M_i^2)} = \int_0^1 dx \frac{1}{[(k^2 - M_i^2)x + k^2(1-x)]^2} = \int_0^1 dx \frac{1}{(M_i^2 x - k^2)^2}, \tag{B.3}$$

so that the dimensionally regularised integral becomes

$$\begin{aligned}
\int \frac{d^n k}{(2\pi)^n} \frac{1}{k^2(k^2 - M_i^2)} &= \int_0^1 dx \int \frac{d^n k}{(2\pi)^n} \frac{1}{(M_i^2 x - k^2)^2} \\
&= \int_0^1 dx \frac{i\Gamma(2 - \frac{n}{2})}{(4\pi)^{\frac{n}{2}} \Gamma(2)} \frac{1}{(M_i^2 x)^{2 - \frac{n}{2}}} \\
&= \frac{i}{16\pi^2} \int_0^1 dx \left(\frac{2}{4-n} - \gamma + \ln 4\pi \right) \left(1 - \frac{4-n}{2} \ln \frac{M_i^2 x}{\mu^2} \right) \\
&= \frac{i}{16\pi^2} \int_0^1 dx \left(\frac{1}{\bar{\epsilon}} - \ln \frac{M_i^2 x}{\mu^2} \right) = \frac{i}{16\pi^2} \left(\frac{1}{\bar{\epsilon}} - \ln \frac{M_i^2}{\mu^2} + 1 \right), \tag{B.4}
\end{aligned}$$

with $\bar{\epsilon}^{-1} = \epsilon^{-1} - \gamma + \ln 4\pi$. Therefore, the vertex function (B.2) is obtained by

$$i\mathcal{V}_{\alpha\beta}^\rho = \frac{1}{16\pi^2} \sum_i \frac{C_{NB,\alpha i}(\mu)}{M_\Psi^2} (y_e^\top y_\nu)_{\beta i} \left(\frac{1}{\bar{\epsilon}} - \ln \frac{M_i^2}{\mu^2} + 1 \right) (2\sigma^{\rho\lambda} q_\lambda P_R). \tag{B.5}$$

Hence, eq. (4.22) is obtained, from which the renormalised Wilson coefficients in eqs. (4.26) and (4.27) follow, as described in the main text.

B.2 Two-loop pure dipole

Next we derive the two-loop contribution $C_{e\gamma}^{(2)}$ following sec. 4.5.

B.2.1 Inner one-loop

We now evaluate the dimensionally regularised integral appearing in the first line of eq. (4.38), corresponding to the inner loop in fig. 4

$$i\mathcal{V}_{h\gamma B}^{\mu\rho}(p, q) = -\frac{8c_B}{v} \sum_{\alpha', i} |\mu_{\alpha' i}|^2 \int \frac{d^n k}{(2\pi)^n} \frac{\text{tr}[(\sigma^{\mu\nu} q_\nu P_R)(\not{k} + M_i)(\sigma^{\rho\lambda} r_\lambda P_L)(\not{k} + \not{p})]}{(k^2 - M_i^2)(k + p)^2}, \tag{B.6}$$

and begin by computing the trace

$$\mathcal{T}^{\mu\rho} := \text{tr}[(\sigma^{\mu\nu} q_\nu P_R)(\not{k} + M_i)(\sigma^{\rho\lambda} r_\lambda P_L)(\not{k} + \not{p})], \tag{B.7}$$

where $P_R = (1 + \gamma_5)/2$. Since a single insertion of γ_5 in the trace involves a totally antisymmetric tensor of rank four and yields a CP-odd structure, such terms do not contribute to the external-loop operator $\mathcal{O}_{e\gamma}$ (which is CP-even). Therefore, keeping only the CP-even part we obtain

$$\mathcal{T}^{\mu\rho} = \frac{1}{4} \text{tr}[\sigma^{\mu\nu} q_\nu \not{k} \sigma^{\rho\lambda} r_\lambda (\not{k} + \not{p})]. \quad (\text{B.8})$$

Since the momentum expansion appropriate for a local operator requires only the term linear in the external momentum q , all higher-order terms in q are set to zero, the denominator may be evaluated in the limit $p \rightarrow 0$, where no infrared divergence arises. In this limit, the trace becomes

$$\begin{aligned} \mathcal{T}^{\mu\rho} &= \frac{1}{4} \text{tr}(\sigma^{\mu\nu} q_\nu \not{k} \sigma^{\rho\lambda} r_\lambda \not{k}) = \frac{1}{4} q_\nu r_\lambda k_\alpha k_\beta \text{tr}(\sigma^{\mu\nu} \gamma^\alpha \sigma^{\rho\lambda} \gamma^\beta) \\ &= q_\nu r_\lambda k_\alpha k_\beta \text{tr}[(g^{\mu\rho} g^{\nu\lambda} - g^{\mu\lambda} g^{\nu\rho}) g^{\alpha\beta} + g^{\mu\beta} (g^{\nu\rho} g^{\lambda\alpha} - g^{\nu\lambda} g^{\rho\alpha}) + g^{\nu\beta} (g^{\mu\lambda} g^{\rho\alpha} - g^{\mu\rho} g^{\lambda\alpha})] \\ &= k^2 [g^{\mu\rho} (q \cdot r) - q^\rho r^\mu] + r^\mu [(q \cdot k) k^\rho - q^\rho k^2] - g^{\mu\rho} [(q \cdot k) (r \cdot k) - (q \cdot r) k^2] \\ &\quad - (q \cdot r) (k^\mu k^\rho - g^{\mu\rho} k^2) + q^\rho [k^\mu (r \cdot k) - r^\mu k^2]. \end{aligned} \quad (\text{B.9})$$

(B.6) together with this trace can be written as

$$i\mathcal{V}_{h\gamma B}^{\mu\rho}(p, q) = -\frac{8c_B}{v} \sum_{\alpha',i} |\mu_{\alpha'i}|^2 \int \frac{d^n k}{(2\pi)^n} \frac{\mathcal{T}^{\mu\rho}}{k^2(k^2 - M_i^2)}. \quad (\text{B.10})$$

Applying the Feynman-parameter formula (B.3) to the denominator of (B.10) yields

$$i\mathcal{V}_{h\gamma B}^{\mu\rho}(p, q) = -\frac{8c_B}{v} \sum_{\alpha',i} |\mu_{\alpha'i}|^2 \int_0^1 dx \int \frac{d^n k}{(2\pi)^n} \frac{\mathcal{T}^{\mu\rho}}{(M_i^2 x - k^2)^2}. \quad (\text{B.11})$$

Substituting the trace (B.9) and performing dimensional regularisation, we obtain

$$\begin{aligned} &\int \frac{d^n k}{(2\pi)^n} \frac{\mathcal{T}^{\mu\rho}}{(M_i^2 x - k^2)^2} \\ &= -\frac{\Gamma(1 - \frac{n}{2})}{(4\pi)^{\frac{n}{2}} \Gamma(2)} \cdot \frac{1}{2} \cdot \frac{n[g^{\mu\rho} (q \cdot r) - q^\rho r^\mu] - 2r^\mu (n-1)q^\rho + 2g^{\mu\rho} (n-1)(q \cdot r)}{(M_i^2 x)^{1-\frac{n}{2}}} \\ &= -\frac{1}{32\pi^2} \left[-\frac{2}{4-n} + (\gamma - 1) - \ln 4\pi \right] \frac{(3n-2)[g^{\mu\rho} (q \cdot r) - q^\rho r^\mu]}{(M_i^2 x)^{1-\frac{n}{2}}} \\ &= -\frac{3n-2}{32\pi^2} \left[-\frac{2}{4-n} + (\gamma - 1) - \ln 4\pi \right] \left(1 - \frac{4-n}{2} \ln \frac{M_i^2 x}{\mu^2} \right) [g^{\mu\rho} (q \cdot r) - q^\rho r^\mu] \\ &= \frac{5}{16\pi^2} \left[\frac{2}{4-n} - (\gamma - 1) + \ln 4\pi - \ln \frac{M_i^2 x}{\mu^2} \right] [g^{\mu\rho} (q \cdot r) - q^\rho r^\mu] \\ &= \frac{5}{16\pi^2} \left(\frac{1}{\bar{\epsilon}} - \ln \frac{M_i^2 x}{\mu^2} + 1 \right) [g^{\mu\rho} (q \cdot r) - q^\rho r^\mu]. \end{aligned} \quad (\text{B.12})$$

Performing the x -integration finally yields

$$i\mathcal{V}_{h\gamma B}^{\mu\rho}(p, q) = -\frac{8c_B}{v} \sum_{\alpha',i} |\mu_{\alpha'i}|^2 \int_0^1 dx \int \frac{d^n k}{(2\pi)^n} \frac{\mathcal{T}^{\mu\rho}}{(M_i^2 x - k^2)^2}$$

$$\begin{aligned}
&= -\frac{5c_B}{2\pi^2 v} (g^{\mu\rho} q \cdot r - q^\rho r^\mu) \sum_{\alpha',i} |\mu_{\alpha'i}|^2 \int_0^1 dx \left(\frac{1}{\bar{\epsilon}} - \ln \frac{M_i^2 x}{\mu^2} + 1 \right) \\
&= -\frac{5c_B}{2\pi^2 v} T_1^{\mu\rho}(p, q) \sum_{\alpha',i} |\mu_{\alpha'i}|^2 \left(\frac{1}{\bar{\epsilon}} - \ln \frac{M_i^2}{\mu^2} + 2 \right).
\end{aligned} \tag{B.13}$$

Keeping only the lowest-order local operator $\mathcal{O}(q)$, we take

$$\begin{aligned}
T_1^{\mu\rho}(p, q) &:= g^{\mu\rho} q \cdot r - q^\rho r^\mu = g^{\mu\rho}(-q \cdot p - q^2) - q^\rho(-q^\mu - p^\mu) \\
&= -g^{\mu\rho} q \cdot p - g^{\mu\rho} q^2 + q^\rho q^\mu + p^\mu q^\rho \\
&\simeq -g^{\mu\rho} q \cdot p + p^\mu q^\rho.
\end{aligned} \tag{B.14}$$

Because this tensor structure is uniquely fixed by gauge invariance of the electromagnetic dipole operator, the effective external-loop vertex is

$$i\mathcal{V}_{h\gamma B}^{\mu\rho}(p, q) = \mathcal{C}_B T_1^{\mu\rho}(p, q), \tag{B.15}$$

with coefficient

$$\mathcal{C}_B = -\frac{5c_B}{2\pi^2 v} \sum_{\alpha'i} |\mu_{\alpha'i}|^2 \left(\frac{1}{\bar{\epsilon}} - \ln \frac{M_i^2}{\mu^2} + 2 \right), \tag{B.16}$$

where $c_\gamma = 1$ and $c_Z = -\tan\theta_W$.

B.2.2 Outer one-loop

The outer 1PI amplitude for each $B = \gamma, Z$ is

$$\begin{aligned}
iI_{\alpha\beta}^{(B)\mu}(q) &= \int \frac{d^n p}{(2\pi)^n} S_\ell(p) (-ig_{L_\beta}^B \gamma_\rho P_L) \Delta_h(p) S_\ell(p+q) (-iy_{\ell_\beta}) D_B^{\rho\sigma}(p+q) [iV_\sigma^\mu(p, q)] \\
&= \delta_{\alpha\beta} \int \frac{d^n p}{(2\pi)^n} \frac{i\cancel{p}}{p^2} (-ig_{L_\beta}^B \delta_{\alpha\gamma} \gamma_\rho P_L) \frac{i}{p^2 - m_h^2} \frac{i(\cancel{p} + \cancel{q})}{(p+q)^2} \\
&\quad \times (-iy_{\ell_\beta} \delta_{\gamma\beta}) \frac{-ig^{\rho\sigma}}{(p+q)^2 - m_B^2} [iV_\sigma^\mu(p, q)] \\
&= \delta_{\alpha\beta} g_{L_\beta}^B y_{\ell_\beta} \int \frac{d^n p}{(2\pi)^n} \frac{\cancel{p} \gamma_\rho P_L (\cancel{p} + \cancel{q}) g^{\rho\sigma}}{p^2 (p^2 - m_h^2) (p+q)^2 [(p+q)^2 - m_B^2]} [iV_\sigma^\mu(p, q)] \\
&= \delta_{\alpha\beta} g_{L_\beta}^B y_{\ell_\beta} \mathcal{C}_B \int \frac{d^n p}{(2\pi)^n} \frac{\cancel{p} \gamma_\rho (\cancel{p} + \cancel{q}) T_1^{\mu\rho}(p, q) P_R}{p^2 (p^2 - m_h^2) (p+q)^2 [(p+q)^2 - m_B^2]}, \tag{B.17}
\end{aligned}$$

where $i\mathcal{V}_\sigma^\mu(p, q)$ is the inner one-loop effective vertex and we have substituted $i\mathcal{V}_\sigma^\mu = i\mathcal{C}_B T_{1\sigma}^\mu$. Furthermore, we decompose the numerator of eq. (B.17) as

$$\cancel{p} \gamma_\rho (\cancel{p} + \cancel{q}) T_1^{\mu\rho} = \cancel{p} \gamma_\rho \cancel{p} T_1^{\mu\rho} + \cancel{p} \gamma_\rho \cancel{q} T_1^{\mu\rho} \tag{B.18}$$

For the first term on the right-hand side, using $\cancel{p} \gamma_\rho \cancel{p} = 2p_\rho \cancel{p} - p^2 \gamma_\rho$, we obtain

$$\begin{aligned}
\cancel{p} \gamma_\rho \cancel{p} (-g^{\mu\rho} q \cdot p + p^\mu q^\rho) &= (2p_\rho \cancel{p} - p^2 \gamma_\rho) (-g^{\mu\rho} q \cdot p + p^\mu q^\rho) \\
&= p^2 \gamma^\mu (q \cdot p) - p^2 p^\mu \cancel{q}.
\end{aligned} \tag{B.19}$$

For the second term on the right-hand side, using $\gamma_\rho \not{q} = q_\rho + i\sigma_{\rho\nu}q^\nu$, we find

$$\begin{aligned} \not{p}\gamma_\rho \not{q}(-g^{\mu\rho}q \cdot p + p^\mu q^\rho) &= (q_\rho + i\sigma_{\rho\nu}q^\nu)(-g^{\mu\rho}q \cdot p + p^\mu q^\rho) \\ &= -\not{p}q^\mu(q \cdot p) - i\not{p}\sigma^{\mu\nu}q_\nu(q \cdot p), \end{aligned} \quad (\text{B.20})$$

where terms of $\mathcal{O}(q^2)$ have been dropped. Combining these results, the numerator of eq. (B.17) can be written as

$$N^\mu := p^2(q \cdot p)\gamma^\mu - p^2p^\mu \not{q} - (q \cdot p)\not{p}q^\mu - i(q \cdot p)\not{p}\sigma^{\mu\nu}q_\nu. \quad (\text{B.21})$$

On the other hand, the denominator of eq. (B.17) is

$$D := p^2(p^2 - m_h^2)(p + q)^2[(p + q)^2 - m_B^2]. \quad (\text{B.22})$$

Since the only external vector available is q_μ , Lorentz invariance implies

$$\int \frac{d^n p}{(2\pi)^n} \frac{p^\alpha p^\beta}{D} = A g^{\alpha\beta} + B q^\alpha q^\beta. \quad (\text{B.23})$$

Using this, we obtain

$$\int \frac{d^n p}{(2\pi)^n} \frac{(q \cdot p)\not{p}}{D} = \gamma_\beta q_\alpha \int \frac{d^n p}{(2\pi)^n} \frac{p^\alpha p^\beta}{D} = (A + Bq^2)\not{q} \xrightarrow{q^2 \rightarrow 0} A\not{q}. \quad (\text{B.24})$$

Hence, after dimensional regularisation the third and fourth terms in eq. (B.21) contribute only longitudinal structures proportional to $q^\mu \not{q}$, which vanish when contracted with the physical polarisation vector satisfying $q \cdot \varepsilon = 0$; they therefore do not contribute to the dipole coefficient. The second term, $-p^2p^\mu \not{q}$, also does not contribute to the dipole part once we sandwich it between external spinors. Thus, only the first term of eq. (B.21) is relevant. Inserting the first term between external spinors and using the Gordon identity [67],

$$\bar{u}(p')\gamma^\mu P_R u(p) = \frac{1}{2m_{\ell_\beta}} \bar{u}(p')[(p' + p)^\mu + i\sigma^{\mu\nu}q_\nu]P_R u(p), \quad q = p' - p, \quad (\text{B.25})$$

we see that the term proportional to $i\sigma^{\mu\nu}q_\nu$ contributes to the dipole. The vector part $(p' + p)^\mu$ reduces on shell to a Dirac current and does not generate any dipole operator. Combining eqs. (B.17), (B.21), and (B.25) and using $y_{\ell_\beta} = \sqrt{2}m_{\ell_\beta}/v$, we obtain

$$\begin{aligned} \bar{u}i\Gamma_{\alpha\beta}^{(B)\mu}(q)u &= \delta_{\alpha\beta} g_{L_\beta}^B \frac{y_{\ell_\beta}}{2m_{\ell_\beta}} \mathcal{C}_B \int \frac{d^n p}{(2\pi)^n} \frac{p^2(q \cdot p)\bar{u}(i\sigma^{\mu\nu}q_\nu P_R)u}{p^2(p^2 - m_h^2)(p + q)^2[(p + q)^2 - m_B^2]} \\ &= \frac{i}{\sqrt{2}v} \delta_{\alpha\beta} g_{L_\beta}^B \mathcal{C}_B (\bar{u}\sigma^{\mu\nu}q_\nu P_R u) I_B, \end{aligned} \quad (\text{B.26})$$

with

$$I_B(a, b; q^2) := \int \frac{d^n p}{(2\pi)^n} \frac{q \cdot p}{(p^2 - a)(p + q)^2[(p + q)^2 - b]}, \quad a := m_h^2, \quad b := m_B^2. \quad (\text{B.27})$$

To simplify I_B , we use the identity $2p \cdot q = (p + q)^2 - p^2 - q^2$ to decompose the numerator and obtain

$$I_B(a, b; q^2) = \frac{1}{2} \int \frac{d^n p}{(2\pi)^n} \frac{1}{p^2 - a}$$

$$\times \left\{ \frac{1}{(p+q)^2 - b} - \frac{p^2}{(p+q)^2[(p+q)^2 - b]} - \frac{q^2}{(p+q)^2[(p+q)^2 - b]} \right\}. \quad (\text{B.28})$$

Introducing $X := (p+q)^2$, the two-point partial fraction

$$\frac{1}{X(X-b)} = \frac{1}{b} \left(\frac{1}{X-b} - \frac{1}{X} \right) \quad (\text{B.29})$$

can be applied to the second and third terms in the curly brackets of eq. (B.28), yielding

$$I_B(a, b; q^2) = \frac{1}{2} \int \frac{d^n p}{(2\pi)^n} \frac{1}{p^2 - a} \left[\frac{1}{X-b} - \frac{p^2}{b} \left(\frac{1}{X-b} - \frac{1}{X} \right) - \frac{q^2}{b} \left(\frac{1}{X-b} - \frac{1}{X} \right) \right]. \quad (\text{B.30})$$

In addition, by employing

$$\frac{p^2}{p^2 - a} = 1 + \frac{a}{p^2 - a}, \quad (\text{B.31})$$

we rewrite the factor p^2 appearing in the numerator of the second term on the right-hand side of eq. (B.30), thereby reducing all contributions to two-point integrals:

$$\begin{aligned} I_B(a, b; q^2) &= \frac{1}{2} \int \frac{d^n p}{(2\pi)^n} \left\{ \frac{1}{(p^2 - a)(X-b)} \right. \\ &\quad \left. - \frac{p^2}{b} \left[\frac{1}{(p^2 - a)(X-b)} - \frac{1}{(p^2 - a)X} \right] - \frac{q^2}{b} \left[\frac{1}{(p^2 - a)(X-b)} - \frac{1}{(p^2 - a)X} \right] \right\} \\ &= \int \frac{d^n p}{(2\pi)^n} \left\{ \frac{1}{2(p^2 - a)(X-b)} - \frac{1}{2b} \left(\frac{1}{X-b} - \frac{1}{X} \right) \right. \\ &\quad \left. - \frac{a}{2b} \left[\frac{1}{(p^2 - a)(X-b)} - \frac{1}{(p^2 - a)X} \right] - \frac{q^2}{2b} \left[\frac{1}{(p^2 - a)(X-b)} - \frac{1}{(p^2 - a)X} \right] \right\} \\ &= \frac{1}{2} J(a, b; q^2) - \frac{1}{2b} A_0(b) \\ &\quad - \frac{a}{2b} [J(a, b; q^2) - J(a, 0; q^2)] - \frac{q^2}{2b} [J(a, b; q^2) - J(a, 0; q^2)], \end{aligned} \quad (\text{B.32})$$

where we have defined [57, 58]

$$A_0(b) := \int \frac{d^n p}{(2\pi)^n} \frac{1}{X-b}, \quad J(a, b; q^2) := \int \frac{d^n p}{(2\pi)^n} \frac{1}{(p^2 - a)(X-b)}. \quad (\text{B.33})$$

In dimensional regularisation, the integral $A_0(0) = \int d^n p / (p+q)^2$ is scaleless and vanishes by cancellation between the UV and IR poles; thus $A_0(0) := 0$. The tadpole integral $A_0(b) = \int d^n p / [(p+q)^2 - b]$ evaluates to

$$\begin{aligned} A_0(b) &:= \int \frac{d^n p}{(2\pi)^n} \frac{1}{(p+q)^2 - b} = - \int \frac{d^n p}{(2\pi)^n} \frac{1}{b - q^2 + 2p \cdot (-q) - p^2} \\ &= - \frac{i\Gamma(1 - \frac{n}{2})}{(4\pi)^{\frac{n}{2}} \Gamma(1)} \frac{1}{b^{1 - \frac{n}{2}}} = - \frac{ib}{16\pi^2} \left[-\frac{2}{4-n} + (\gamma - 1) - \ln 4\pi + \ln \frac{b}{\mu^2} \right] \\ &= \frac{ib}{16\pi^2} \left(\frac{1}{\epsilon} + 1 - \ln \frac{b}{\mu^2} \right), \end{aligned} \quad (\text{B.34})$$

where the last expression makes explicit that the result does not depend on either p or q . Next we evaluate $J(a, b; q^2)$. Using the Feynman-parameter formula

$$\begin{aligned} \frac{1}{(p^2 - a)[(p + q)^2 - b]} &= \int_0^1 dx \frac{1}{\{(p^2 - a)(1 - x) + [(p + q)^2 - b]x\}^2} \\ &= \int_0^1 dx \frac{1}{[a(1 - x) + bx - q^2 x - 2p \cdot qx - p^2]^2}, \end{aligned} \quad (\text{B.35})$$

we obtain

$$\begin{aligned} J(a, b; q^2) &= \int_0^1 dx \int \frac{d^n p}{(2\pi)^n} \frac{1}{[a(1 - x) + bx - q^2 x + 2p \cdot (-qx) - p^2]^2} \\ &= \frac{i\Gamma(2 - \frac{n}{2})}{(4\pi)^{\frac{n}{2}} \Gamma(2)} \int_0^1 dx \frac{1}{[a(1 - x) + bx - q^2 x(1 - x)]^{2 - \frac{n}{2}}} \\ &= \frac{i}{16\pi^2} \left(\frac{2}{4 - n} - \gamma + \ln 4\pi \right) \int_0^1 dx \left[1 - \frac{4 - n}{2} \ln \frac{a(1 - x) + bx - q^2 x(1 - x)}{\mu^2} \right] \\ &= \frac{i}{16\pi^2} \left[\frac{1}{\bar{\epsilon}} - \int_0^1 dx \ln \frac{a(1 - x) + bx - q^2 x(1 - x)}{\mu^2} \right] \\ &=: \frac{i}{16\pi^2} \left[\frac{1}{\bar{\epsilon}} - F(a, b; q^2) \right], \end{aligned} \quad (\text{B.36})$$

where $F(a, b; q^2)$ denotes the finite part of the x -integral and is dimensionless. Substituting eqs. (B.34) and (B.36) into eq. (B.32) and rearranging, we find

$$\begin{aligned} I_B(a, b; q^2) &= \frac{i}{32\pi^2} \left\{ \left[\frac{1}{\bar{\epsilon}} - F(a, b; q^2) \right] - \frac{1}{b} \cdot b \left(\frac{1}{\bar{\epsilon}} + 1 - \ln \frac{b}{\mu^2} \right) \right. \\ &\quad - \frac{a}{b} \left[\frac{1}{\bar{\epsilon}} - F(a, b; q^2) - \frac{1}{\bar{\epsilon}} + F(a, 0; q^2) \right] \\ &\quad \left. - \frac{q^2}{b} \left[\frac{1}{\bar{\epsilon}} - F(a, b; q^2) - \frac{1}{\bar{\epsilon}} + F(a, 0; q^2) \right] \right\} \\ &= \frac{i}{32\pi^2} \left\{ \left[\ln \frac{b}{\mu^2} - F(a, b; q^2) - 1 \right] + \frac{a}{b} [F(a, b; q^2) - F(a, 0; q^2)] \right. \\ &\quad \left. + \frac{q^2}{b} [F(a, b; q^2) - F(a, 0; q^2)] \right\}. \end{aligned} \quad (\text{B.37})$$

Since the UV pole $\bar{\epsilon}^{-1}$ does not depend on q^2 , the constant term arising purely from $A_0(b)$ (the "+1" in eq. (B.34)) must cancel against the constant part of $F(a, b; q^2 \rightarrow 0)$. Evaluating

$$F(a, b; 0) = \int_0^1 dx \ln \frac{a(1 - x) + bx}{\mu^2} = \frac{a \ln \frac{a}{\mu^2} - b \ln \frac{b}{\mu^2}}{a - b} - 1, \quad (\text{B.38})$$

$$F(a, 0; 0) = \int_0^1 dx \ln \frac{a(1 - x)}{\mu^2} = \ln \frac{a}{\mu^2} - 1, \quad (\text{B.39})$$

and inserting these into the curly brackets of eq. (B.37), keeping only the constant terms in the limit $q^2 \rightarrow 0$, one finds

$$\left[\ln \frac{b}{\mu^2} - F(a, b; 0) - 1 \right] + \frac{a}{b} [F(a, b; 0) - F(a, 0; 0)]$$

$$\begin{aligned}
&= \ln \frac{b}{\mu^2} - 1 + \frac{1}{b} \left(a \ln \frac{a}{\mu^2} - b \ln \frac{b}{\mu^2} \right) + 1 - \frac{a}{b} - \frac{a}{b} \left(\ln \frac{a}{\mu^2} - 1 \right) \\
&= 0.
\end{aligned} \tag{B.40}$$

Thus, the constants cancel exactly, and only the difference of the finite functions enters. Here, we define $\Delta F(a, b; q^2)$ as

$$\Delta F(a, b; q^2) := F(a, b; q^2) - F(a, 0; q^2), \tag{B.41}$$

and together with eq. (B.36) we extract the finite part from

$$\begin{aligned}
J(a, b; q^2) - J(a, 0; q^2) &= -\frac{i}{16\pi^2} \int_0^1 dx \ln \frac{a(1-x) + bx - q^2 x(1-x)}{a(1-x) - q^2 x(1-x)} \\
&=: -\frac{i}{16\pi^2} \Delta F(a, b; q^2).
\end{aligned} \tag{B.42}$$

Using this definition, the quantity $\Delta F(a, b; q^2)$ is finite and contains neither the UV pole $\bar{\epsilon}^{-1}$ nor the renormalisation scale μ . Rewriting eq. (B.32) in terms of $\Delta F(a, b; q^2)$ from eq. (B.42) and $F(a, b; q^2)$ from eq. (B.36), we obtain

$$I_B(a, b; q^2) = -\frac{i}{32\pi^2} \left[F(a, b; q^2) + \left(1 - \ln \frac{b}{\mu^2} \right) - \frac{a}{b} \Delta F(a, b; q^2) - \frac{q^2}{b} \Delta F(a, b; q^2) \right]. \tag{B.43}$$

If we were to substitute $q^2 \rightarrow 0$ directly into this expression, all terms of order $\mathcal{O}(q^0)$ would cancel according to eq. (B.40), yielding zero. However, this is only an apparent cancellation coming from the longitudinal part. The physically relevant finite constant originates from a non-uniform limit at the endpoints, because the limit $q^2 \rightarrow 0$ and the x -integration do not commute in the presence of logarithmic terms $\ln[a(1-x) + bx - q^2 x(1-x)]$ that become singular near $x = 0, 1$. Therefore, one must keep the order of integration and limiting procedure as in eqs. (B.44)–(B.46) below. Treating $\Delta F(a, b; q^2)$ as a primitive function with respect to b , differentiation gives

$$\frac{\partial}{\partial b} \Delta F(a, b; q^2) = \int_0^1 dx \frac{x}{a(1-x) + bx - q^2 x(1-x)}. \tag{B.44}$$

Using eq. (B.44), we express $\Delta F(a, b; q^2)$ appearing in eq. (B.43) as an integral over $b' \in [0, b]$ with the initial condition $\Delta F(b' = 0) = 0$:

$$\Delta F(a, b; q^2) = \int_0^b db' \int_0^1 dx \frac{x}{a(1-x) + b'x - q^2 x(1-x)}. \tag{B.45}$$

Performing the b' -integration first, we obtain

$$\int_0^b \frac{db'}{a(1-x) + b'x - q^2 x(1-x)} = \frac{1}{x} \ln \frac{a(1-x) + bx - q^2 x(1-x)}{a(1-x) - q^2 x(1-x)}. \tag{B.46}$$

Substituting eqs. (B.45) and (B.46) into eq. (B.43), we find

$$I_B(a, b; q^2) = -\frac{i}{32\pi^2} \left[F(a, b; q^2) + \left(1 - \ln \frac{b}{\mu^2} \right) \right]$$

$$- \left(\frac{a}{b} + \frac{q^2}{b} \right) \int_0^1 dx \ln \frac{a(1-x) + bx - q^2 x(1-x)}{a(1-x) - q^2 x(1-x)} \Big]. \quad (\text{B.47})$$

Before taking the limit $q^2 \rightarrow 0$, the constant terms originating from J and A_0 cancel against each other, as follows from eqs. (B.32) and (B.40). Hence,

$$I_B(a, b; q^2) = \frac{i}{32\pi^2} \int_0^1 dx \left[\left(\frac{a}{b} + \frac{q^2}{b} \right) \ln \frac{a(1-x) + bx - q^2 x(1-x)}{a(1-x) - q^2 x(1-x)} \right. \\ \left. - \ln \frac{a(1-x) + bx - q^2 x(1-x)}{b} \right]. \quad (\text{B.48})$$

In what follows we keep only the finite part. We may therefore set $q^2 \rightarrow 0$ and perform the remaining x -integration, which leads to

$$I_B(a, b; 0) = \frac{i}{32\pi^2} \int_0^1 dx \left[\frac{a}{b} \ln \frac{a(1-x) + bx}{a(1-x)} - \ln \frac{a(1-x) + bx}{b} \right]. \quad (\text{B.49})$$

The remaining task is a straightforward integration of elementary functions; defining the functions

$$f(x) := \ln[a(1-x) + bx], \quad g(x) := \ln[a(1-x)], \quad (\text{B.50})$$

we can rewrite eq. (B.49) as

$$I_B(a, b; 0) = \frac{i}{32\pi^2} \int_0^1 dx \left[\left(\frac{a}{b} - 1 \right) f(x) - \frac{a}{b} g(x) + \ln b \right]. \quad (\text{B.51})$$

Using integration by parts, one finds

$$\int_0^1 dx f(x) = \int_0^1 dx \ln[a(1-x) + bx] = \frac{b \ln b - a \ln a}{b - a} - 1, \quad (\text{B.52})$$

$$\int_0^1 dx g(x) = \int_0^1 dx \ln[a(1-x)] = \ln a + \int_0^1 dx \ln(1-x) = \ln a - 1. \quad (\text{B.53})$$

Substituting eqs. (B.52) and (B.53) into eq. (B.51), we obtain

$$I_B(a, b; 0) = \frac{i}{32\pi^2} \left[\left(\frac{a}{b} - 1 \right) \left(\frac{b \ln b - a \ln a}{b - a} - 1 \right) - \frac{a}{b} (\ln a - 1) + \ln b \right] \\ = \frac{i}{32\pi^2} \left[-\frac{1}{b} (b \ln b - a \ln a) - \frac{a}{b} + 1 - \frac{a}{b} \ln a + \frac{a}{b} + \ln b \right] \\ = \frac{i}{32\pi^2} \left(-\ln b + \frac{a}{b} \ln a - \frac{a}{b} + 1 - \frac{a}{b} \ln a + \frac{a}{b} + \ln b \right) \\ = \frac{i}{32\pi^2}. \quad (\text{B.54})$$

Thus, $I_B(a, b; 0)$ reduces to the constant $i/(32\pi^2)$, independent of the specific values of $a = m_h^2$ and $b = m_B^2$. Inserting this into eq. (B.26), we arrive at

$$\Gamma_{\alpha\beta}^{(B)\mu}(q) = -\frac{1}{64\sqrt{2}\pi^2 v} \sum_{B=\gamma, Z} c_B g_{L_\beta}^{(B)} \mathcal{C}_B (2\sigma^{\mu\nu} q_\nu P_R). \quad (\text{B.55})$$

Following the procedure described in the main text, and employing this expression together with eq. (4.41), we obtain the renormalised Wilson coefficients given in eqs. (4.52) and (4.53).

C One-loop β -function of QED

In this appendix, we derive the one-loop RGE of QED from the β -function.

C.1 Renormalisation of QED

Let us write the QED Lagrangian as

$$\mathcal{L}_{\text{QED}} = -\frac{1}{4}F_{\mu\nu}F^{\mu\nu} + \bar{\psi}(iD - m)\psi, \quad D = \gamma^\mu(\partial_\mu + ieA_\mu). \quad (\text{C.1})$$

We compute the fermion self-energy, the vacuum polarisation, and the vertex function:



Eq. (C.1) is understood in terms of bare quantities:

$$\mathcal{L}_{\text{QED}} = -\frac{1}{4}F_{0\mu\nu}F_0^{\mu\nu} + \bar{\psi}_0[i(\not{D} + ie\not{A}_0) - m_0]\psi_0. \quad (\text{C.3})$$

Before setting up perturbation theory, we rewrite the bare fields and parameters in terms of renormalised ones,

$$\psi_0 = \sqrt{Z_2}\psi, \quad A_{0\mu} = \sqrt{Z_3}A_\mu, \quad m_0 = Z_m m, \quad e_0 = Z_e e. \quad (\text{C.4})$$

Using (C.4) in (C.3) gives

$$\begin{aligned} \mathcal{L}_{\text{QED}} &= -\frac{1}{4}Z_3F_{\mu\nu}F^{\mu\nu} + Z_2\bar{\psi}\left[i(\not{D} + ie\not{A}) - Z_m m\right]\psi \\ &= -\frac{1}{4}F_{\mu\nu}F^{\mu\nu} + \bar{\psi}\left[i(\not{D} + ie\not{A}) - m\right]\psi \\ &\quad - \frac{1}{4}(Z_3 - 1)F_{\mu\nu}F^{\mu\nu} + i(Z_2 - 1)\bar{\psi}\not{D}\psi \\ &\quad - (Z_2 Z_m - 1)m\bar{\psi}\psi - (Z_e Z_2 \sqrt{Z_3} - 1)e\bar{\psi}\not{A}\psi. \end{aligned} \quad (\text{C.5})$$

Here we have introduced

$$Z_1 := Z_e Z_2 \sqrt{Z_3}, \quad (\text{C.6})$$

and we define

$$Z_i = 1 + \delta Z_i^{(1)}, \quad (i = 1, 2, 3), \quad \delta Z_m^{(1)} = (Z_2 Z_m - 1)m. \quad (\text{C.7})$$

With these, the Lagrangian (C.5) may be written as

$$\begin{aligned} \mathcal{L}_{\text{QED}} &= -\frac{1}{4}F_{\mu\nu}F^{\mu\nu} + \bar{\psi}\left[i(\not{D} + ie\not{A}) - m\right]\psi \\ &\quad - \frac{1}{4}\delta Z_3^{(1)}F_{\mu\nu}F^{\mu\nu} + \bar{\psi}(i\delta Z_2^{(1)}\not{D} - \delta Z_m^{(1)})\psi - \delta Z_1^{(1)}e\bar{\psi}\not{A}\psi, \end{aligned} \quad (\text{C.8})$$

where the second line represents the counterterm Lagrangian $\mathcal{L}_{\text{count}}$. Note that this is equivalent to the bare Lagrangian (C.3). The quantities $\delta Z_i^{(1)}$ ($i = 1, 2, 3$) and $\delta Z_m^{(1)}$

incorporate loop corrections (i.e. quantum effects) and appear as additional interaction vertices in the Feynman rules: from the Fourier transformations of the second line of (C.8), we obtain the counterterm vertices

$$\text{---} \otimes \text{---} = i(\not{p} \delta Z_2^{(1)} - \delta Z_m^{(1)}), \quad (\text{C.9})$$

$$\text{~~~~~} \otimes \text{~~~~~} = -i\delta Z_3^{(1)}(g^{\mu\nu}q^2 - q^\mu q^\nu), \quad (C.10)$$

$$= ie\gamma^\mu \delta Z_1^{(1)}. \quad (C.11)$$

Although (C.9)–(C.11) look like tree-level vertices, they actually contain loop effects through the counterterms.

C.2 Fermion self-energy

Isolating the one-loop counterterm contribution, the self-energy graph satisfies

$$\frac{1}{i} \tilde{\Sigma}_{1\text{PI}}(\not{p}) + i(\not{p}Z_2^{(1)} - m) = \text{.....} \text{---} \text{.....} + \text{---} \otimes \text{---} \quad (\text{C.12})$$

Here, $\frac{1}{i} \tilde{\Sigma}_{1\text{PI}}$ represents the one-loop 1PI graphs with two external legs amputated. Evaluating the first term on the r.h.s. of (C.12), we obtain

$$\begin{aligned}
 \text{Diagram: } & \text{A Feynman diagram showing a loop with a wavy line. The loop is labeled } p-k \text{ at the top. The wavy line is labeled } p \text{ at the bottom left and } p \text{ at the bottom right. The loop has a clockwise arrow. The wavy line has an arrow pointing right. The loop is connected to the wavy line at two points, labeled } \mu \text{ and } \nu \text{ on the wavy line.} \\
 & \text{Equation: } \int \frac{d^n k}{(2\pi)^4} (-ie\gamma^\mu) \frac{i(\not{k} + m)}{k^2 - m^2} (-ie\gamma^\nu) \frac{-ig_{\mu\nu}}{(p-k)^2} \\
 & = \frac{ie^2}{16\pi^2} \left[(\not{p} - 4m) \frac{1}{\epsilon} + \int_0^1 dx (-2x\not{p} + 4m) \ln \frac{(m^2 - p^2 x)(1-x)}{\mu^2} \right], \quad (\text{C.13})
 \end{aligned}$$

where $\bar{\epsilon}^{-1} := \epsilon^{-1} - \gamma + \ln 4\pi$, and we kept the external momentum p general (although on shell $p^2 = m^2$) since we will also take the derivative with respect to p .

The on-shell renormalisation conditions require that the one-loop correction in (C.12) does not shift the physical mass, so

$$\frac{1}{i} \tilde{\Sigma}_{\text{1PI}}(\not{p}) + i(\not{p} \delta Z_2^{(1)} - m) \Big|_{\not{p}=m} = \text{.....} \text{---} \text{.....} + \text{---} \otimes \text{---} = 0, \quad (\text{C.14})$$

and expanding around $\mathcal{P} = m$ to zeroth and first order gives

$$\frac{1}{i} \tilde{\Sigma}_{1\text{PI}}(m^2) + i(m\delta Z_2^{(1)} - \delta Z_m^{(1)}) = 0, \quad (\text{C.15})$$

$$\frac{d}{d\psi} \frac{1}{i} \tilde{\Sigma}_{1\text{PI}}(p^2) \bigg|_{\psi=m} + i\delta Z_2^{(1)} = 0. \quad (\text{C.16})$$

From (C.16) we therefore obtain

$$\delta Z_2^{(1)} = -\frac{\alpha}{4\pi} \left(\frac{1}{\bar{\epsilon}} + \ln \frac{\mu^2}{m^2} + 5 + 2 \ln \frac{m_\gamma^2}{m^2} \right), \quad \alpha = \frac{e^2}{4\pi}, \quad (\text{C.17})$$

where we introduced an infrared regulator m_γ . Substituting (C.17) into (C.12) yields

$$\delta Z_m^{(1)} = -\frac{\alpha m}{\pi} \left(\frac{1}{\bar{\epsilon}} - \ln \frac{\mu^2}{m^2} + \frac{5}{4} + \frac{1}{2} \ln \frac{m_\gamma^2}{m^2} \right). \quad (\text{C.18})$$

C.3 Vacuum polarisation

We now compute the vacuum polarisation. The one-loop Feynman graph is

$$i\Pi_2^{\mu\nu}(q) := \frac{\text{.....}}{q} \begin{array}{c} \text{---} \\ \text{---} \\ \text{---} \\ \text{---} \\ \text{---} \end{array} \frac{\text{.....}}{q} \quad , \quad (\text{C.19})$$

and can be written as

$$\begin{aligned}
i\pi_2^{\mu\nu}(q) &= (-ie)^2(-1) \int \frac{d^4k}{(2\pi)^4} \text{tr} \left(\gamma^\mu \frac{i}{k-m} \gamma^\nu \frac{i}{k+q-m} \right) \\
&= -i(g^{\mu\nu}q^2 - q^\mu q^\nu)e^2 \frac{1}{2\pi^2} \int_0^1 dx \ x(1-x) \left[\frac{1}{\epsilon} + \ln \frac{\mu^2}{m^2 - q^2 x(1-x)} \right] \\
&=: -i(g^{\mu\nu}q^2 - q^\mu q^\nu)e^2 \Pi_2(q^2), \tag{C.20}
\end{aligned}$$

where

$$\Pi_2(q^2) = \frac{1}{2\pi^2} \int_0^1 dx \, x(1-x) \left[\frac{1}{\bar{\epsilon}} + \ln \frac{\mu^2}{m^2 - q^2 x(1-x)} \right]. \quad (\text{C.21})$$

Imposing the charge non-renormalisation condition, i.e. Ward–Takahashi identity,



$$\text{Diagram: circle with a loop inside} + \text{wavy line} \otimes \text{wavy line} = i\pi_2^{\mu\nu}(q) - i\delta Z_3^{(1)}(g^{\mu\nu}q^2 - q^\mu q^\nu) = 0, \quad (\text{C.22})$$

yields

$$\begin{aligned} i\pi_2^{\mu\nu}(q) - i\delta Z_3^{(1)}(g^{\mu\nu}q^2 - q^\mu q^\nu) \\ = -i(g^{\mu\nu}q^2 - q^\mu q^\nu) \left[e^2 \Pi_2(q^2) + \delta Z_3^{(1)} \right] = 0. \end{aligned} \quad (\text{C.23})$$

Evaluating this relation at the photon on-shell point $q^2 = 0$, we obtain

$$\begin{aligned}\delta Z_3^{(1)} &= -e^2 \Pi_2(q^2 = 0) = -\frac{e^2}{2\pi^2} \int_0^1 dx \, x(1-x) \left(\frac{1}{\bar{\epsilon}} + \ln \frac{\mu^2}{m^2} \right) \\ &= -\frac{e^2}{12\pi^2} \left(\frac{1}{\bar{\epsilon}} + \ln \frac{\mu^2}{m^2} \right) = -\frac{\alpha}{3\pi} \left(\frac{1}{\bar{\epsilon}} + \ln \frac{\mu^2}{m^2} \right).\end{aligned}\quad (\text{C.24})$$

C.4 Vertex correction

Let us now compute the one-loop vertex function with external legs amputated:

$$\bar{u}_{\mathbf{p}',s'} \delta I^\mu(p',p) u_{\mathbf{p},s} := \text{Diagram} \quad (C.25)$$

By the Feynman rules,

$$\bar{u}_{\mathbf{p}',s'} \delta \Gamma^\mu(p',p) u_{\mathbf{p},s} = \bar{u}_{\mathbf{p}',s'} \int \frac{d^n k}{(2\pi)^n} \frac{-ig_{\nu\rho}}{(p-k)^2} (-ie\gamma^\nu) \frac{i(\not{k} + m)}{k'^2 - m^2} (-ie\gamma^\mu) \frac{i(\not{k} + m)}{k^2 - m^2} (-ie\gamma^\rho) u_{\mathbf{p},s}, \quad (\text{C.26})$$

and the Gordon identity yields [67]

$$\begin{aligned} \delta\Gamma^\mu(p', p) &= -e^3 \int \frac{d^n k}{(2\pi)^n} \frac{\gamma^\nu(\not{k}' + m)\gamma^\mu(\not{k} + m)\gamma_\nu}{(p - k)^2(k'^2 - m^2)(k^2 - m^2)} \\ &=: -ie \left[\gamma^\mu F_1(q^2) + \frac{i\sigma^{\mu\nu}q_\nu}{2m} F_2(q^2) \right], \end{aligned} \quad (\text{C.27})$$

where F_1 and F_2 are form factors that contain the one-loop corrections. F_1 is given by

$$F_1(q^2) := 1 + \frac{e^2}{16\pi^2} \left\{ \frac{1}{\epsilon} - 1 + 2 \int_0^1 dx \int_0^1 dy \int_0^1 dz \delta(x+y+z-1) \right. \\ \left. \times \left[\ln \frac{\mu^2}{\Delta} + \frac{(1-x)(1-y)q^2 + (1-4z+z^2)m^2}{\Delta} \right] \right\}, \quad (\text{C.28})$$

with $\Delta := m^2(1-z)^2 - q^2xy$. Writing the quantum correction part of F_1 as f_1 , one may express $F_1(q^2) = 1 + f_1(q^2)$ with

$$f_1(q^2) = \frac{e^2}{16\pi^2} \left\{ \frac{1}{\bar{\epsilon}} - 1 + 2 \int_0^1 dx \int_0^1 dy \int_0^1 dz \, \delta(x+y+z-1) \right. \\ \left. \times \left[\ln \frac{\mu^2}{\Delta} + \frac{(1-x)(1-y)q^2 + (1-4z+z^2)m^2}{\Delta} \right] \right\}. \quad (\text{C.29})$$

At $q^2 = 0$, Δ reduces to

$$\Delta(q^2 = 0) = m^2(1 - z)^2. \quad (\text{C.30})$$

However, an infrared divergence appears here again, which we regulate by introducing a small photon mass m_γ ,

$$f_1(q^2 = 0) = \frac{\alpha}{4\pi} \left(\frac{1}{\bar{\epsilon}} + \ln \frac{\mu^2}{m^2} + 5 + 2 \ln \frac{m_\gamma^2}{m^2} \right), \quad \alpha = \frac{e^2}{4\pi}. \quad (\text{C.31})$$

By definition (C.27), the form factor F_1 corrects the vertex $-ie\gamma^\mu$. Hence, just as in the two-point functions, the quantum correction $-ie\gamma^\mu f_1(q^2 = 0)$ must be cancelled by the counterterm (C.11), leading to

$$-ie\gamma^\mu\delta Z_1^{(1)} - ie\gamma^\mu f_1(q^2=0) = 0 \quad \Rightarrow \quad \delta Z_1^{(1)} = -f_1(q^2=0). \quad (\text{C.32})$$

Therefore, from (C.31),

$$\delta Z_1^{(1)} = -\frac{\alpha}{4\pi} \left(\frac{1}{\bar{\epsilon}} + \ln \frac{\mu^2}{m^2} + 5 + 2 \ln \frac{m_\gamma^2}{m^2} \right). \quad (\text{C.33})$$

In fact, this is identical to $\delta Z_2^{(1)}$ in (C.17):

$$\delta Z_1^{(1)} = \delta Z_2^{(1)}. \quad (\text{C.34})$$

This equality is not accidental: it is guaranteed by gauge invariance and follows from the Ward–Takahashi identity [26].

We now compute $F_2(q^2)$. From (C.27), the one-loop form factor is

$$F_2(q^2) := \frac{e^2}{8\pi^2} \int_0^1 dx \int_0^1 dy \int_0^1 dz \delta(x+y+z-1) \frac{2m^2 z(1-z)}{\Delta}. \quad (\text{C.35})$$

Using $\Delta = m^2(1-z)^2 - q^2 xy$, the value at $q^2 = 0$ is

$$\begin{aligned} F_2(q^2 = 0) &= \frac{e^2}{8\pi^2} \int_0^1 dx \int_0^1 dy \int_0^1 dz \delta(x+y+z-1) \frac{2m^2 z(1-z)}{m^2(1-z)^2} \\ &= \frac{e^2}{4\pi^2} \int_0^1 dz \int_0^{1-z} dx \frac{z}{1-z} = \frac{e^2}{4\pi^2} \int_0^1 dz z = \frac{e^2}{8\pi^2} = \frac{\alpha}{2\pi}. \end{aligned} \quad (\text{C.36})$$

This correction is called the anomalous magnetic moment of the electron, i.e., the deviation of the g -factor $g = 2[1 + F_2(0)]$:

$$\frac{g-2}{2} = F_2(0) = \frac{\alpha}{2\pi} \simeq 0.0011614, \quad \alpha \simeq \frac{1}{137.036}, \quad (\text{C.37})$$

in excellent agreement with the experimental value $(g-2)/2 = 0.0011597$.

C.5 One-loop β -function

In the following we only need the ultraviolet pole, so we drop finite $\bar{\epsilon}$ -dependent terms and replace $\bar{\epsilon}^{-1}$ by ϵ^{-1} . To obtain the one-loop β -function of QED, start from (C.6),

$$Z_e = Z_1 Z_2^{-1} Z_3^{-1/2}, \quad (\text{C.38})$$

from which it follows that the one-loop counterterm for the electric charge is

$$\delta Z_e^{(1)} = \delta Z_1^{(1)} - \delta Z_2^{(1)} - \frac{1}{2} \delta Z_3^{(1)}. \quad (\text{C.39})$$

Extracting the ultraviolet-divergent parts, and using (C.34) which implies $\delta Z_1^{(1)} = \delta Z_2^{(1)}$, we obtain

$$\delta Z_e^{(1)} = -\frac{1}{2} \delta Z_3^{(1)}. \quad (\text{C.40})$$

Inserting into $\delta Z_3^{(1)}$ the UV-divergent piece of (C.24), $(-\alpha/3\pi\epsilon)$, gives

$$\delta Z_e^{(1)} = \frac{\alpha}{6\pi\epsilon} = \frac{e^2}{24\pi^2\epsilon}. \quad (\text{C.41})$$

Since the bare charge is independent of the renormalisation scale μ , eq. (C.4) implies

$$0 = \mu \frac{d}{d\mu} e_0 = \mu \frac{d}{d\mu} (\mu^\epsilon e Z_e) = \mu^\epsilon e Z_e \left(\epsilon + \frac{\mu}{e} \frac{de}{d\mu} + \frac{\mu}{Z_e} \frac{dZ_e}{d\mu} \right). \quad (\text{C.42})$$

At leading order in e one has $Z_e = Z_e^{(0)} = 1$, hence

$$\mu \frac{de}{d\mu} = -e\epsilon. \quad (\text{C.43})$$

At the next order, using (C.41),

$$\mu \frac{dZ_e}{d\mu} = \mu \frac{d}{d\mu} \left(1 + \frac{e^2}{24\pi^2\epsilon} \right) = \frac{e}{12\pi^2\epsilon} \cdot \mu \frac{de}{d\mu} = \frac{e}{12\pi^2\epsilon} \cdot (-e\epsilon) = -\frac{e^2}{12\pi^2}, \quad (\text{C.44})$$

where we used (C.43). Substituting (C.44) into (C.42), the one-loop QED β -function is

$$\beta(e) := \mu \frac{de}{d\mu} \simeq -e\epsilon - e \frac{\mu}{Z_e^{(0)}} \frac{dZ_e}{d\mu} = -e\epsilon + \frac{e^3}{12\pi^2}. \quad (\text{C.45})$$

Taking the limit $\epsilon \rightarrow 0$ yields the familiar form [26]

$$\beta(e) = \frac{e^3}{12\pi^2}. \quad (\text{C.46})$$

References

- [1] A.D. Sakharov, *Violation of CP Invariance, C asymmetry, and baryon asymmetry of the universe*, *Pisma Zh. Eksp. Teor. Fiz.* **5** (1967) 32.
- [2] N.S. Manton, *Topology in the weinberg-salam theory*, *Phys. Rev. D* **28** (1983) 2019.
- [3] F.R. Klinkhamer and N.S. Manton, *A saddle-point solution in the weinberg-salam theory*, *Phys. Rev. D* **30** (1984) 2212.
- [4] M. Fukugita and T. Yanagida, *Baryogenesis without grand unification*, *Physics Letters B* **174** (1986) 45.
- [5] P. Minkowski, $\mu \rightarrow e\gamma$ at a Rate of One Out of 10^9 Muon Decays?, *Phys. Lett. B* **67** (1977) 421.
- [6] T. Yanagida, *Horizontal gauge symmetry and masses of neutrinos*, *Conf. Proc. C* **7902131** (1979) 95.
- [7] M. Gell-Mann, P. Ramond and R. Slansky, *Complex Spinors and Unified Theories*, *Conf. Proc. C* **790927** (1979) 315 [[1306.4669](#)].
- [8] R.N. Mohapatra and G. Senjanović, *Neutrino mass and spontaneous parity nonconservation*, *Phys. Rev. Lett.* **44** (1980) 912.
- [9] W. Buchmuller, P. Di Bari and M. Plumacher, *Leptogenesis for pedestrians*, *Annals of Physics* **315** (2005) 305.
- [10] S. Davidson, E. Nardi and Y. Nir, *Leptogenesis*, *Physics Reports* **466** (2008) 105.
- [11] C.S. Fong, E. Nardi and A. Riotto, *Leptogenesis in the universe*, *Advances in High Energy Physics* **2012** (2012) 158303.

[12] N.F. Bell, B.J. Kayser and S.S.C. Law, *Electromagnetic leptogenesis*, *Phys. Rev. D* **78** (2008) 085024.

[13] R. Takada, *Electromagnetic leptogenesis — an EFT-consistent analysis via Wilson coefficients. Part I. Low-scale, non-resonant regime*, *JHEP* **12** (2025) 010 [[2509.07698](#)].

[14] R. Takada, *Electromagnetic Leptogenesis — an EFT-Consistent Analysis via Wilson Coefficients. Part II. Low-Scale, Resonant Regime*, [2510.21089](#).

[15] A. Pilaftsis and T.E. Underwood, *Resonant leptogenesis*, *Nuclear Physics B* **692** (2004) 303.

[16] S. Weinberg, *Baryon- and lepton-nonconserving processes*, *Phys. Rev. Lett.* **43** (1979) 1566.

[17] G. Isidori, F. Wilsch and D. Wyler, *The standard model effective field theory at work*, *Rev. Mod. Phys.* **96** (2024) 015006.

[18] S.M. Barr and A. Zee, *Electric dipole moment of the electron and of the neutron*, *Phys. Rev. Lett.* **65** (1990) 21.

[19] S.M. Barr and A. Zee, *Electric dipole moment of the electron and of the neutron*, *Phys. Rev. Lett.* **65** (1990) 2920.

[20] K. Afanaciev et al., *New limit on the mu+ -> e+ gamma decay with the MEG II experiment*, *Eur. Phys. J. C* **85** (2025) 1177 [[2504.15711](#)].

[21] T.S. Roussy et al., *An improved bound on the electron's electric dipole moment*, *Science* **381** (2023) 46.

[22] THE MUON $g - 2$ COLLABORATION collaboration, *Measurement of the positive muon anomalous magnetic moment to 0.20 ppm*, *Phys. Rev. Lett.* **131** (2023) 161802.

[23] Planck Collaboration, N. Aghanim, Y. Akrami, M. Ashdown, J. Aumont, C. Baccigalupi et al., *Planck 2018 results. VI. Cosmological parameters*, *Astronomy & Astrophysics* **641** (2020) A6 [[1807.06209](#)].

[24] A. Aparici, K. Kim, A. Santamaria and J. Wudka, *Right-handed neutrino magnetic moments*, *Phys. Rev. D* **80** (2009) 013010.

[25] S. Patra and S. Rao, *A Simple Model for Magnetic Inelastic Dark Matter (MiDM)*, [1112.3454](#).

[26] M.D. Schwartz, *Quantum Field Theory and the Standard Model*, Cambridge University Press (2013).

[27] M.E. Machacek and M.T. Vaughn, *Two-loop renormalization group equations in a general quantum field theory: (i). wave function renormalization*, *Nuclear Physics B* **222** (1983) 83.

[28] M.E. Machacek and M.T. Vaughn, *Two-loop renormalization group equations in a general quantum field theory (ii). yukawa couplings*, *Nuclear Physics B* **236** (1984) 221.

[29] B. Grzadkowski, M. Iskrzynski, M. Misiak and J. Rosiek, *Dimension-Six Terms in the Standard Model Lagrangian*, *JHEP* **10** (2010) 085 [[1008.4884](#)].

[30] I. Brivio and M. Trott, *The standard model as an effective field theory*, *Physics Reports* **793** (2019) 1.

[31] S.S.C. Law, *Neutrino Models and Leptogenesis*, Ph.D. thesis, Melbourne U., 2008. [0901.1232](#).

[32] G. Magill, R. Plestid, M. Pospelov and Y.-D. Tsai, *Dipole portal to heavy neutral leptons*, *Phys. Rev. D* **98** (2018) 115015.

[33] W. Buchmuller, P. Di Bari and M. Plumacher, *Cosmic microwave background, matter - antimatter asymmetry and neutrino masses*, *Nucl. Phys. B* **643** (2002) 367 [[hep-ph/0205349](#)].

[34] M. D’Onofrio, K. Rummukainen and A. Tranberg, *Sphaleron rate in the minimal standard model*, *Phys. Rev. Lett.* **113** (2014) 141602.

[35] M. D’Onofrio and K. Rummukainen, *Standard model cross-over on the lattice*, *Phys. Rev. D* **93** (2016) 025003.

[36] K. Babu, C. Leung and J. Pantaleone, *Renormalization of the neutrino mass operator*, *Physics Letters B* **319** (1993) 191.

[37] S. Davidson, M. Gorbahn and A. Santamaria, *From transition magnetic moments to majorana neutrino masses*, *Phys. Lett. B* **626** (2005) 151 [[hep-ph/0506085](#)].

[38] Z. Maki, M. Nakagawa and S. Sakata, *Remarks on the unified model of elementary particles*, *Progress of Theoretical Physics* **28** (1962) 870.

[39] B. Pontecorvo, *Mesonium and Antimesonium*, *Sov. Phys. JETP* **6** (1958) 429.

[40] B. Pontecorvo, *Inverse Beta Processes and Nonconservation of Lepton Charge*, *Sov. Phys. JETP* **7** (1958) 172.

[41] B. Pontecorvo, *Neutrino Experiments and the Problem of Conservation of Leptonic Charge*, *Sov. Phys. JETP* **26** (1968) 984.

[42] V. Gribov and B. Pontecorvo, *Neutrino astronomy and lepton charge*, *Physics Letters B* **28** (1969) 493.

[43] I. Esteban, M.C. Gonzalez-Garcia, M. Maltoni, T. Schwetz and A. Zhou, *The fate of hints: updated global analysis of three-flavor neutrino oscillations*, *JHEP* **09** (2020) 178 [[2007.14792](#)].

[44] I. Esteban, M.C. Gonzalez-Garcia, M. Maltoni, I. Martinez-Soler, J.P. Pinheiro and T. Schwetz, *NuFit-6.0: updated global analysis of three-flavor neutrino oscillations*, *JHEP* **12** (2024) 216 [[2410.05380](#)].

[45] KATRIN collaboration, *Direct neutrino-mass measurement based on 259 days of KATRIN data*, *Science* **388** (2025) adq9592 [[2406.13516](#)].

[46] R.N. Mohapatra and G. Senjanović, *Neutrino masses and mixings in gauge models with spontaneous parity violation*, *Phys. Rev. D* **23** (1981) 165.

[47] M. Magg and C. Wetterich, *Neutrino Mass Problem and Gauge Hierarchy*, *Phys. Lett. B* **94** (1980) 61.

[48] J. Schechter and J.W.F. Valle, *Neutrino masses in $su(2) \otimes u(1)$ theories*, *Phys. Rev. D* **22** (1980) 2227.

[49] C. Wetterich, *Neutrino Masses and the Scale of B-L Violation*, *Nucl. Phys. B* **187** (1981) 343.

[50] G. Lazarides, Q. Shafi and C. Wetterich, *Proton lifetime and fermion masses in an $so(10)$ model*, *Nuclear Physics B* **181** (1981) 287.

[51] R. Foot, H. Lew, X.G. He and G.C. Joshi, *Seesaw Neutrino Masses Induced by a Triplet of Leptons*, *Z. Phys. C* **44** (1989) 441.

[52] E. Ma, *Pathways to naturally small neutrino masses*, *Phys. Rev. Lett.* **81** (1998) 1171.

[53] E. Ma and D.P. Roy, *Heavy triplet leptons and new gauge boson*, *Nucl. Phys. B* **644** (2002) 290 [[hep-ph/0206150](#)].

[54] E.E. Jenkins, A.V. Manohar and P. Stoffer, *Low-Energy Effective Field Theory below the Electroweak Scale: Operators and Matching*, *JHEP* **03** (2018) 016 [[1709.04486](#)].

[55] E.E. Jenkins, A.V. Manohar and M. Trott, *Renormalization Group Evolution of the Standard Model Dimension Six Operators I: Formalism and lambda Dependence*, *JHEP* **10** (2013) 087 [[1308.2627](#)].

[56] E.E. Jenkins, A.V. Manohar and P. Stoffer, *Low-Energy Effective Field Theory below the Electroweak Scale: Anomalous Dimensions*, *JHEP* **01** (2018) 084 [[1711.05270](#)].

[57] G. Passarino and M. Veltman, *One-loop corrections for e^+e^- annihilation into $\mu^+\mu^-$ in the weinberg model*, *Nuclear Physics B* **160** (1979) 151.

[58] J.M. Campbell, E.W.N. Glover and D.J. Miller, *One loop tensor integrals in dimensional regularization*, *Nucl. Phys. B* **498** (1997) 397 [[hep-ph/9612413](#)].

[59] T. Kugo, *Quantum Theory of Gauge Fields, Vol. II*, no. 24 in New Physics Series, Baifukan, Tokyo (July, 1989).

[60] Y. Kuno and Y. Okada, *Muon decay and physics beyond the standard model*, *Rev. Mod. Phys.* **73** (2001) 151.

[61] D.J. Griffiths, *Introduction to elementary particles*, Physics textbook, Wiley, New York, NY (2008).

[62] M. Pospelov and A. Ritz, *Electric dipole moments as probes of new physics*, *Annals of Physics* **318** (2005) 119.

[63] T. Aoyama et al., *The anomalous magnetic moment of the muon in the Standard Model*, *Phys. Rept.* **887** (2020) 1 [[2006.04822](#)].

[64] C. Froggatt and H. Nielsen, *Hierarchy of quark masses, cabibbo angles and cp violation*, *Nuclear Physics B* **147** (1979) 277.

[65] K.S. Babu and C.N. Leung, *Classification of effective neutrino mass operators*, *Nucl. Phys. B* **619** (2001) 667 [[hep-ph/0106054](#)].

[66] I. Bischer and W. Rodejohann, *General neutrino interactions from an effective field theory perspective*, *Nucl. Phys. B* **947** (2019) 114746 [[1905.08699](#)].

[67] M.E. Peskin and D.V. Schroeder, *An Introduction to quantum field theory*, Addison-Wesley, Reading, USA (1995), [10.1201/9780429503559](#).